In compliance with the
Canadian Privacy Legislation
some supporting forms
may have been removed from
this dissertation.

While these forms may be included
in the document page count,
their removal does not represent
any loss of content from the dissertation.

University of Alberta

Repair Techniques for Locally Buckled Energy Pipelines Using Fibre Reinforced Polymer Composites

by

Imran A. Khawaja

A thesis submitted to the Faculty of Graduate Studies and Research in partial fulfillment of the requirements for the degree of Master of Science

in

Structural Engineering

Department of Civil and Environmental Engineering

Edmonton, Alberta

FALL 2003

National Library
of Canada

Acquisitions and
Bibliographic Services

395 Wellington Street
Ottawa ON K1A 0N4
Canada

Bibliothèque nationale
du Canada

Acquisisitons et
services bibliographiques

395, rue Wellington
Ottawa ON K1A 0N4
Canada

Your file Votre référence
ISBN: 0-612-87801-5
Our file Notre référence
ISBN: 0-612-87801-5

The author has granted a non-exclusive licence allowing the National Library of Canada to reproduce, loan, distribute or sell copies of this thesis in microform, paper or electronic formats.

The author retains ownership of the copyright in this thesis. Neither the thesis nor substantial extracts from it may be printed or otherwise reproduced without the author's permission.

L'auteur a accordé une licence non exclusive permettant à la Bibliothèque nationale du Canada de reproduire, prêter, distribuer ou vendre des copies de cette thèse sous la forme de microfiche/film, de reproduction sur papier ou sur format électronique.

L'auteur conserve la propriété du droit d'auteur qui protège cette thèse. Ni la thèse ni des extraits substantiels de celle-ci ne doivent être imprimés ou aturement reproduits sans son autorisation.

Canada

University of Alberta

Library Release Form

Name of Author:	Imran A. Khawaja
Title of Thesis:	Repair Techniques for Locally Buckled Energy Pipelines Using Fibre Reinforced Polymer Composites
Degree:	Master of Science
Year this Degree is Granted:	2003

Permission is hereby granted to the University of Alberta Library to produce single copies of this thesis and to lend or sell such copies for private, scholarly or scientific research purposes only.

The author reserves all other publication and other rights in association with the copyright in the thesis, and except as herein before provided; neither the thesis nor any substantial portion thereof may be printed or otherwise reproduced in any material from whatever without the author's prior written permission.

Dated: August 28, 2003

University of Alberta

Faculty of Graduate Studies and Research

The undersigned certify that they have read, and recommend to the Faculty of Graduate Studies and Research for acceptance, a thesis entitled Repair Techniques for Locally Buckled Energy Pipelines using Fibre Reinforced Polymer Composites submitted by Imran A. Khawaja in partial fulfillment of the requirements for the degree of Master of Science in Structural Engineering.

Dr. J.J. Roger Cheng, Supervisor

Dr. Alaa Elwi, Committee Chair and Examiner

Dr. Ben Jar, Committee Member

Dated: August 28, 2003

ABSTRACT

Steel pipelines are the most economical and efficient mode of transporting oil and natural gas. When buried pipelines pass through discontinuous permafrost regions in Canadian north, local buckling appears in the pipe wall due to extremely high stresses generated by frost heave, slope moment and thaw settlement of the soil. Several wrinkles have been found in Norman Wells line in Northwest Territory since 1998.

The common rehabilitation method is to replace the wrinkled section of the pipe with unwrinkled one. This method is extremely expensive. Another method is to provide external steel sleeve on the wrinkled portion of the pipe however studies have revealed that this method is not effective in the long run.

This research program is designed to develop optimum repair techniques using fibre reinforced polymer (FRP) composites. Experiments and finite element analysis (FEA) have been used. The effects of several repair techniques on the behaviour of the pipe are discussed and effective repair techniques are developed.

ACKNOWLEDGEMENTS

The author sincerely thanks to his supervisor Dr. J.J. Roger Cheng for his guidance, support and encouragement throughout this project.

The author acknowledges the financial support for this research project from Enbridge Pipelines Inc. and ISIS (Intelligent Sensing for Innovative Structures) Canada. The author acknowledges the technical support from Larry Burden and Richard Helfrich at I.F. Morrison Structural Engineering Laboratory at University of Alberta.

Author would like to thank all the faculty members of Structural Engineering at the University of Alberta for their teaching during M.Sc. program. Author also thanks fellow graduate students Oliver Youzwishen, Syed Salman Mobeen, Munawar Hussain and Nadeem Khattak for their assistance during numerical and experimental works.

Last but not least, the author would like to acknowledge the support and encouragement from his family members especially parents, Dr. and Mrs. Nawaz Ali and brother, Dr. Nisar Ali.

TABLE OF CONTENTS

1	**INTRODUCTION**		**1**
	1.1	GENERAL	1
	1.2	STATEMENT OF PROBLEM	1
	1.3	CURRENT METHODS OF REPAIR	2
	1.4	OBJECTIVES AND SCOPE	2
	1.5	OVERVIEW OF THESIS	3
2	**LITERATURE REVIEW AND PREVIOUS INVESTIGATIONS**		**6**
	2.1	GENERAL	6
	2.2	CAUSES OF LOCAL BUCKLING	6
		2.2.1 Temperature Differential Effect	7
		2.2.2 Poisson's Effect	7
		2.2.3 Soil Movement and Settlement Effect	8
	2.3	NORMAN WELLS PIPELINE-A CASE STUDY	8
	2.4	BEHAVIOUR OF WRINKLED PIPES	9
	2.5	REHABILITATION METHODS FOR WRINKLED PIPES	10
		2.5.1 Rehabilitation by Replacing the Wrinkled section of the Pipe	11
		2.5.2 Rehabilitation by External Steel Sleeve	11
		2.5.3 Rehabilitation by FRP Sleeves	12
		2.5.3.1 FRP Composites	12
		2.5.3.2 Sleeve Geometry	13
	2.6	PREVIOUS EXPERIMENTAL RESULTS	14
		2.6.1 Half-Scale Test Results	15
		2.6.2 Full-Scale Test Results	16

3 EXPERIMENTAL PROGRAM 29

3.1 EXPERIMENTAL OBJECTIVES AND TEST PARAMETERS 29
3.2 TEST SPECIMENS AND PREPARATIONS 30
3.3 TEST SETUP AND BOUNDARY CONDITIONS 31
3.3.1 Test Frame 31
3.3.2 Boundary Conditions 32
3.4 INSTRUMENTATION 32
3.4.1 Strain Gauges 33
3.4.2 Cable Transducers 33
3.4.3 Load Cells 34
3.4.4 Rotation Meters 34
3.4.5 LVDTs 34
3.5 TEST PROCEDURE 35
3.5.1 General Test Procedure 35
3.5.1.1 Internal Pressure 35
3.5.1.2 Axial Load 35
3.5.1.3 Flexural Bending 36
3.5.2 Pre-wrinkle Test Procedure 37
3.5.3 Post-wrinkle Repair of Specimens 38
3.5.3.1 Test No.1 39
3.5.3.2 Test No.2 39
3.5.3.3 Test No.3 39
3.5.4 Post-repair Test Procedure 39
3.5.5 Problems and Difficulties during Tests 40

4 EXPERIMENTAL RESULTS 55

4.1 OBJECTIVE 55

4.2 MATERIAL PROPERTIES 55
4.3 DATA CALCULATIONS 56
4.4 DISCUSSION OF EXPERIMENTS 57
4.4.1 Test-1 58
4.4.2 Test-2 60
4.4.3 Test-3 62

5 FINITE ELEMENT ANALYSIS 78

5.1 GENERAL 78
5.2 FINITE ELEMENT MODEL 79
5.2.1 Mesh and Element Selection 79
5.2.2 Boundary Conditions 79
5.2.3 Imperfection 80
5.2.4 Loading Conditions 80
5.2.4.1 Internal Pressure 80
5.2.4.2 Axial Loads 81
5.2.4.3 Curvature 82
5.2.5 Sleeve Application 82
5.2.6 Analysis Procedure 82
5.3 SLEEVE GEOMETRY OR CONFIGURATION 83
5.3.1 Single Sleeve Configuration (SS) 83
5.3.2 Odd Sleeve Configuration (OS) 84
5.3.3 Even Sleeve Configuration (ES) 84
5.4 PARAMETERS 85
5.4.1 Single Sleeve 86
5.4.2 Odd Sleeve 87
5.4.3 Even Sleeve 88
5.5 SLEEVE STIFFNESS 91
5.5.1 Single Sleeve 91

5.5.2 Odd Sleeve 93
5.5.3 Even Sleeve 96
5.6 COMPARISON 97
5.6.1 Comparison between Even and Odd Sleeve Configurations 98
5.6.2 Comparison between Even and Double Sleeve Configurations 99
5.6.3 Comparison between Single and Odd Sleeve Configurations 98
5.6.4 Overall Comparison 100
5.7 SEQUENTIAL SLEEVE REPAIR 100

6 CONCLUSIONS AND RECOMMENDATIONS 127

6.1 GENERAL 127
6.2 SLEEVE LENGTH 127
6.3 GAP SIZE 128
6.4 SLEEVE STIFFNESS 130
6.5 CONCLUSIONS 131
6.6 OPTIMUM SLEEVE DESIGN 132
6.7 RECOMMENDATIONS 133

REFERENCES 135

LIST OF TABLES

Table 2-1 Material Properties of NPS 6 Pipe (Youzwishen and Cheng, 2001) 18

Table 2-2 Test Matrix for NPS 6 Pipe Specimen (Youzwishen and Cheng, 2001) 18

Table 2-3 Material Properties of Carbon Fibre (Youzwishen and Cheng, 2001) 19

Table 2-4 Material Properties of FTS-GE-30 Glass Fibre (Youzwishen and Cheng, 2001) 19

Table 2-5 Test Matrix for NPS 12 Pipe Specimen (Youzwishen and Cheng, 2001) 20

Table 2-6 Material Properties of NPS 12 Pipe (Youzwishen and Cheng, 2001) 20

Table 3-1 Typical Physical Properties of Mbrace EG 900 42

LIST OF FIGURES

Figure 1.1	Local buckling in the pipe wall	4
Figure 1.2	Typical moment-curvature behaviour of a locally buckled pipe	4
Figure 1.3	Global moment vs. curvature for single steel sleeve repair	5
Figure 2.1	Local buckling in Norman Wells Pipeline	21
Figure 2.2	Digging of Norman Wells Pipeline	21
Figure 2.3	Local buckle of a pipe	22
Figure 2.4	Buckling modes of pipe (Dorey et al., 2001)	23
Figure 2.5	Fracture of a wrinkled pipe under cyclic loading (Das et al., 2002)	24
Figure 2.6	Moment-curvature behaviour of NPS 6 specimens (Youzwishen and Cheng, 2001)	24
Figure 2.7	Failure modes of NPS 6 specimens tested by Youzwishen and Cheng (2001)	25
Figure 2.8	Repair techniques or schemes used by Youzwishen and Cheng (2001)	26
Figure 2.9	Mid-span moment vs. global curvature for NPS 12 tests (Youzwishen and Cheng, 2001)	27
Figure 2.10	Fracture pattern of sleeve for 12-GO-12-M specimen	27
Figure 2.11	"Diamond" secondary buckling of 12-GO-6-M specimen	28
Figure 3.1	Repair techniques or schemes used in this project	43
Figure 3.2	Water is being filled in the specimen in vertical position	44
Figure 3.3	Cross-sectional view of channel sections	45
Figure 3.4	Test setup	46
Figure 3.5	Sketches showing shear and constant moment regions	47
Figure 3.6	Boundary condition used for test specimens	48
Figure 3.7	Rockers were placed between end plates and prestressing bars	49
Figure 3.8	Locations of instrumentation on the specimen	50
Figure 3.9	Cable transducers used to measure deflection of the pipe	50
Figure 3.10	Instrumentations	51
Figure 3.11	Steel collars in pre-wrinkle test	52

Figure 3.12	Marking on the pipe showing geometry of the sleeves in test-3	53
Figure 3.13	Marking on putty for middle sleeves in test-3	53
Figure 3.14	Formwork for removing air voids from epoxy putty	54
Figure 3.15	Strain gauge and demecs on the middle sleeve	54
Figure 4.1	Primary wrinkle	64
Figure 4.2	Location of primary wrinkle and sleeve marking for test-1	65
Figure 4.3	Odd sleeve configuration used in test-1	66
Figure 4.4	Demecs and strain gauge on the middle sleeve in test-1	67
Figure 4.5	Reloading of the specimen for Post-repair test-1	67
Figure 4.6	Moment-curvature behaviour of the specimen in test-1	68
Figure 4.7	Strain in the middle sleeve at wrinkle crest	68
Figure 4.8	Fibre fracture at wrinkle crest in test-1	69
Figure 4.9	Failure mode of the pipe in FEA model for test-1	69
Figure 4.10	Comparison between test and FEA results	70
Figure 4.11	Deflection of the specimen at the end of test-1	70
Figure 4.12	Unsymmetrical odd sleeve geometry used in test-2	71
Figure 4.13	Strain gauges and demecs on the middle sleeve in test-2	71
Figure 4.14	Steel collar was applied on the middle sleeve in test-2	72
Figure 4.15	Moment-curvature behaviour in test-2	72
Figure 4.16	Moment-curvature behaviour at higher pressure in test-2	73
Figure 4.17	Secondary wrinkle in test-2 and FEA	73
Figure 4.18	Deflection of the specimen at the end of test-2	74
Figure 4.19	Sleeve configuration and marking on the specimen for test-3	74
Figure 4.20	Marking on epoxy putty for the middle sleeve in test- 3	75
Figure 4.21	Strain gauges on the specimen and the middle sleeves in test-3	75
Figure 4.22	Secondary wrinkle in test- 3 and FE model	76
Figure 4.23	Moment-curvature behaviour of the specimen in test-3	77
Figure 5.1	FE Model of the pipe	102
Figure 5.2	Boundary conditions	102
Figure 5.3	Single sleeve configuration	103
Figure 5.4	Odd sleeve configuration	103

Figure 5.5	Even sleeve configuration	104
Figure 5.6	The effect of varying sleeve length for single sleeve	105
Figure 5.7	The effect of varying middle sleeve length for odd sleeve configuration	106
Figure 5.8	The effect of varying gap size for odd sleeve configuration	107
Figure 5.9	The effect of wider gaps on odd sleeve configuration	108
Figure 5.10	The effect of varying thickness of odd sleeve configuraion	108
Figure 5.11	The effect of varying length of middle sleeves for even sleeve configuration	109
Figure 5.12	The effect of varying side gap sizes for even sleeve configuration	109
Figure 5.13	The effect of varying side gap sizes for even sleeve configuration	110
Figure 5.14	The effect of varying side gap sizes for even sleeve configuration	110
Figure 5.15	The effect of varying side gap sizes for even sleeve configuration	111
Figure 5.16	The effect of varying side gap sizes for even sleeve configuration	111
Figure 5.17	The effect of side sleeve length for even sleeve configuration	112
Figure 5.18	Inward buckling in a 0.33d single sleeve	112
Figure 5.19	The effect of varying stiffness ratios ($E_s t_s / E_p t_p$) for single sleeve	113
Figure 5.20	The effect of varying stiffness ratios ($E_s t_s / E_p t_p$) for single sleeve	113
Figure 5.21	Failure mode of a 0.50d single sleeve ($\rho = 0.11$)	114
Figure 5.22	Failure mode of a 0.50d single sleeve ($\rho = 0.41$)	114
Figure 5.23	The effect of varying stiffness ratios (ρ) for odd sleeve configuration	115
Figure 5.24	The effect of varying stiffness ratios (ρ) for odd sleeve configuration	115
Figure 5.25	Combined effect of varying gap sizes, middle sleeve length and stiffness ratio for odd sleeve configuration	116
Figure 5.26	Combined effect of varying gap sizes and stiffness ratios for odd sleeve configuration	116
Figure 5.27	The growth of the primary wrinkle for lower stiffness ratios	117
Figure 5.28	Secondary wrinkle outside sleeved region for shorter gap sizes	117
Figure 5.29	The growth of the primary wrinkle	118
Figure 5.30	Secondary wrinkle outside sleeved region	118
Figure 5.31	Secondary wrinkle within sleeved region for longer gap sizes	119
Figure 5.32	Effect of varying stiffness ratios for even sleeve configuration	119

Figure 5.33	Combined effect of varying stiffness ratios and side gap sizes on the secondary moment for even sleeve configuration	120
Figure 5.34	The growth of the primary wrinkle for lower stiffness ratio	120
Figure 5.35	Secondary wrinkle outside sleeved region	121
Figure 5.36	Secondary wrinkle inside sleeved region	121
Figure 5.37	Comparison between even and odd sleeve configurations	122
Figure 5.38	Comparison between even and odd sleeve configurations	122
Figure 5.39	Comparison between double and even sleeve configurations	123
Figure 5.40	Comparison between single and odd sleeve configurations	123
Figure 5.41	Comparison among all sleeve configurations	124
Figure 5.42	Initially double sleeves were applied for a sequential repair	124
Figure 5.43	0.33d side sleeves were applied on the secondary wrinkle	125
Figure 5.44	0.33d sleeves were applied on the tertiary wrinkle	125
Figure 5.45	Moment-curvature behaviour of a sequential repair	126

LIST OF SYMBOLS

A	Cross sectional area of the pipe
d	Outside diameter of the pipe
d_i	Inside diameter of the pipe
DS	Double sleeve configuration
E	Young's modulus of elasticity
E_s	Modulus of elasticity of sleeve in hoop direction
E_p	Modulus of elasticity of steel pipe
E_1	Elastic modulus in the local fibre direction; elastic modulus for the FRP sleeve in the global longitudinal direction
E_2	Elastic modulus transverse to the local fibre direction; elastic modulus for the FRP sleeve in the global hoop direction
Elong.	Elongation
ES	Even sleeve configuration
GS	Side gap size (longitudinal distance between middle and side sleeves)
L_s	Length of shear span
L_{1-2}	Longitudinal distance between rotation meters
L	Pipe length between load points
M_T	Total mid-span moment
MG	Middle gap size (longitudinal distance between middle sleeves)
MS	Length of the middle sleeve(s)
OS	Odd sleeve configuration
P	Total axial load
p	Internal pressure
p_{end}	External pressure applied to end caps in finite element simulation
LC5, LC6	Axial load in prestressing bars
R_E, R_W	East, West side vertical reaction loads in experiments
SS	Single sleeve configuration
SSL	Length of side sleeves
t	wall thickness

t_p	Wall thickness of pipe
t_s	Thickness of sleeve
w_1	Primary wrinkle
w_2	Secondary wrinkle

Greek Symbols

α	Coefficient of thermal expansion
$\Delta_{\%}$	Elongation
ΔX_3	Vertical displacement at mid-length of pipe
Δ_1, Δ_2	Relative longitudinal displacement of load points
Δ_E, Δ_W	Longitudinal displacement of east and west side reactions
ΔT	Temperature differential = $T_{operating} - T_{installation}$
ε_{ult1}	ultimate strain in the local fibre direction
Φ	Global pipe curvature
$\mu\varepsilon$	Micro strain ($1\mu\varepsilon = 1x10^{-6}$ mm/mm)
ν	Poisson's ratio
ρ	Ratio between sleeve to pipe stiffness ($E_s t_s / E_p t_p$)
σ_α	Longitudinal stress due to thermal expansion
σ_h	Hoop stress due to internal pressure
σ_l	Longitudinal stress due to internal pressure
σ_v	Longitudinal stress due to Poisson's effect
σ_{ult}	Ultimate stress
σ_{ult1}	Ultimate stress in the local fibre direction
$\sigma_{ult\ dyn.}$	Dynamic ultimate stress
$\sigma_{ult\ stat.}$	Static ultimate stress
σ_y	Yield stress
$\sigma_{y\ dyn}$	Dynamic yield stress
$\sigma_{y\ stat}$	Static yield stress
θ_1, θ_2	Pipe rotation measured with RVDTs

1. INTRODUCTION

1.1 GENERAL

Steel pipelines are the most economical and efficient mode of transporting oil and natural gas. Canadian transmission pipelines transport 95% of the crude oil and natural gas produced in Canada, which account for almost two-thirds of Canada's total energy supply. Transmission pipelines also provide Canada with access to valuable export markets. They deliver crude oil and natural gas to connecting US pipelines that serve four main US markets in the Northwest, Northeast, Midwest, and West regions.

It is necessary to ensure the integrity of the pipelines since they contain substances that can be hazardous to the surrounding environment. Leakage or outflow of crude oil or gas can impose disastrous damage to infrastructure and the surrounding environment. Leakage can be caused by soil settlement, corrosion, and pipe buckling. Environmental and geological conditions are the major contributors towards abnormal loading on the pipes.

1.2 STATEMENT OF PROBLEM

Buried pipelines are subjected to various load combinations such as fluid pressure, axial loads, and bending moments. When a pipeline passes through discontinuous permafrost in the Canadian north, the soil has the ability to interact with the pipeline through frost heave, slope movement, and thaw settlement, and all these can produce extreme loading in the pipe wall. When the stresses in the pipe wall reach a certain limit, the pipe will deform plastically, and wrinkling (buckling) appears locally in the pipe wall, as shown in **Figure 1.1**. Once a wrinkle appears, it will grow continuously if it is not repaired or replaced. Even though local buckling of the pipe does not cause immediate failure, it is necessary to stop or decrease the wrinkle's rate of growth so that serviceability and integrity of the pipeline is maintained. Typical moment-curvature behaviour of a pipe

under combined internal pressure, axial load, and bending moment is shown in **Figure 1.2**.

1.3 CURRENT METHODS OF REPAIR

The most commonly used method for repairing a locally buckled pipe is to remove the wrinkled section of the pipe and replace it with a thicker new one. This method is very expensive because the pipeline has to be shut down, heavy construction equipment has to be brought on the site, and care has to be taken to prevent the leakage of oil or gas.

Another method of repair is to provide external steel sleeve reinforcement at the wrinkle location to prevent further growth of the wrinkle. Steel sleeve repair was studied numerically by Yoosef-Ghodsi and Murray (1999). The study has shown that steel sleeve stops the growth of the primary wrinkle but another secondary wrinkle develops next to the sleeve because of the rigidity of the steel sleeve. The results show that the secondary wrinkle grows faster than the primary wrinkle, which limits the effectiveness of this repair method. Moment-curvature behaviour of a locally buckled pipe repaired with a single steel sleeve of length "d" is shown in **Figure 1.3** (Youzwishen and Cheng, 2001).

In order to find a more effective repair method, use of Fibre Reinforced Polymer (FRP) composites was studied by Youzwishen and Cheng (2001) as the repair material. It is very economical to repair the buckled pipe with FRP composite sleeves since the sleeves can be applied to the pipe without the help of heavy equipment and without shutting down the pipeline operation. Youzwishen and Cheng (2001) concluded that the thickness and layout of the FRP sleeves and the timing of the repair would alter the behaviour of a repaired pipe. However, no design recommendation was provided for the wrinkled pipes repaired by FRP sleeves.

1.4 OBJECTIVES AND SCOPE

The main objective of this research program is to develop effective, economical, and optimum repair techniques for locally buckled pipes by using FRP sleeves. The effect of

various geometrical and material parameters of FRP sleeves on the behaviour of repaired pipes is also examined.

Both experimental and numerical studies are used in this research program. Three full-scale tests of NPS 12 (12.75 inch in diameter) pipes are conducted. Glass Fibre Reinforced Polymer (GFRP) is used as the rehabilitation material. The finite element program ABAQUS/Standard Version 5.8-1 (Hibbitt, Karlsson, & Sorenson, Inc., HKS, 1999a) is used in the numerical simulation of the test specimens and the parametric study to develop the optimum design of FRP sleeves.

1.5 OVERVIEW OF THESIS

The thesis is divided into six chapters. The first chapter provides a general introduction, statement of problem, and objectives of the project. Chapter 2 consists of previous findings and literature related to the research topic. Chapter 3 contains the experimental program, test setup, instrumentation, and test procedures. Test results and the behaviour of test specimens with different repair techniques are discussed in Chapter 4. Chapter 5 includes Finite Element Analysis (FEA) of the pipe behaviour under varying parameters. Several repair techniques and their effects on the behaviour of the pipe, based on the FEA, are discussed in Chapter 5. Conclusions and recommendations are given in Chapter 6.

Figure 1.1 Local buckling in the pipe wall

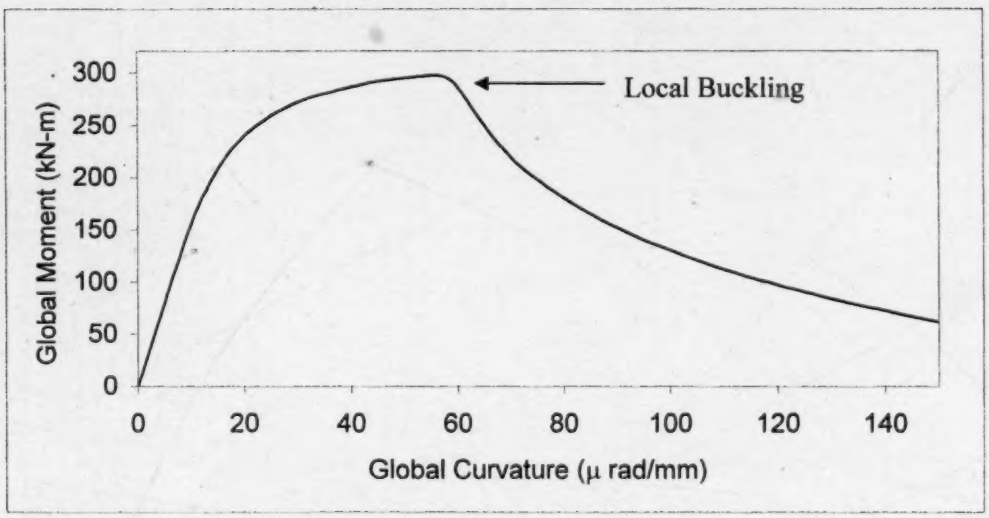

Figure 1.2 Typical moment-curvature behaviour of a locally buckled pipe

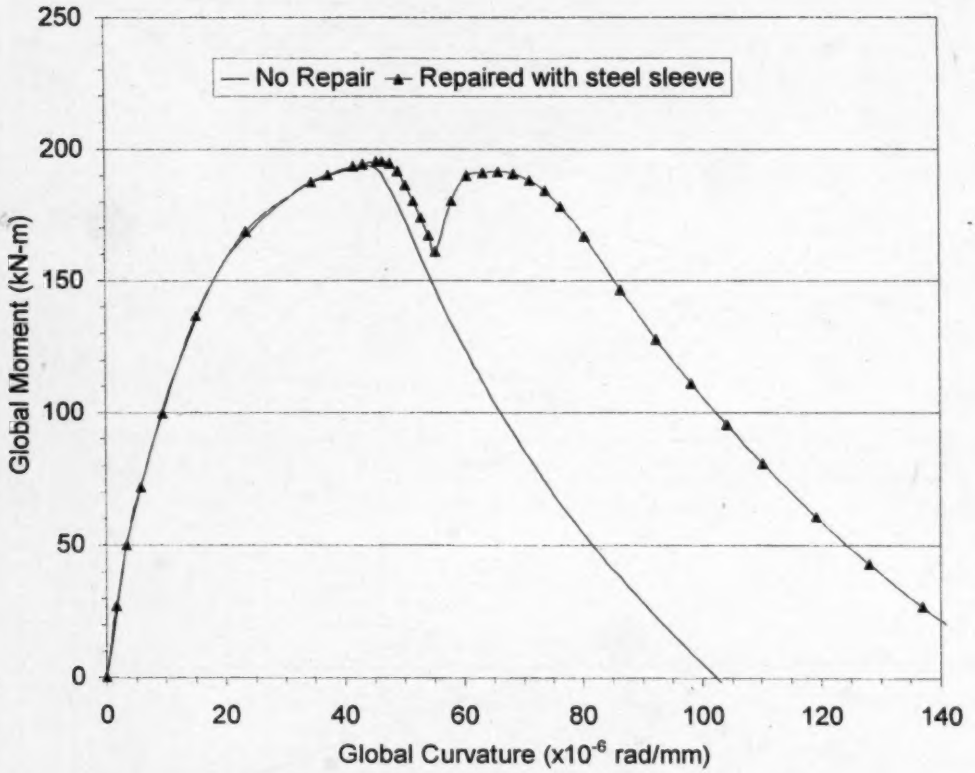

Figure 1.3 Global moment vs. curvature for single steel sleeve repair

2. LITERATURE REVIEW AND PREVIOUS INVESTIGATIONS

2.1 GENERAL

Experimental studies, finite element analyses (FEA) and modelling, and field studies of the local buckling behaviour of line pipes subjected to combined loading have been carried out at the University of Alberta over the last ten years by Mohareb et al. (1994), Souza et al. (1994), Zhou and Murray (1993), Yoosef-Ghodsi and Murray (1994), Dorey et al. (2001), Youzwishen and Cheng (2001) and Das et al. (2002).

In this chapter the main findings and conclusions of previous studies on this subject are discussed, starting with the main causes of local buckling in line pipes buried in permafrost regions. A brief discussion of Norman Wells pipeline is given in section 2.3 as a case study. Behaviour of the wrinkled pipe is discussed in section 2.4. Various rehabilitation methods for a locally buckled pipe are discussed in section 2.5. Finally, results of experiments previously conducted on the subject matter are explained in section 2.6.

2.2 CAUSES OF LOCAL BUCKLING

The pipelines passing through discontinuous permafrost regions are susceptible to differential settlement caused by freeze and thaw effect of the soil. A pipe segment bends as a result of settlement of the soil underneath. The segment of the pipe in thaw-stable regions remains in its original position and a curvature is formed due to discontinuity in the vertical alignment of the pipe. With the increase in settlement, the curvature also increases and so do the stresses in the pipe. The combination of the soil settlement, temperature differential effect, and operational internal pressure can cause high compressive stresses in the pipe wall, eventually leading to local buckling (or wrinkling) of the pipe.

2.2.1 Temperature Differential Effect

In Canada, pipelines are usually installed in the winter season when heavy equipment and machinery have easy access on snow routes. During this season, the ambient temperature on site is around –30°C, and the typical operational temperature of the pipeline in the summer is +15°C. The positive temperature differential (ΔT) of +45°C cause the pipe to expand during operation, but since the pipeline is restrained in the longitudinal direction, compressive stresses are produced in the pipe wall. Theses stresses can be determined by the following expression:

(2.1) $$\sigma_\alpha = -E \cdot \alpha \cdot \Delta T$$

where:

E = Young's modulus of elasticity (MPa)

α = Coefficient of thermal expansion (/°C)

ΔT = Temperature Differential (°C)

Negative sign in Equation (2.1) indicates compressive stresses.

2.2.2 Poisson's Effect

A pipe under internal operational pressure expands in the hoop direction. Consequently, the pipe contracts in the longitudinal direction due to the Poisson's effect. Since the pipe is restrained in the longitudinal direction, longitudinal tensile stresses are developed in the pipe wall. The longitudinal tensile stresses can be calculated by:

(2.2) $$\sigma_v = \nu \sigma_h = \nu \left(\frac{p d_i}{2000\, t}\right)$$

where:

ν = Poisson's Ratio

σ_h= Hoop stress in the pipe (MPa)

p = Internal pressure in the pipe (kPa)

d_i = Inside diameter of the pipe (mm)

t = Wall thickness of the pipe (mm)

2.2.3 Soil Movement and Settlement Effect

Soil movement along a pipe installed on a sloped surface inflict tensile axial forces at the top of the slope where the pipe is pulled and compressive axial loads at the bottom of the slope where the soil is pushing on the pipe. Due to several environmental effects like soil consolidation, frost heave, undulation, inclined movement etc., differential soil settlement occurs along the pipe length. Overall, a pipeline behaves as a beam structure supported continuously by the soil underneath it. When a portion or segment of the soil region settles down, the pipe segment at that location undergoes local deformation in that region, and flexural stresses are then built up in the pipe wall. When the flexural (compressive) stresses reach the ultimate local buckling resistance of the pipe, a wrinkle or buckle appears on the compression side of the pipe, as shown in **Figure 2.1**.

After initiation of buckling, if these loads are applied continuously, very large deformations can occur in the pipe. Failure can either be a serviceability problem or fracture of the pipe wall. In the former case, even though the pipe remains intact, the pipe may no longer perform the function for which it was designed.

2.3 NORMAN WELLS PIPELINE – A CASE STUDY

The Norman Wells pipeline has been in operation since 1985, and it is the first completely buried oil pipeline in Canada's permafrost terrain. The length of the pipeline is 869 km, and its diameter is 323 mm. It is owned and operated by Enbridge Pipelines (NW) Inc. It carries crude oil from Norman Wells, Northwest Territories to Zama, Alberta. It passes through regions of discontinuous permafrost that are susceptible to differential settlement. With the increase in settlement, curvature also increases (**Figure 2.2**) and so do the stresses (Wilkie et al., 2000). Extreme stresses in the pipe wall eventually cause wrinkling in the pipe.

The Norman Wells pipeline is monitored regularly by various instruments and Geopig runs. Geopig is an internal geometry tool, which detects pipe movement associated with slope instability and differential thaw settlement (Wilkie et al., 2000). A wrinkle was found along the Norman Wells pipeline in 1998 (**Figure 2.3**), and instrumentation including strain gauges and extensometers were installed to monitor the development of the wrinkle (Afhami et al., 2000) that same year. The wrinkled portion was cut out and replaced with a thicker pipe in 1999 because of the continuing growth of the wrinkle (Wilkie et al., 2000). A finite element analysis of the wrinkled segment was carried out by Yoosef-Ghodsi et al. (2000); a good agreement was obtained from the study.

2.4 BEHAVIOUR OF WRINKLED PIPES

A pipe subjected to combined axial load, bending moment, and internal pressure can fail in local buckling on the side of the maximum compressive fibre. Typical moment-curvature behaviour of a pipe under combined loading is shown in **Figure 1.2**. As the curvature increases, the moment also increases. After reaching at the peak value, the moment starts decreasing because local buckling occurs in the pipe wall. Due to the softening effect at the wrinkle, a plastic hinge condition is formed at the buckled location and the pipe cannot resist the moment previously achieved. Elastic unloading of the pipe segment occurs away from the wrinkle to maintain equilibrium in the system and if the loading is continued after buckling, very large deformations can occur in the pipe (Zhou and Murray, 1995).

The buckling modes of the pipe can be grouped into two types, i.e. a "bulge" buckle and a "diamond-shape" buckle. When the buckle consists of dips, it is referred to as inward or diamond buckle. When a bulge is developed and the pipe wall in the bulge moves outward then it is referred to as an outward buckle or bulging mode. The type of buckling mode is primarily dependent on the internal pressure. Specimens without internal pressure or with very low internal pressure buckle in diamond mode irrespective of applied axial load. Pipes with higher d/t ratios have a greater tendency to buckle in diamond modes. Specimens with significant internal pressure buckle in bulging modes

(Zhou and Murray, 1995). Typical buckling modes are shown in **Figure 2.4** (Dorey et al., 2001).

Experimental and analytical studies have recently been conducted at the University of Alberta on assessing the risk of fracture of the pipe due to wrinkling. It has been found that the pipe may not fail in fracture when only monotonically increasing compressive axial strain is applied. If the pipe is subjected to cycles of loading and unloading, fracture due to low cycle fatigue can occur in the wrinkled region (**Figure 2.5**). It has been found that strain reversal at the wrinkle location will produce fracture after only a few cycles of loading and unloading of axial load and/or bending under internal pressure (Das et al., 2002).

2.5 REHABILITATION METHODS FOR WRINKLED PIPES

When wrinkling appears in the pipe, a plastic hinge condition is formed at the location of the wrinkle. This will cause the pipe to deform further with little flexural resistance. If growth of the wrinkle is not stopped or slowed down, eventually, the pipe will no longer be serviceable or may even fracture under cyclic loading. Even though wrinkle or local buckling may not cause immediate failure to the pipe, it is necessary to repair the pipe to keep it serviceable in the long run.

When the pipe is buckled locally, it can be repaired either by replacing the buckled portion with a new pipe section or by applying external sleeve(s) at the wrinkled location. The mode of failure is very important for external sleeve repair since effective repair is possible only if an outward wrinkle or bulging buckle appears in the pipe wall. When a pipe fails in a diamond or inward buckle, there is no possibility to repair it with external sleeve(s).

2.5.1 Rehabilitation by Replacing the Wrinkled Section of the Pipe

One common method to rectify the local buckling problem is to replace the affected portion of the wrinkled pipe with a thicker one. However this can be a very expensive method because the line has to be shutdown and supply has to be stopped. Moreover heavy equipment may be needed on the site and oil or gas in the pipe that may cause damage to the surrounding environment has to be removed.

2.5.2 Rehabilitation by External Steel Sleeve

Another method of repair is to provide external steel sleeve reinforcement at the wrinkle location to prevent its further growth. Steel sleeve repair was studied numerically by Yoosef-Ghodsi and Murray (1999). Analysis was divided into two stages. In the first stage a plain pipe model was developed and subjected to simulated field conditions and loadings. Loading was applied on the model until wrinkling appeared in the pipe wall. In the second stage the response of the wrinkled model was analyzed on the basis of different remedial actions. Three types of analyses were conducted: no-sleeve, short sleeved, and long sleeved models. In the case of no-sleeve model, the original (initial) wrinkle grows further and no new wrinkles appear. In the cases of sleeved models, even though the initial wrinkle stopped from growing further due to rigidity of the sleeve, new wrinkles appeared adjacent to the sleeve. The size of new wrinkles in the sleeved models exceeded the size of the initial wrinkle when bending is provided to the model. This denotes the limited effectiveness of the single steel sleeve. The results show that in the long run the wrinkles grow to the same extent in both sleeved and non-sleeved models grow almost the same amount in wrinkles. Also there is no difference in the behaviour of the pipe when long or short steel sleeves are used.

2.5.3 Rehabilitation by FRP Sleeves

Analytical and experimental studies on using FRP composites as the rehabilitation material started at the University of Alberta in 2000. The behaviour of the repaired pipe was studied by applying external FRP sleeves. It was observed that the behaviour of a repaired pipe depended largely on the methods, techniques or configurations in which sleeves were applied. It also depended on geometrical and material properties (length, thickness, stiffness, gap etc.) of the sleeves. The concept of providing multiple sleeves rather than one single sleeve was also developed. Multiple sleeves are divided into two main configurations i.e. odd (three) and even (two or four) sleeve configurations. More sleeve configurations are discussed in details in section 5.3.

2.5.3.1 FRP Composites

A composite is a structural material consisting of two or more constituents. The constituents are combined in such a way that they keep their individual physical states and are not soluble in each other nor do they form a new chemical compound. One constituent is called the reinforcing phase and the one in which it is embedded is called the matrix (Kaw A.K., 1997).

Fibre reinforced polymer (FRP) composites usually consist of high performance fibres as reinforcing phases and polymers as matrices. The fibres have very high stiffness and strength. FRP materials have been used in different fields including structural applications. Research is being conducted on using FRP materials with concrete, masonry, steel and other structural materials to enhance the performance of structural members and systems.

Composite materials possess two major advantages over other materials. Firstly, they possess higher parameters of specific modulus and specific strength. Specific modulus is defined as the ratio between Young's modulus (E) and the density of material. Specific strength is defined as the ratio between the strength and density of material. Secondly,

composite materials possess high corrosion resistance, high impact resistance and high wear resistance (Kaw A.K., 1997).

The major fibres in use today are glass, carbon and aramid. Glass fibre is low cost, high strength, has high chemical resistance and good insulating properties. Glass fibre is more corrosion resistant than carbon fibre that is why it is more attractive for pipeline repair in highly corrosive environments. Carbon fibre has very high specific stiffness, specific ultimate strength and high fatigue strength. Aramid fibre has low density, high tensile strength and high impact resistance. Its compressive strength is very low and therefore it is not recommended for structural applications involving high compressive loads. Also it degrades under sunlight.

Most FRP material properties can be custom-designed and therefore it is an ideal material for repair. Unlike the traditional method of replacing the wrinkled pipe with a new pipe section, FRP sleeve repair does not need the shutdown of supply. Unlike steel sleeves, FRP sleeve repair does not need welding and therefore heavy machinery and equipment are not required at the site. FRP sleeve design or configuration can easily be made on site and geometrical and material properties of the design can be changed easily and economically. FRP sleeve repair is economical, efficient, fast and easy method of repairing the locally buckled pipeline.

2.5.3.2 Sleeve Geometry

Numerical studies by Yoosef-Ghodsi and Murray (1999) showed that the use of a single steel sleeve has little impact on the behaviour of the wrinkled pipe. Unlike single steel sleeves, both experimental and analytical studies by Youzwishen and Cheng (2001) have shown that geometrical properties of FRP composite sleeves have significant influence on the behaviour of a wrinkled pipe. In post buckling behaviour of the repaired pipe, the ductility is of significant importance. If the growth rate of the initial (referred to as primary) wrinkle is slowed down, the moment capacity and the ductility of the pipe can be improved. By adjusting certain parameters of the sleeves, the wrinkle growth rate can

be slowed down. The ability of sleeves to control the wrinkle growth rate determines their effectiveness.

Three sleeve configurations, single, odd (three) and even (two or four) sleeves, were studied by Youzwishen and Cheng (2001). Odd and even sleeve repairs provide a much larger range of pipe behaviour compared to single sleeve repairs. The post-repair behaviour of the pipe can significantly be varied by varying sleeve design parameters for odd and even sleeves. Most of design parameters of the single sleeve do not significantly alter the post-buckling behaviour of the pipe.

The odd sleeve design places a large amount of sleeve material over the top of the wrinkle, making it more difficult to slow the wrinkle growth to a level showing larger improvements in moment capacity at high values of curvature. In the case of an even sleeve design, material is provided to the edges of the wrinkle, which enables it to manipulate the growth rate of the wrinkle. In other words odd sleeves stop the wrinkle while even sleeve allows it to grow at a slower rate (Youzwishen and Cheng, 2001).

Other geometrical parameters like gap size between the sleeves and length of the sleeves also affect the behaviour of the repaired pipe. Timing of the sleeve repair is also an important factor. If repair is made sooner, the repaired pipe exhibits more favourable post buckling behaviour. But in the field, timing of the repair likely cannot be controlled since inspection is usually made once a year and a wrinkle can appear at any time between two consecutive inspections.

2.6 PREVIOUS EXPERIMENTAL RESULTS

Four half-scale and two full-scale tests were conducted previously by Youzwishen and Cheng (2001). NPS 6 pipe specimens were used for half-scale tests whereas NPS 12 pipe specimens were used for full-scale tests. All pipe specimens were plain. The test procedure consisted of two phases, i.e. pre-wrinkle testing and post repair testing. In the pre-wrinkle test, a plain pipe was loaded to produce local buckling in the specimen. A four-point bending system was used. When wrinkling appeared in the pipe wall, the

loading was removed and the pipe was repaired with FRP sleeves. In the post repair phase, the repaired pipe was loaded to study the behaviour after rehabilitation. The test procedure and set-up are detailed in chapter 3.

2.6.1 Half-Scale Test Results

The specimens for half-scale tests had a diameter of 167.95 mm, a wall thickness of 3.22 mm, length of approximately 3054 mm and a d/t ratio of 52.2. The steel used for the pipe was API-5L X52 grade, with a specified minimum yield strength (SMYS) of 52 ksi or 359 MPa and a nominal tensile strength of 413 MPa. Material properties of NPS 6 specimens, determined from tension coupon tests by Youzwishen and Cheng (2001) are listed in Table 2-1.

The first NPS 6 specimen (6-NS) was not repaired and it served as a bench mark for the repaired specimens. The second (6-CO-9-M) and third (6-CE-18-E) specimens were repaired with uni-axial carbon fibre (CFRP) sleeves and the fourth specimen (6-GE-10-L) was repaired with glass fibre (GFRP) sleeves. Material properties of the test matrix is given in Table 2-2 and material properties for carbon and glass fibres are given in Tables 2-3 and 2-4.

Moment-curvature behaviour of all test specimens is shown in **Figure 2.6**. It can be observed that as the curvature is increased, a maximum moment is reached. When a local buckle appears in the pipe, a rapid drop in moment capacity is observed.

In the first test, it was difficult to maintain axial load due to the large axial deformation of the pipe after buckling and the softening effect of the wrinkle. After a curvature of 120 μ rad/mm axial load was not maintained and curvature was increased through vertical displacement at the load points only. The behaviour of the specimen seems to be un-realistic between curvatures of approximately 120 and 140 μ rad/mm.

The Second specimen was repaired with three sleeves (referred to as odd sleeve configuration) after local buckling appeared in the pipe. The third and fourth specimens were repaired with four sleeves (even sleeve configuration). In all three repair tests, the post-buckling moment capacity of the pipe increases after it is repaired with FRP sleeves. Moment capacity reaches a maximum value and then drops down, due to the fracture of the middle sleeve.

From **Figure 2.6**, it can be observed that the timing of repair is an important factor. The sooner the pipe is repaired the higher is its post buckling capacity. When we compare 6-CO-9-M and 6-CE-18-E, it appears that even sleeve design provides more ductility than odd sleeve design. The rate of drop in moment capacity after fibre fracture is less in the even sleeve configuration than in the odd sleeve configuration. We can also notice that GFRP provides very good ductility to the pipe. Failure modes of the NPS 6 specimens are shown in **Figure 2.7.**

2.6.2 Full-Scale Test Results

Full-scale test specimens were 4070 mm long, had a diameter of 323.9 mm, a wall thickness of 6.33 mm and a d/t ratio of 52. All pipes were X60, with a nominal yield strength of 414 MPa. However from pipe material coupons tested by Youzwishen and Cheng (2001), the average static yield strength was 520 MPa, the ultimate tensile strength was 550 MPa, and the average modulus of elasticity (E) of coupons was 192,128 MPa. A test matrix is given in Table 2-5 and material properties of NPS 12 specimens, determined from coupon tests are listed in Table 2-6.

In two full-scale tests, three glass fibre reinforced polymer (GFRP) sleeves were applied on the pipe. Sleeve repair techniques that were used in those two tests are shown in **Figure 2.8**.

Spacing between two adjacent sleeves (referred to as gap size) was 0.25d in both the tests where "d" is the pipe diameter. In the first test, length of all the sleeves was 0.50d. In the

second test, the length of the middle sleeve was increased to 1.0d and that of the side sleeves was decreased to 0.33d. Sleeve to pipe stiffness ($E_s.t_s$ / $E_p.t_p$) ratios of 0.11 and 0.13 were used in test-1 and test-2 respectively. In the first test, one sleeve was composed of a glass fibre section over the wrinkle (middle sleeve) and two carbon fibre sections away from the wrinkle (side sleeves). Originally, a sleeve system consisting entirely of glass fibre was planned, but due to material shortages, there was only enough glass fibre to cover the critical section over the wrinkle.

Moment-curvature behaviours for NPS 12 specimens are shown in **Figure 2.9**. The trends of the curves prior to local buckling and prior to repair are similar to those given in **Figure 2.6** for the NPS 6 pipe tests since the d/t ratios of both types of specimens were similar. When the post-repair behaviour of the NPS 12 specimens is examined, we see also a similar trend to the NPS 6 tests. Post buckling capacity of the specimens increase following the application of FRP sleeves and then drop after reaching the maximum values. The first specimen (12-GO-6-M) failed in the middle sleeve due to fibre fracture as shown in **Figure 2.10**. Fibre fracture indicates that the growth of the primary wrinkle was not stopped. The middle sleeve was not stiff enough to resist strains generated by the growth of the primary wrinkle. The second specimen (12-GO-12-M) failed due to an inward buckle as shown in **Figure 2.11**.

The sleeve fracture problem was observed in the most experiments conducted by Youzwishen and Cheng (2001). It was found that the method in which the sleeve is applied to the pipe has a major impact on the integrity of the sleeve. Timing of the application of sleeves is also a major factor for sleeve fracture. There is a lesser chance of sleeve fracture when it is applied earlier since less strain occurs in the sleeve prior to the appearance of a secondary wrinkle. If a sleeve repair is applied too late, fracture of the sleeve becomes more likely. By increasing the global stiffness of the sleeve, strain in the fibres can be reduced and fracture possibility avoided.

Table 2-1 - Material Properties of NPS 6 Pipe (Youzwishen and Cheng, 2001)

Specimen	t (mm)	$\sigma_{y\ stat.}$ (MPa)	$\sigma_{y\ dyn.}$ (MPa)	$\sigma_{ult\ stat.}$ (MPa)	$\sigma_{ult\ dyn.}$ (MPa)	E (MPa)	Elong. (%)
1	3.220	413	428	463	488	188883	26.5
2	3.220	410	424	468	493	195018	30.2
3	3.229	417	434	483	508	196571	32.9
Average	3.223	413	429	471	496	193491	29.9
Std. Dev.	0.005	4	5	10	10	4065	3.2
Co. Var. (%)	0.2	0.9	1.2	2.2	2.1	2.1	10.6

Table 2-2 - Test Matrix for NPS 6 Pipe Specimens (Youzwishen and Cheng, 2001)

Specimen No.	Specimen ID	Sleeve Material	Sleeve Configuration	Main Sleeve Length(s) (mm)	Sleeve Thickness (mm)	Repair Timing
1	6-NS	none (control)	-	-	-	-
2	6-CO-9-M	Uniaxial Carbon	odd	150	0.99	moderate
3	6-CE-18-E	Uniaxial Carbon	even	75	1.98	early
4	6-GE-10-L	FTS-GE-30 Glass	even	75	3.00	late

Table 2-3 - Material Properties of Carbon Fibre

(Youzwishen and Cheng, 2001)

Specimen	t (mm) [1]	E_1 (MPa)	$\sigma_{ult\ 1}$ (MPa)	$\varepsilon_{ult\ 1}$ (%)
C-1	0.110	229207	3443	1.38
C-2	0.110	197338	3249	1.60
C-3	0.110	233653	3728	1.56
C-4	0.110	233864	3802	1.56
C-5	0.110	232073	3392	1.50
Average	0.110	225227	3523	1.52
Std. Dev.	0.000	15701	234	0.09
Co. Var. (%)	0.0	7.0	6.6	5.6

[1] Manufacturer's specified thickness for one layer of fibre sheet

Table 2-4 - Material Properties of FTS-GE-30 Glass Fibre

(Youzwishen and Cheng, 2001)

Specimen	t (mm) [1]	E_1 (MPa)	$\sigma_{ult\ 1}$ (MPa)	$\varepsilon_{ult\ 1}$ (%)
G1-1	0.149	74049	1060	1.54
G1-2	0.149	69642	883	1.69
G1-3	0.149	70857	1029	1.66
G1-4	0.149	81469	1077	1.35
G1-5	0.149	80550	1235	1.61
Average	0.149	75313	1057	1.57
Std. Dev.	0.000	5453	125	0.13
Co. Var. (%)	0.0	7.2	11.9	8.5

[1] Manufacturer's specified thickness for one layer of fibre sheet

Table 2-5 - Test Matrix for NPS 12 Pipe Test Specimens

(Youzwishen and Cheng, 2001)

Test No.	Specimen ID	Sleeve Material	Sleeve Configuration	Main Sleeve Length(s) (mm)	Sleeve Thickness (mm)	Repair Timing
1	12-GO-12-M	FTS-GE-30 Glass	Odd	150	3.60	moderate
2	12-GO-6-M	MBrace EG 900 Glass	Odd	300	4.40	moderate

Table 2-6 - Material Properties of NPS 12 Pipe

(Youzwishen and Cheng, 2001)

Specimen	t (mm)	$\sigma_{y\ stat.}$ (MPa)	$\sigma_{y\ dyn.}$ (MPa)	$\sigma_{ult\ stat.}$ (MPa)	$\sigma_{ult\ dyn.}$ (MPa)	E (MPa)	Elong. (%)
12-1	6.276	497	507	537	569	195071	27.3
12-2	6.311	525	547	555	583	196493	24.8
12-3	6.417	537	564	559	587	188678	22.4
12-4	6.438	525	539	532.000	563	197736	27.1
12-5*	6.498	547	561	553.000	584	188585	7.2
12-6*	6.473	541	561	544.000	580	190853	5.8
12-7*	6.426	527	543	534.000	567	191218	7.1
12-8*	6.379	486	505	526.000	556	188393	14.3
Average	6.402	523	541	543	574	192128	25.4
Std. Dev.	0.077	21	23	12	11	3780	2.3
Co. Var. (%)	1.2	4.1	4.3	2.2	2.0	2.0	9.1

* Specimens 12-5 to 12-8 fractured outside gauge marks and therefore were not included in the calculation of the elongation average and standard deviation.

Figure 2.1 Local buckling in Norman Wells Pipeline

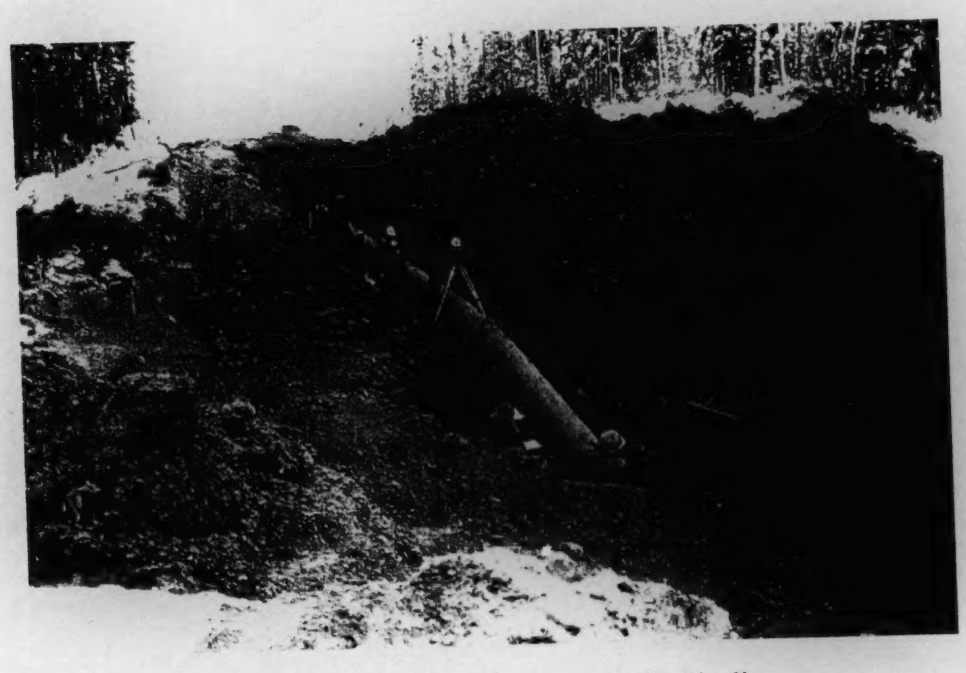

Figure 2.2 Digging of Norman Wells Pipeline

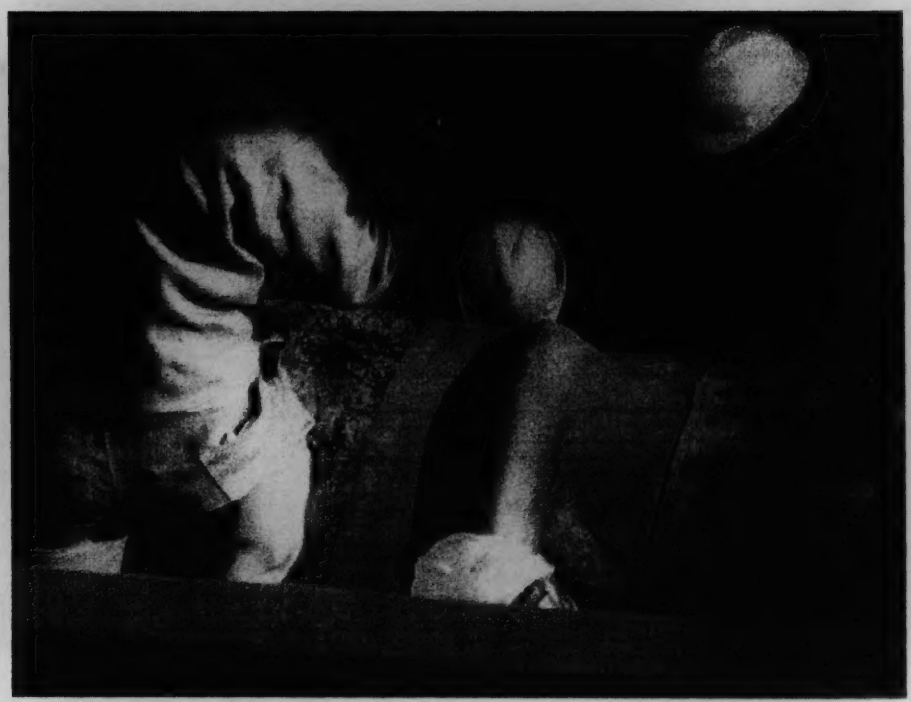

Figure 2.3 Local buckle of a pipe

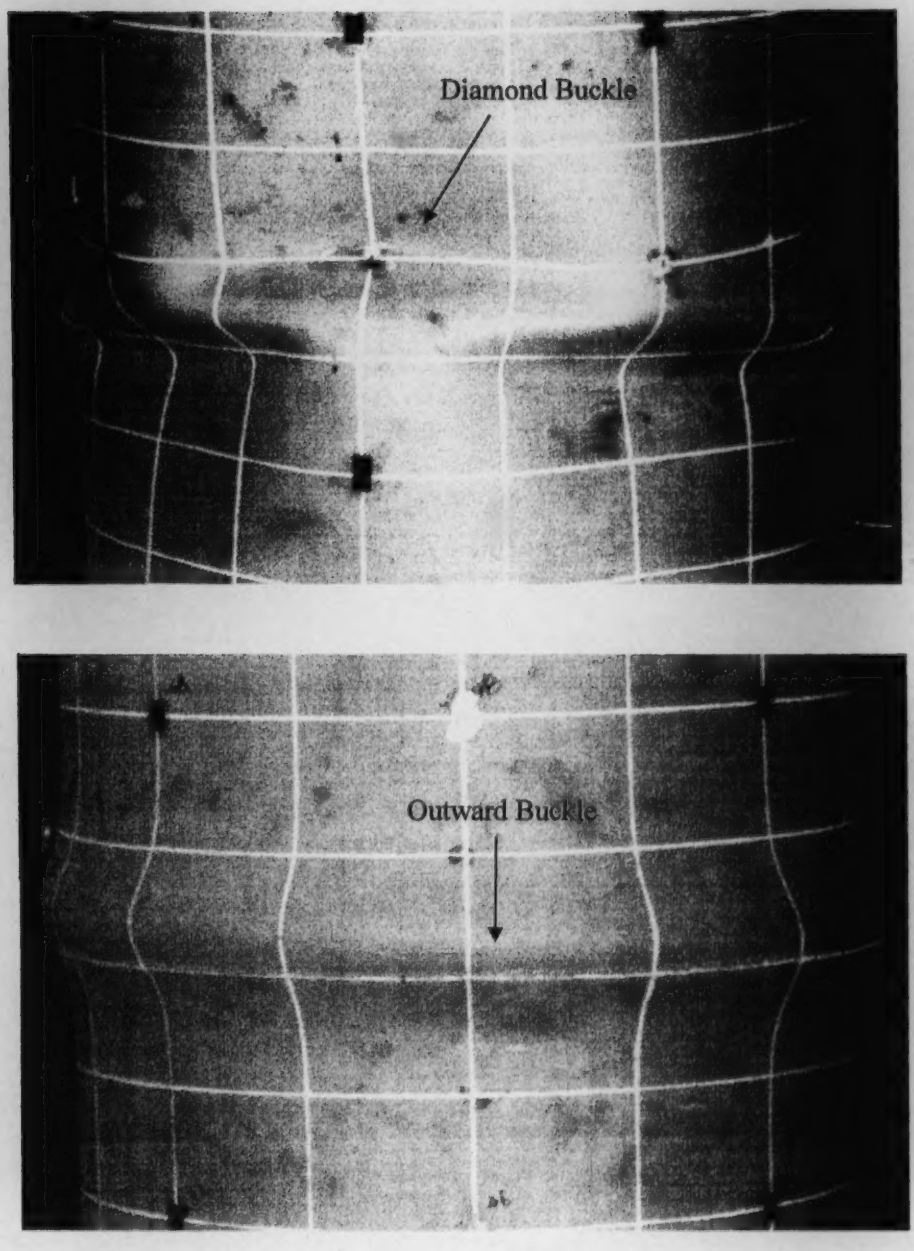

Figure 2.4 Buckling modes of pipe (Dorey et al., 2001)

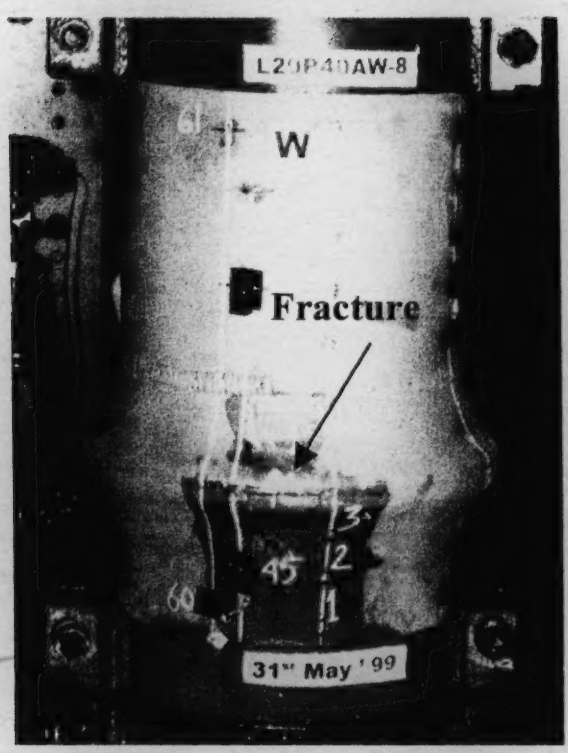

Figure 2.5 Fracture of a wrinkled pipe under cyclic loading (Das et al., 2002)

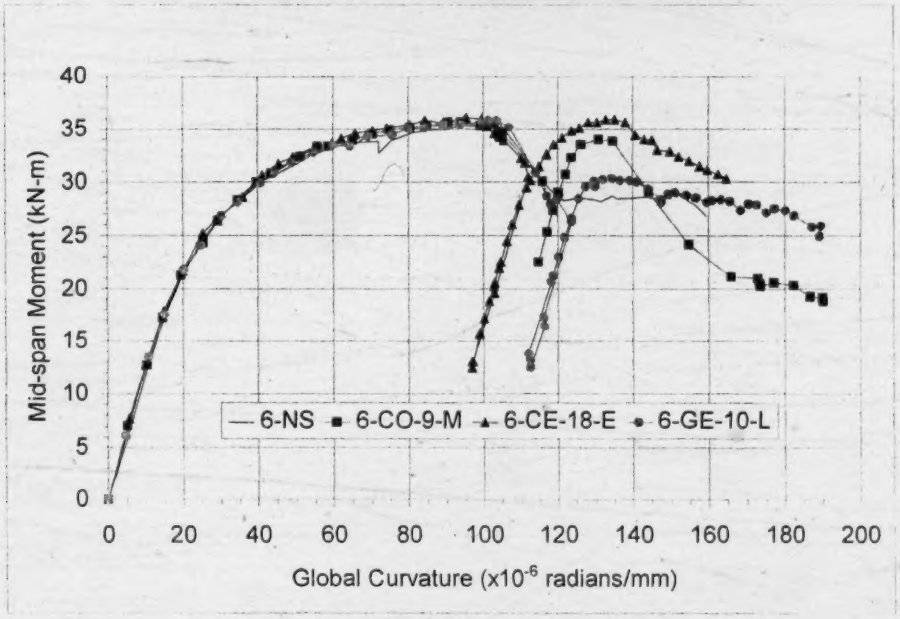

Figure 2.6 Moment-curvature behaviour of NPS 6 specimens (Youzwishen and Cheng, 2001)

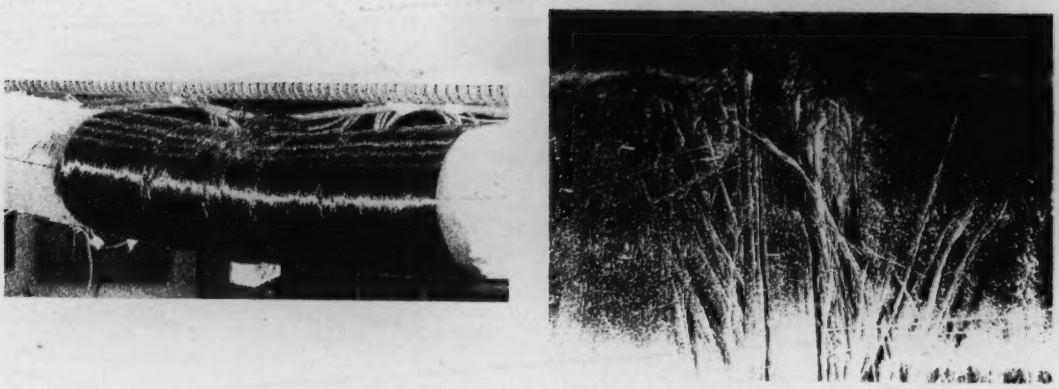

Test-2 (6-CO-9-M)

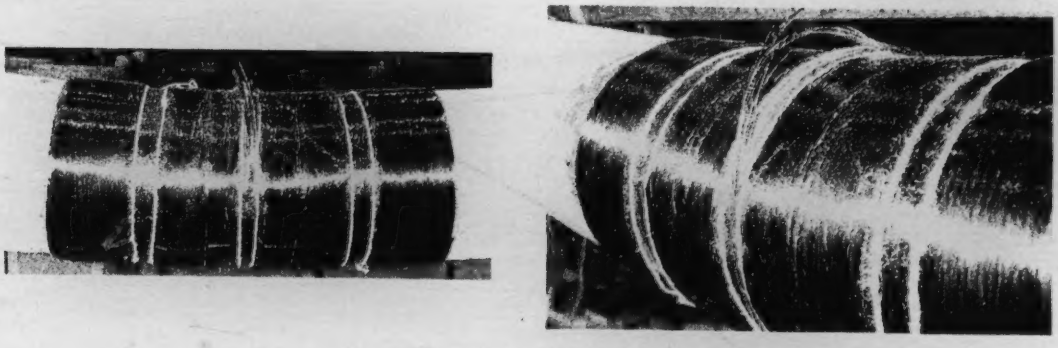

Test-3 (6-CE-18-E)

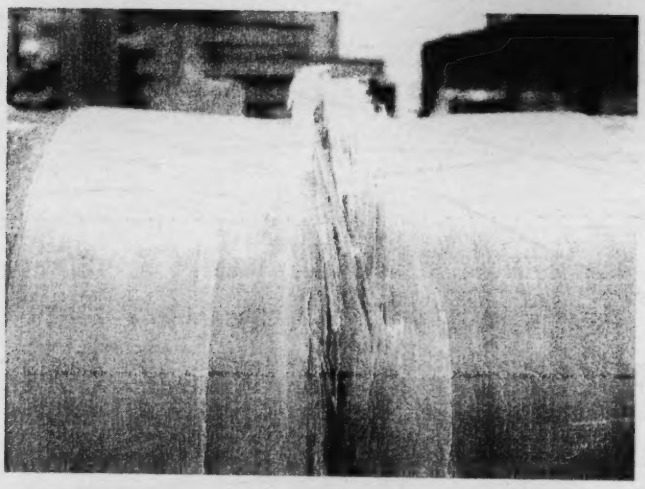

Test-4 (6-GE-10-L)

Figure 2.7 Failure modes of NPS 6 specimens tested by Youzwishen and Cheng (2001)

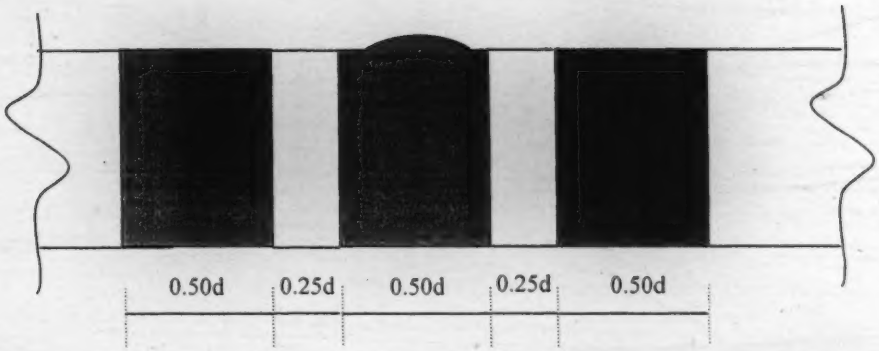

Test-1 (12-GO-12-M)

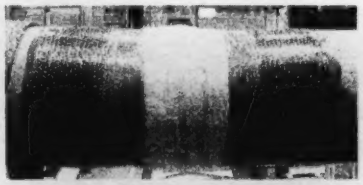

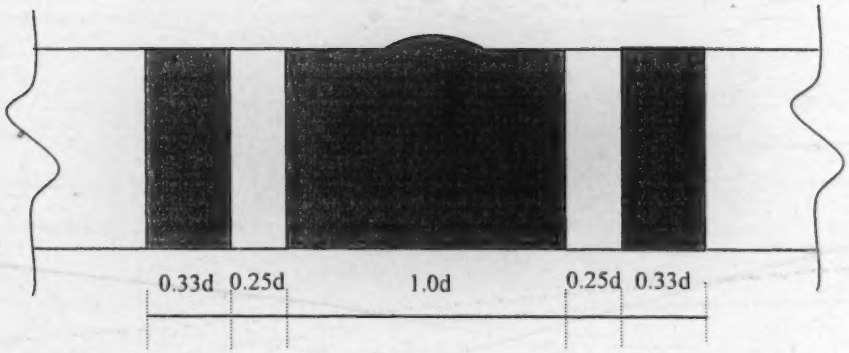

Test-2 (12-GO-6-M)

Figure 2.8 Repair techniques or schemes used by Youzwishen and Cheng (2001)

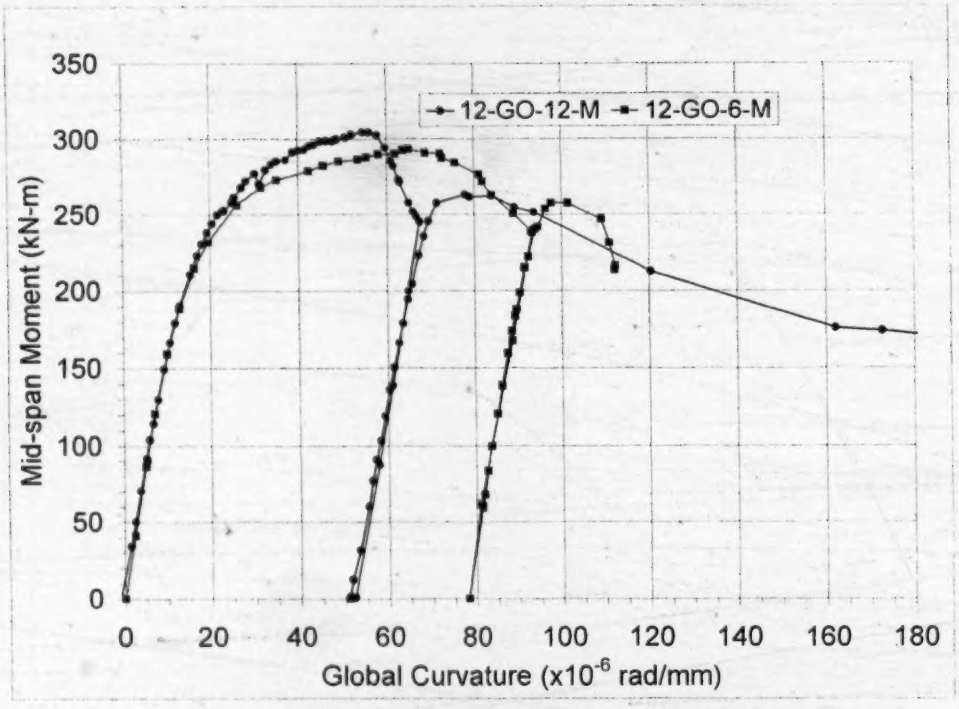

Figure 2.9 Mid-span moment vs. global curvature for NPS 12 tests (Youzwishen and Cheng, 2001)

Figure 2.10 Fracture pattern of sleeve for 12-GO-12-M specimen

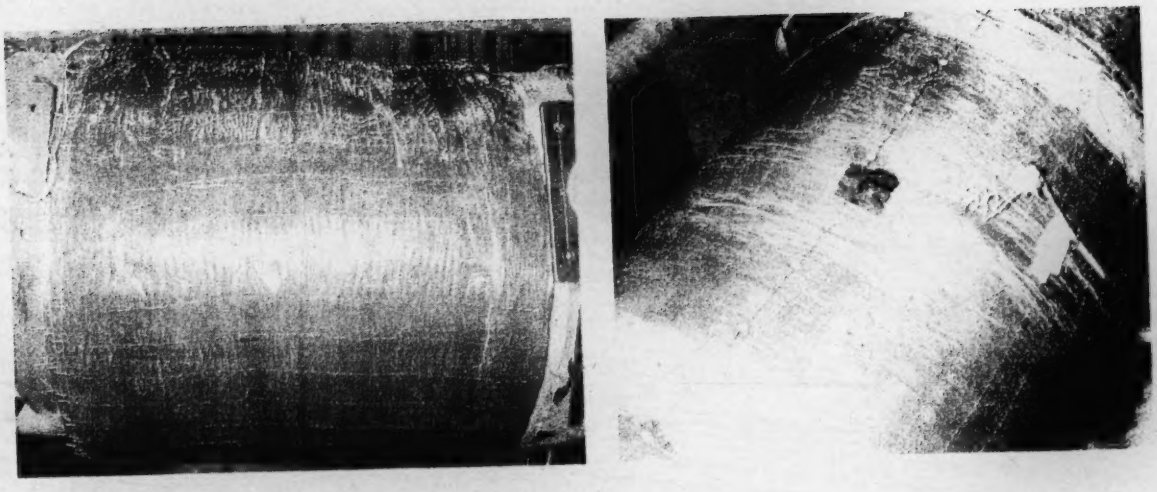

Figure 2.11 "Diamond" secondary buckling of 12-GO-6-M specimen

3. EXPERIMENTAL PROGRAM

3.1 EXPERIMENTAL OBJECTIVES AND TEST PARAMETERS

Four half-scale tests on NPS 6 pipe and two full-scale tests on NPS 12 pipe specimens were conducted previously by Youzwishen and Cheng (2001). Test results are discussed in section 2.6. During previous tests, most of the repaired pipe specimens failed either because of fibre fracture or inward buckling. Fibre fracture occurred because of continuous growth of the primary (initial) wrinkle and the inability of the middle sleeve to stop it. When the pipe fails in inward buckling, it is not possible to repair it again by external sleeves. Both these modes of failure are deemed undesirable.

The main goal of the experimental program in this research is to obtain more laboratory results observing the behaviour of wrinkled pipes repaired with FRP sleeve(s), which can, then, be compared to the analytical results and thus achieve a design configuration to overcome fibre fracture and inward buckling problems.

Three experiments were conducted on NPS 12 pipe specimens in this research program. Pipes were taken from the same batch used by Youzwishen and Cheng (2001). The specimens were tested under the same loading conditions and the setup used by Youzwishen and Cheng (2001). However, repair techniques or schemes (sleeve configurations) and the timing of repair were different from those used by Youzwishen. The MBrace EG900 E-glass reinforcement system was used for sleeve design. This type of glass fibre reinforced polymer (GFRP) contains uniaxial glass fibre sheets. Sleeves were made by placing fibre sheets in various layers. Design thickness of each layer was 0.353 mm. Typical physical properties of the system provided by the manufacturer are given in **Table 3.1**.

In two full-scale tests conducted by Youzwishen and Cheng (2001), three glass fibre reinforced polymer (GFRP) sleeves were used over the buckled region. Sketches for repair techniques used in those two tests have already been shown in **Figure 2.8**.

The repair techniques used in this project were different from the previous schemes in terms of gap size, sleeve length, and stiffness ratio. Sketches for repair schemes used in the experimental program of this project are shown in **Figure 3.1**. The repair techniques or schemes for each test will be discussed further in section 3.5.3.

3.2 TEST SPECIMENS AND PREPARATIONS

Three tests were conducted in this project. Test specimens were approximately 4070 mm long with an outside diameter of 323.9 mm and a wall thickness of 6.33 mm. This results in a depth to thickness ratio of approximately 52 for the specimen. All pipes were X60, with a nominal yield strength of 414 MPa. However from pipe material coupons tested by Youzwishen and Cheng (2001), the average static yield strength was 523 MPa, the ultimate tensile strength was 550 MPa, and the average modulus of elasticity (E) of coupons was 192,128 MPa. Since the same batch of pipe specimens is used in this project, no further coupon tests have been conducted to get material properties.

Preparation of the specimen begins with marking to facilitate welding of end plates, proper placement of instrumentation, load points, and reactions. Marking was done firstly by dividing the specimen transversely into four equal 90-degree segments. Secondly, longitudinal marking was done with the help of marking thread. All points on the pipe were accurately marked for strain gauges, rotation meters, load straps, cable transducers, and reactions. The centreline of the pipe along the length was also marked so that proper location of instruments and alignment of end plates could be obtained.

The end plates were then welded to the pipe. The function of the end plates was to transfer the axial load to the pipe and to contain the water in order to apply internal pressure. The welding setup was made along a steel column fixed in a vertical position.

The specimen was aligned and centred properly on the end plates with the help of a plumb and welded perpendicularly to the plates. One of the end plates is shown in **Figure 3.2**. Before welding, one hole was drilled in each of the end plates for water intake.

The next step was filling up the specimen with water. To avoid any air void in the specimen, it was filled in a vertical position as shown in **Figure 3.2**. An inlet valve and hose were attached to the hole at the bottom of the pipe, while the top hole served as a vent. After filling up the pipe completely with water, the valve at the bottom end plate was closed, and the vent hole at the top end plate was plugged.

The last step was to install strain gauges. The pipe surface was smoothed and cleaned before installing the strain gauges. The details of strain gauge location will be presented in section 3.4.

3.3 TEST SETUP AND BOUNDARY CONDITIONS

3.3.1 Test Frame

Experiments were conducted in the I.F. Morrison Structural Laboratory at the University of Alberta. The test setup consisted of two heavy channel sections as shown in **Figure 3.3**. The channel sections were placed back to back, with a gap of 50 mm between them, and held to the strong floor via a stub beam at each end of the sections. The channels were approximately 860 mm above the strong floor of the laboratory so that sufficient space could be provided to jacks to apply point loads. The gap between two channel sections was also provided to accommodate the loading rods, cable transducers, and other instrumentation. The clear spacing between specimen and channel sections was 559 mm to provide enough spacing to steel collars and load straps connected with point load jacks. The test setup is shown in **Figure 3.4**. The point loads were located 1200 mm from the centreline of the reactions, thereby producing a constant moment region of 1370 mm, as shown in **Figure 3.5**. The length to diameter (L/d) ratio for the constant curvature section was 4.23 and shear span to diameter ratio was 3.71.

3.3.2 Boundary Conditions

A pin-roller boundary condition was used for the specimen. The end reactions consisted of a knife-edge assembly mounted on top of steel rollers as shown in **Figure 3.6**. The rollers were then mounted on a smooth, steel bearing pad. The knife-edge simulated the pin connection and allowed in-plane rotation of the specimen. It also allowed the pipe ends to move longitudinally. Concrete saddles were placed between the specimen and the knife-edge assembly to provide sufficient bearing area between the specimen and the reaction plates.

Flexible Nylon straps were used to apply the point load. The flexibility of the straps and their friction connection to the transfer beam allowed the pipe to rotate and translate at the load points without constraint.

Axial load was applied by means of two external prestressing rods (Dywidag bars). The cross sectional area of each rod was 806 mm^2 with an ultimate strength of 890 kN. The rods were anchored to end plates through square-shaped anchor plates and prestressing nuts. Prestressing rods tend to remain straight since they are in tension while the pipe ends tend to rotate when curvature is applied to the pipe specimen. To avoid serious deformation in the plates and rods due to their opposite movement, rockers were placed between the end plates and the rod anchorage, as shown in **Figure 3.7**. The prestressing rods remained straight by means of rockers while the end plates rotated with the specimen.

3.4 INSTRUMENTATION

Electronic measuring devices such as strain gauges, load cells, rotation meters, linear variable displacement transformers (LVDTs), cable transducers, and pressure transducers were used.

3.4.1 Strain Gauges

A total of 11 strain gauges were used to measure local strain in the pipe at different locations. The strain gauges were indicated by S1 through S11. The locations of strain gauges are shown in **Figure 3.8**. During the test, strain gauges helped in predicting the location of the primary wrinkle. Local strain in the pipe at or near the primary wrinkle increased significantly. Strain gauges S1 and S2 were placed at the mid-height of the pipe along the mid-length of the shear span. S1 was orientated in the hoop direction to measure strain due to internal pressure, and S2 was orientated longitudinally to measure the strain due to axial load at the beginning of the test. Strain gauges S3 through S11 were placed longitudinally in the constant moment region and symmetric about the centreline at a distance of 242.5 mm centre to centre. Five strain gauges, i.e. S3, S5, S7, S9 and S11, were placed at the compression face while four others, i.e. S4, S6, S8 and S10, were placed on the tension face of the specimen.

3.4.2 Cable Transducers

Five cable transducers were used to measure vertical deflection of the pipe in the constant moment region. Cable transducers were indicated by X1 through X5 as shown in **Figures 3.9** and **3.10**. X3 was placed at mid-length of the specimen. The purpose of providing X1 and X5 was to measure deflection at load straps, but it was not possible to place transducers X1 and X5 directly under load points because load cells did not concede any space. However deflection at load points was measured by a rigid lever arm. A wire from the transducer on the floor was connected to the tip of the lever. Another wire was then used to connect the pipe to the lever at the load point. Then by using similar triangles, displacement at load points was calculated. Transducers X2 and X4 were placed at 335 mm on each side of X3.

A pressure transducer was used to measure the internal pressure in the pipe. It was placed at the outlet of the water pump that was used to pressurize the pipe, as shown in **Figure**

3.10. For hydraulic pressure, a pneumatically controlled pump system was used to control the jack stroke.

3.4.3 Load Cells

Six load cells were used to measure the applied loads during the test. They were indicated by LC1 through LC6 as shown in **Figure 3.11**. Two load cells LC1 and LC2 were placed on east and west side reactions respectively to measure the applied load. Two load cells LC3 and LC4 were placed to measure point loads applied through Nylon straps. Two load cells LC5 and LC6, as shown in **Figure 3.10**, were placed on the prestressing rods to measure the axial load.

3.4.4 Rotation Meters

Two rotation meters indicated by R1 and R2 were used to measure the in-plane rotation of the pipe. Both R1 and R2 were placed directly under load points (nylon straps) by means of a steel angle section as shown in **Figure 3.10**. A nut was welded on the pipe and the angle section was then bolted to the nut. Global curvature of the pipe was calculated by measuring the rotations and the gauge length between the two meters.

3.4.5 LVDTs

Three LVDTs indicated by L1 to L3 in **Figures 3.5** and **3.8** were used to measure longitudinal displacements. During the four-point bending test, as loads are applied, the reaction points tend to move outwards and the load points move inwards. Shear span is varied as a result of this movement, which must be known to calculate the applied moment. L1 and L2 were attached to east and west side reactions respectively to measure longitudinal outward movement of the reactions (**Figure 3.10**), where as L3 was placed on load straps to measure inward moment of the load straps. L3 was mounted on a frame made up of two wood pieces connected by a steel bar and resting on pointed screws as

shown in **Figure 3.11**. The screws provided a friction connection to prevent slippage of the wooden frame.

3.5 TEST PROCEDURE

When the specimen was ready to move into the test setup, the reaction rollers were locked to prevent any movement of the rollers. Water added plaster of paris was applied on concrete saddles so that the specimen could not slip. The specimen was placed on the test frame with the help of a 10-ton crane.

The specimen was ready for testing when all the instrumentation had been placed.

3.5.1 General Test Procedure

Three types of loads were applied to the specimen. First, internal pressure was applied to the specimen and then axial load was applied. Both internal pressure and axial loads were kept constant throughout the test. Flexural bending was applied by two point loads, placed at equal distances from the supports and the centerline of the specimen, as shown in **Figure 3.5**.

3.5.1.1 *Internal Pressure*

An internal pressure of 3.3 MPa (479 psi) was applied to the specimens. This was based on actual pressure in the Normal Wells pipeline. It is corresponding to 20% of SMYS (specified minimum yield strength) in the hoop direction. A hydraulic pump was used to apply the internal pressure. The pressure was kept constant throughout the test procedure.

3.5.1.2 *Axial Load*

The total axial load applied to the specimen was kept at 710 kN, which corresponded to 17% of specified yield strength in the pipe wall. Axial load was applied to the pipe through end plates by using two Dywidag bars (prestressing rods). Two holes had already

been drilled in the end plates at the mid-height of the pipe, symmetric about the vertical plane of the pipe. The bars were passed through the holes and prestressed by hydraulic jacks. This set-up eliminated out-of-plane action. Each Dywidag bar applied 355 kN of axial load on the end plates of the specimens. Load cells were put on eastern ends of the bars to measure axial load. The bars were anchored to the plate by means of prestressing nuts and anchor plates. Load jacks were put on western ends of the bars and were fixed with the help of nuts and anchor plates. The jacks were set to bear against the end plate. Prestressing bars were placed into tension when the jacks were extended. Reaction to tension in the bars resulted in compression in the pipe.

3.5.1.3 *Flexural Bending*

A four-point bending test was used to provide bending or curvature to the pipe. Two equal point loads, 1370 mm apart from each other, were applied at a distance of 1200 mm from the centre of each reaction, as shown in **Figures 3.5** and **3.8**. The loads were applied using hydraulic jacks that worked vertically to the pipe. This resulted in a region of zero shear and constant moment between two load points. The constant moment region also provided a region of constant curvature, which allowed the study of moment-curvature behaviour of the specimens.

Stocky HSS sections were used as transfer beams. A high-strength alloyed steel threaded rod and bolt was used to connect hydraulic jacks with the transfer beams that were holed at the centre line. Nylon loading straps were used to transfer loads to the pipe from HSS beams connected to the jacks. This minimises the local effects of loading. The load jacks were placed against two heavy channel sections used as load frame beams. Loads from the jacks were transferred by means of Nylon straps into tension when the jacks were extended.

3.5.2 Pre-Wrinkle Test Procedure

Steel collars as shown in **Figure 3.10**, were placed on the specimen at a clear spacing of approximately 50 mm from each other so that the primary wrinkle could appear near the mid-length of the pipe. The collars were not snugged at this point. Dywidag bars and load cells were placed. Then instrumentation such as strain gauges, LVDTs, cable transducers, and hydraulic lines were connected. Bolts around the reaction load cells were backed off so that the applied load would be carried by load cells. Reaction rollers were unfastened to allow free movement of the reaction points during the tests. A zero reading was taken.

When all setting and instrumentation were completed, loading of the specimen started with internal pressure. A total pressure of 3.3 MPa (479 psi) was applied. After applying the internal pressure, steel collars were snugged. Snugging the steel collars after applying internal pressure, eliminated any possibility of imperfection, which might have been created if the collars were snugged earlier. A reading was taken after applying the internal pressure.

A total axial load of 710 kN was applied with each prestressing rod having 355 kN. A third reading was taken after applying axial load. Both internal pressure and axial load were kept constant during the test.

Point loads were applied by increasing the stroke of the jacks. The test progressed by increasing jack stroke, i.e. it was a stroke controlled test. Readings were taken after every 1 mm of jack stroke. The stroke of the jack was increased until applied load appeared to be decreasing. A primary wrinkle was observed when strain in the pipe wall increased significantly at or near the wrinkle location and load appeared to drop.

When the wrinkle reached a height of approximately 6 to 8 mm, the pipe was unloaded so that a repair could be made. The unloading was done in the reversed order. After removing point loads, axial load was removed and then internal pressure was removed.

Steel collars, prestressing bars, load cells, jack loads and other instrumentation were removed so that FRP sleeves could be applied to the wrinkled specimen.

3.5.3 Post-wrinkle Repair of Specimens

As mentioned above, all the instrumentation, prestressing rods, and load cells were removed from the specimen since they might obstruct the sleeve application. The sleeve area was cleaned and marked as shown in **Figure 3.12**.

Sleeves were placed in three steps. Firstly, a thin layer of primer epoxy was applied around the wrinkled region on the pipe. Epoxy was allowed to become tacky for 15-30 minutes. This layer served as a base layer and made for easier placement of the sleeve. Epoxy also provided a good bond between the pipe and the sleeves.

In the second step, as shown in **Figure 3.13**, epoxy putty was placed around the wrinkle to provide a smooth surface along the wrinkle wave-length. To avoid air gaps in the putty, a formwork was made as shown in **Figure 3.14**. The formwork was applied and screwed tight on freshly applied putty. The putty was allowed to cure for 24-hours before sleeves were applied.

The third step was the placement of FRP sleeves. FRP strips were cut into the required length and width. Resin was applied on FRP strips which were wrapped onto the specimen with the fibres orientated in the hoop direction to the pipe. One coating of resin was applied between each layer of fibre. A final coating was applied on the last layer of the FRP as a protective layer. The sleeves were allowed to cure for 7-days.

In the following subsections, sleeve configurations used for each test will be described briefly before discussing the post-repair test procedure.

3.5.3.1 *Test No.1*

Three sleeves, each consisting of 7-layers of FRP sheet, were made. This is referred to as an odd sleeve geometry or configuration. One sleeve referred to as the main or middle sleeve was placed directly on the primary wrinkle and two sleeves referred to as the side sleeves were placed on both sides at an equal distance from the middle sleeve. The lengths of the middle and side sleeves were 0.50d and 0.33d, respectively. A symmetrical gap size of 0.25d was provided between the middle and side sleeves.

3.5.3.2 *Test No.2*

Three FRP sleeves, each consisting of 10-layers of FRP sheet, were applied similar to those used in Test No.1, but a different sleeve configuration was used. The length of the middle sleeve was 0.42d. Unsymmetrical side sleeves were used in this test. One side sleeve was 0.33d long and the other one was 0.42d long. A symmetrical gap size of 0.42d was provided between the middle and side sleeves.

3.5.3.3 *Test No.3*

Four FRP sleeves, each consisting of 11-layers of FRP sheet, were made. This is referred to as an even sleeve configuration. In the case of even sleeve configuration, two middle sleeves are placed with a gap between them referred to as a middle gap. The lengths of the middle sleeves were 0.25d and the middle gap was 0.08d. Two symmetrical side sleeves, 0.33d long were used. A gap size of 0.125d was provided between the middle and side sleeves.

3.5.4 Post-repair Test Procedure

After 7-day's curing of sleeves, the pipe was ready to be retested. The same test setup and boundary conditions were used as were already discussed in section 3.3 and the same instrumentation was applied as was mentioned in section 3.4, except for the strain gauges.

No additional strain gauge was applied on the pipe this time. Instead, strain gauges were applied to the sleeves.

In the first test, one strain gauge was applied in the centre of the middle sleeve along the hoop direction to monitor strain in the sleeve during the test. 50 mm demecs were also applied on the middle sleeve both in longitudinal and hoop directions of the middle sleeve to monitor strain in the sleeve and to verify readings from the strain gauge. The demecs and strain gauge are shown in **Figure 3.15.** In the second test, six strain gauges were placed on the middle sleeve. In the third test, two strain gauges were placed on each middle sleeve, and one was placed in the middle gap.

The prestressing bars and instrumentation were then re-connected to the pipe. The same procedure of loading was followed as discussed in the pre-wrinkle test procedure in section 3.5.2, but unlike the pre-wrinkle test, no steel collar was placed in the post-repair test. The first test was ended when fibre in the middle sleeve fractured followed by the ultimate strain value of the fibre being reached. A decrease in point loads and global moment was also observed after reaching their maximum values. The second test was ended when the jack stroke was exhausted. The third test was ended when a secondary wrinkle appeared followed by a drop in point loads and moment. The result of each test is discussed in the next chapter.

3.5.5 Problems and Difficulties during Tests

A complete and thorough monitoring of all instruments was required during testing so that any instrumentation failure could be detected immediately. Cable transducer wires and spot welds were very delicate and prone to break. It was also necessary to keep an eye on the readings of rotation meters because sometimes they stopped functioning properly and needed to be changed or to be fixed. At higher point loads, it was difficult to maintain the axial load. It was necessary to keep an eye on internal pressure so that it may not increase or decrease during the test. LVDTs are very sensitive and may sometimes

produce misleading results due to friction. Cutting of FRP sheet into desired strip sizes was also an arduous task.

Table 3-1

Typical Physical Properties of Mbrace EG 900 Fibre

Fibre Modulus	10.5 msi	~72,413 MPa
Design Thickness	0.0139 in.	0.353 mm
Ultimate tensile elongation	2.0 %	2.0%
Design Tensile Modulus	10.5 msi	~72,413 MPa
Design Strength	220 ksi	~1517 MPa
Ultimate Strength	251 ksi	~1730 MPa
Fibre Density	0.093 lb/in.^{3}	~2.55x10^{-5} N/mm^3
Sheet Width	19.7 in.	500 mm

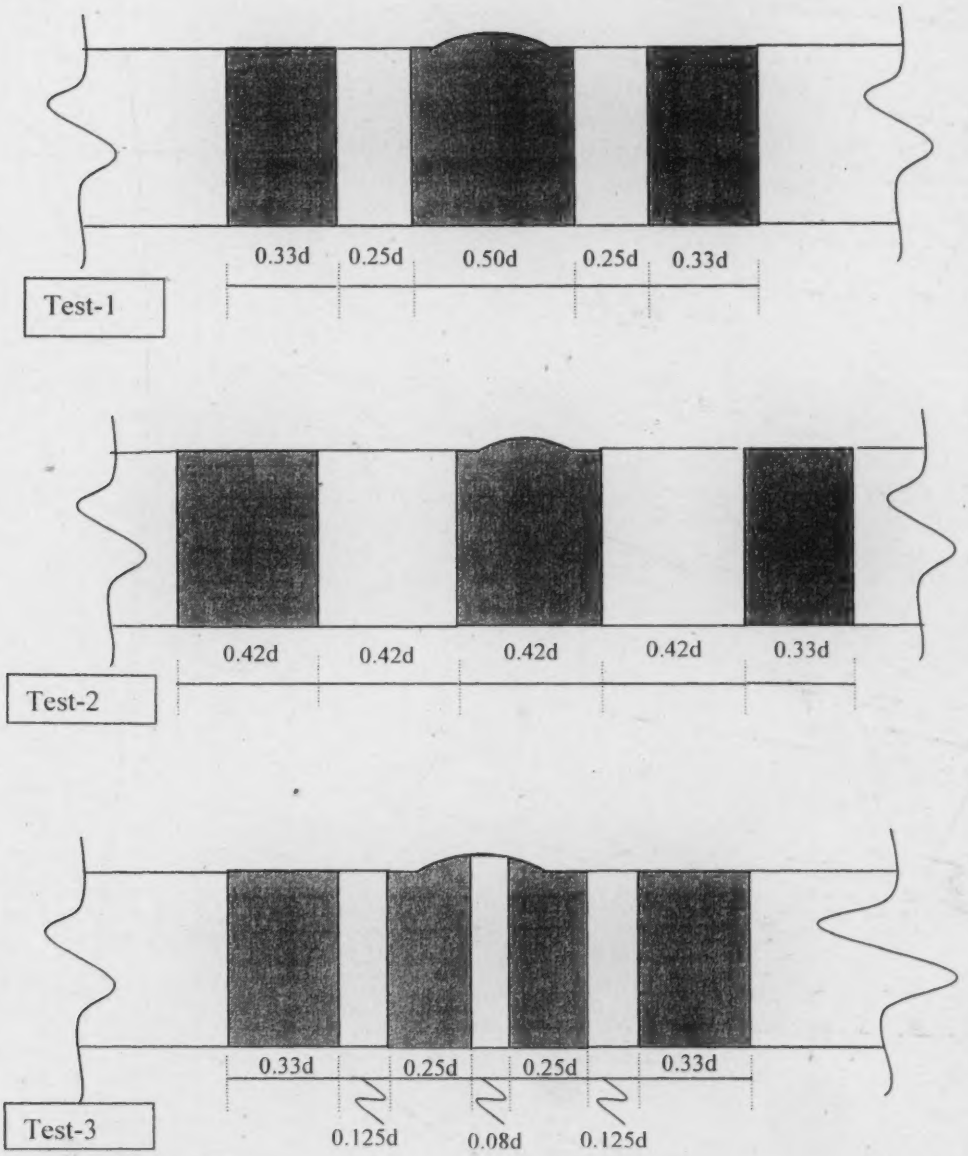

Figure 3.1 Repair techniques or schemes used in this project

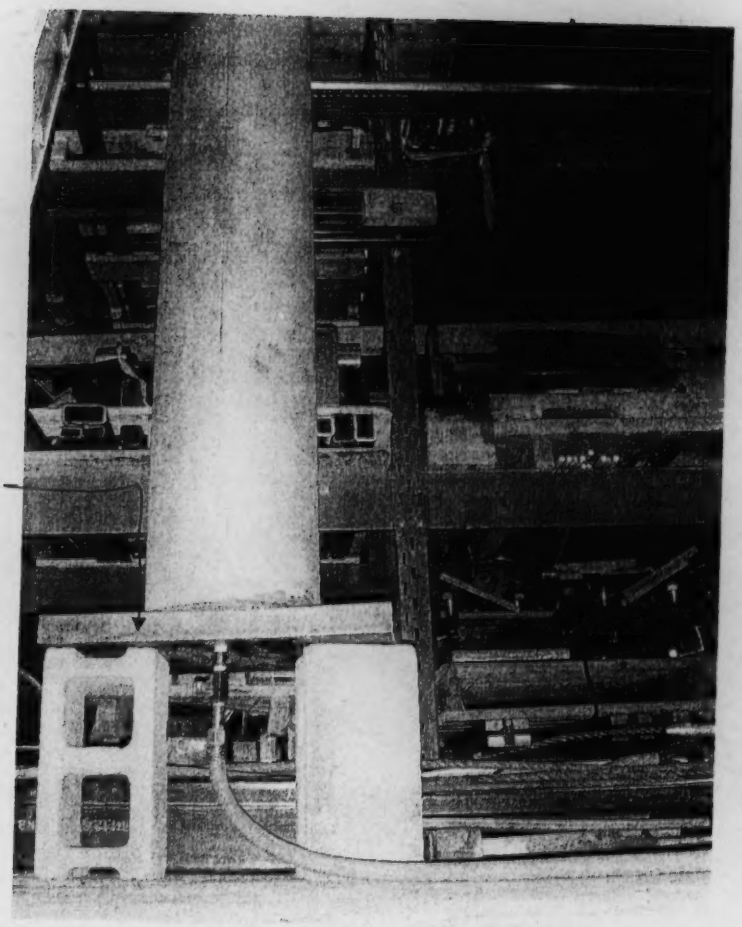

Figure 3.2 Water is being filled in the specimen in vertical position

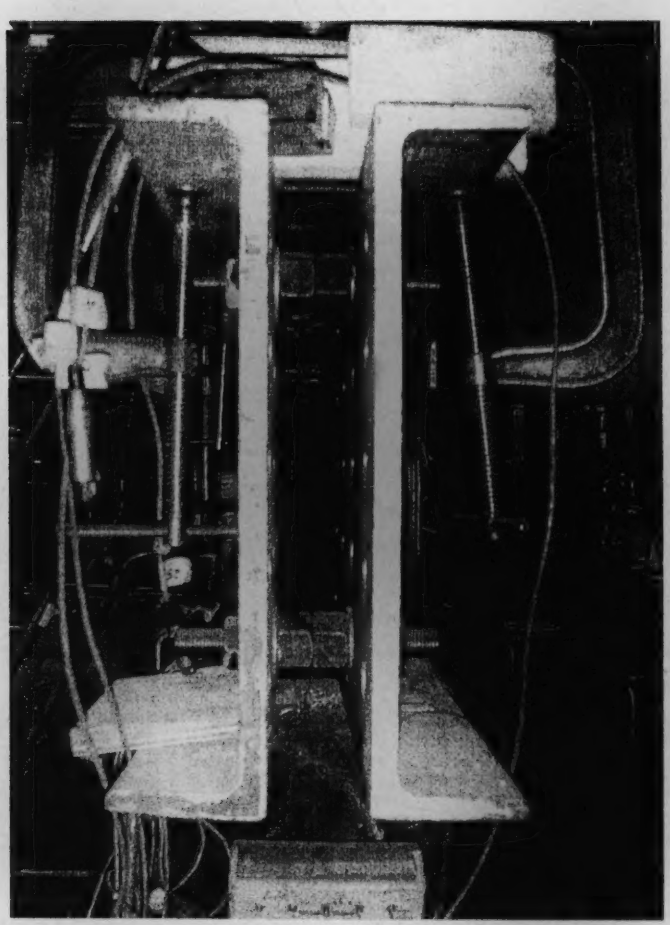

Figure 3.3 Cross-sectional view of channel sections

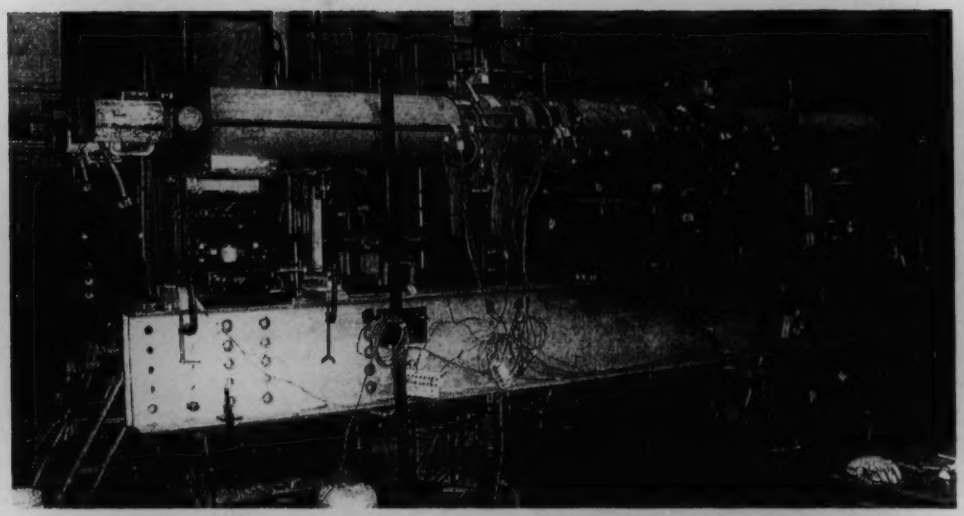

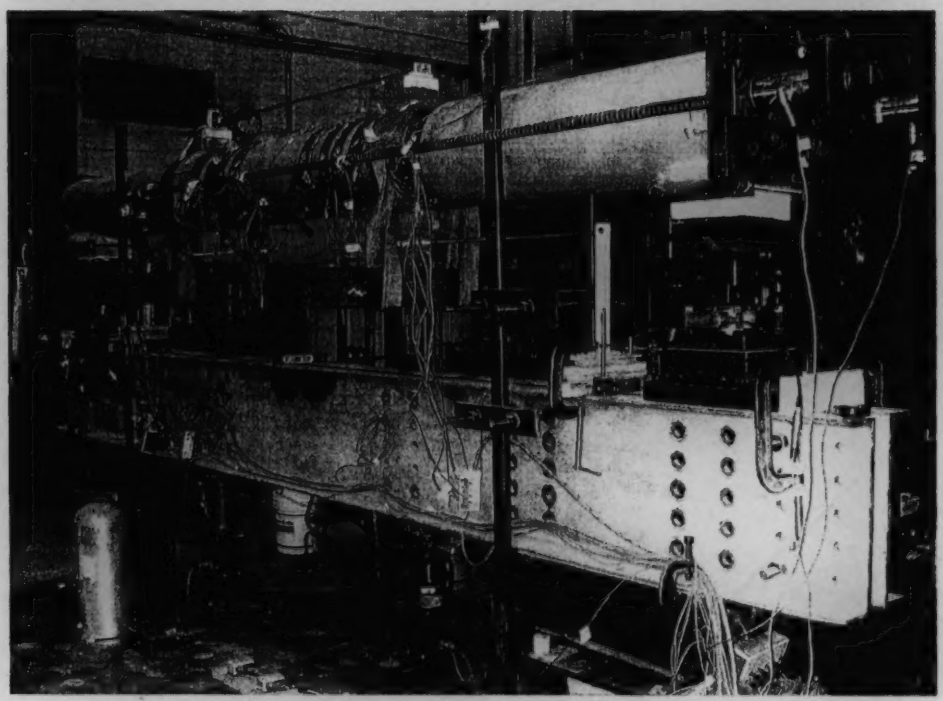

Figure 3.4 Test setup

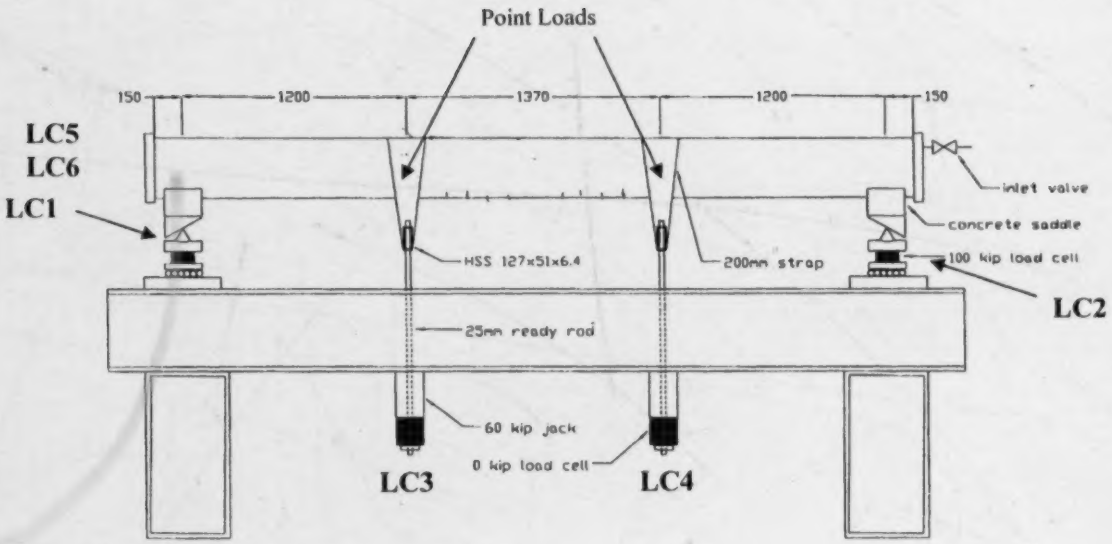

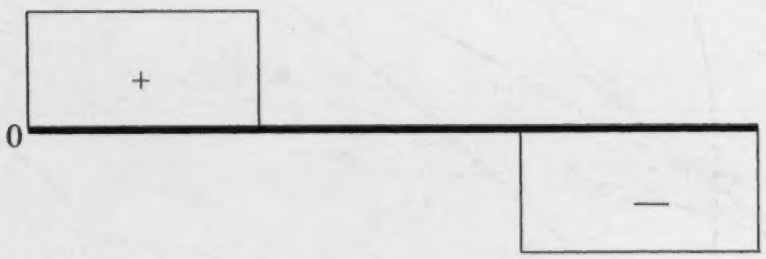

Shear Force Diagram

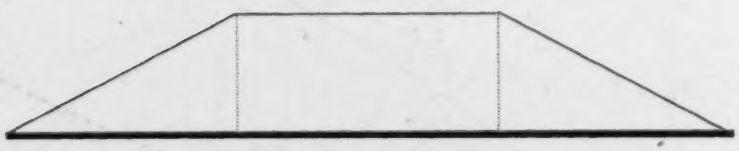

Bending Moment Diagram

Figure 3.5 Sketches showing shear and constant moment regions

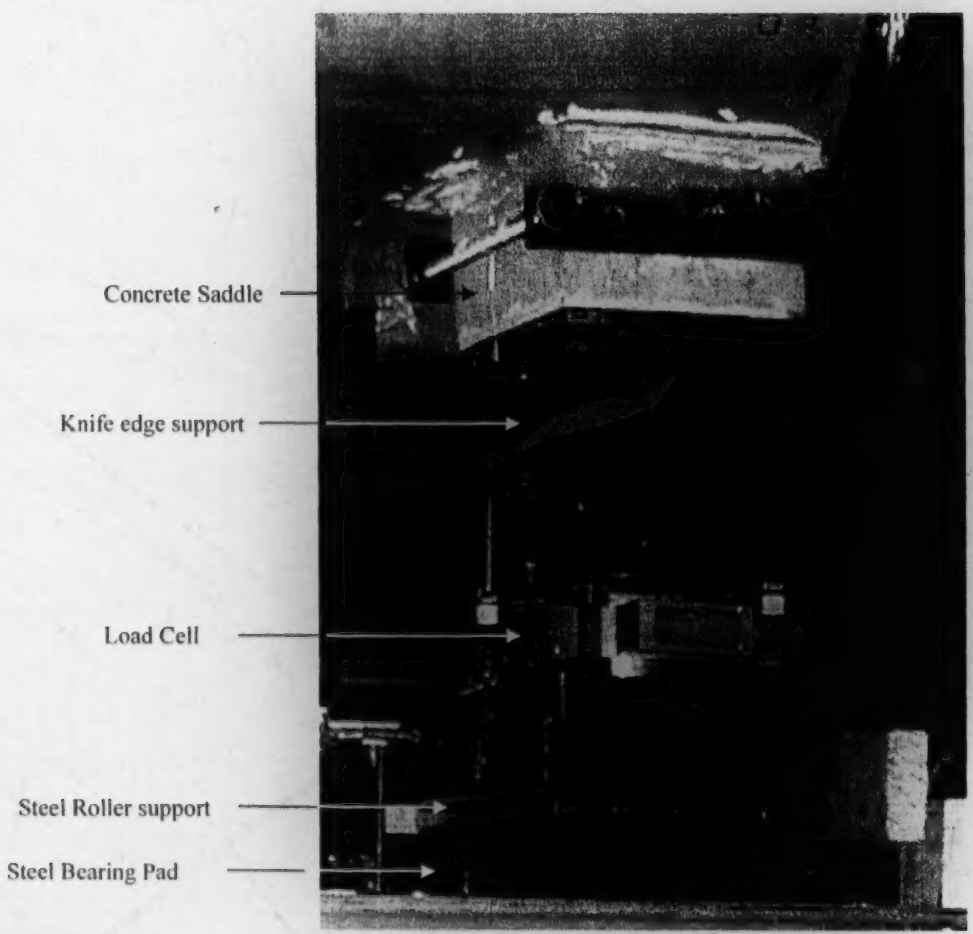

Figure 3.6 Boundary condition used for test specimens

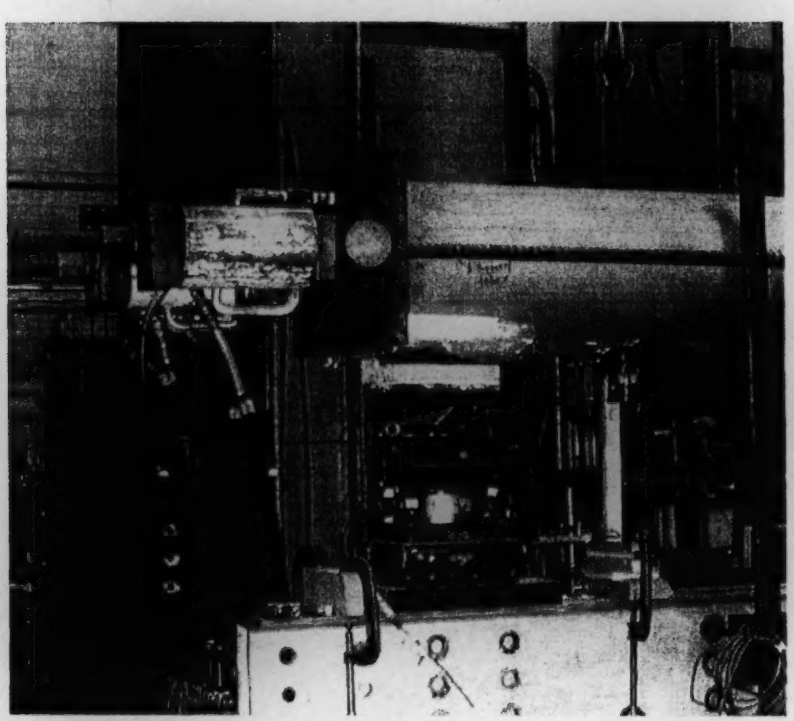

Figure 3.7 Rockers were placed between end plates and prestressing bars

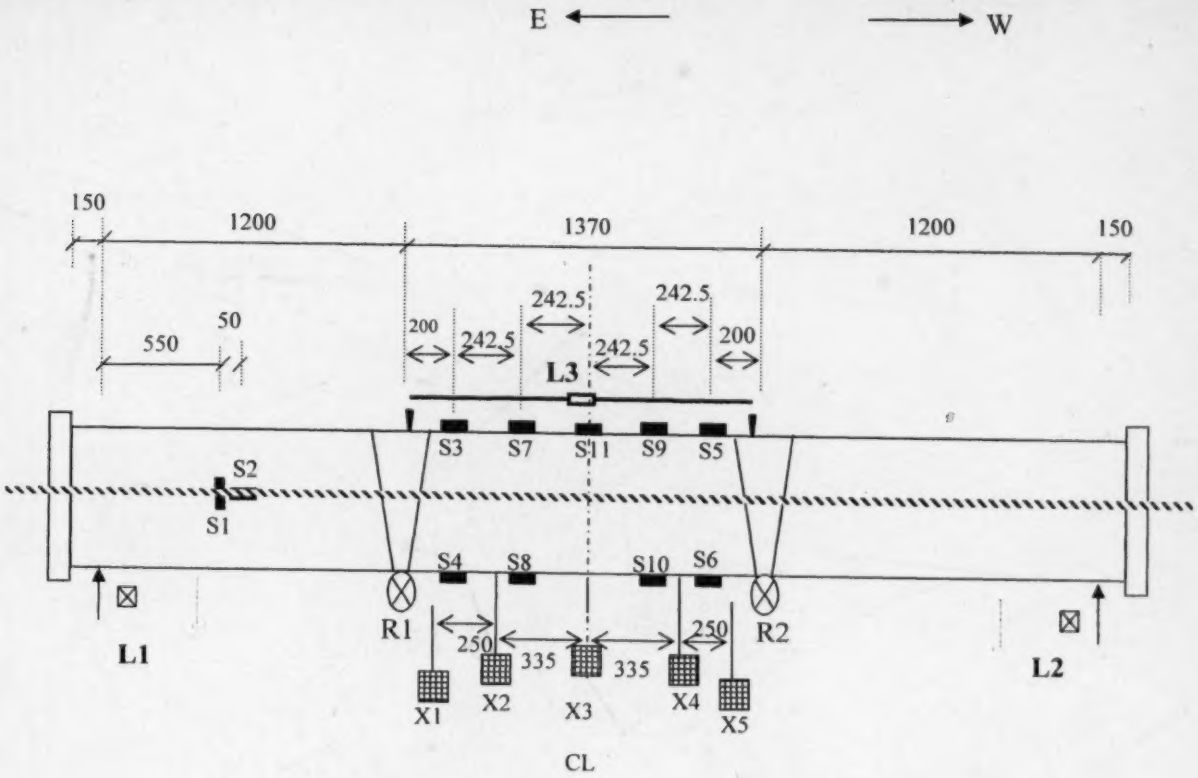

Figure 3.8 Locations of instrumentation on the specimen

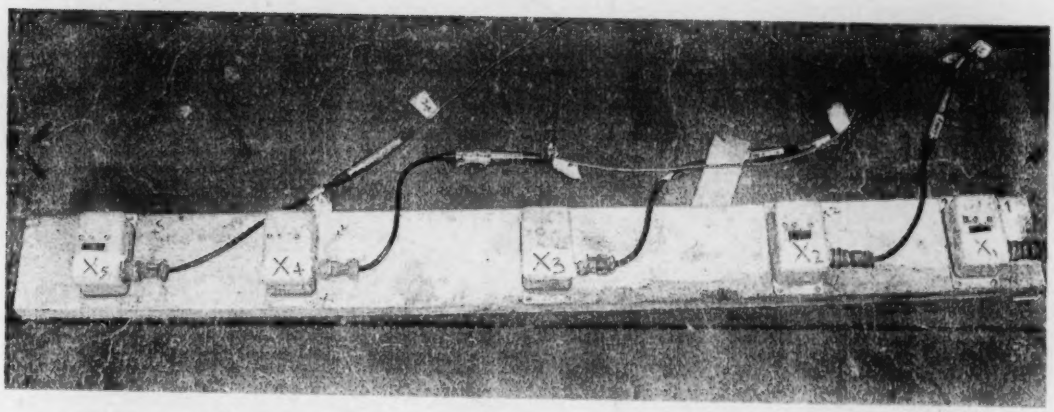

Figure 3.9 Cable transducers used to measure deflection of the pipe

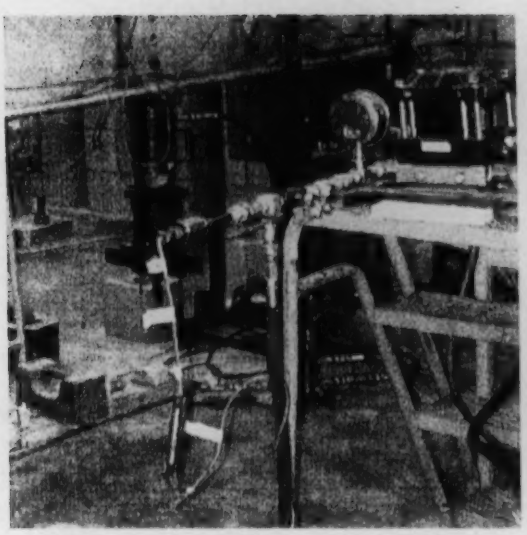

Pressure transducer was placed at the outlet of the water pump

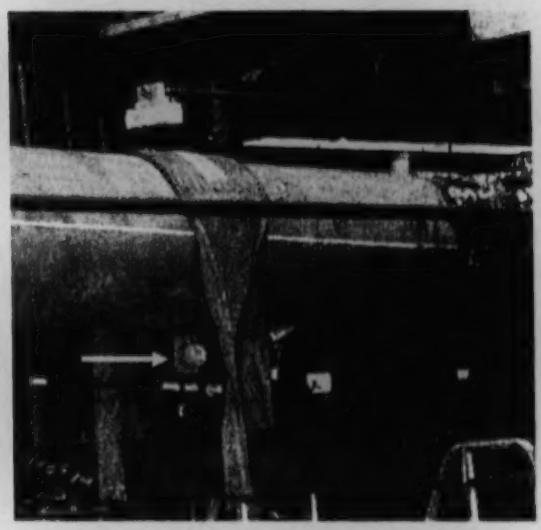

Rotation meter were fixed at the location of load straps

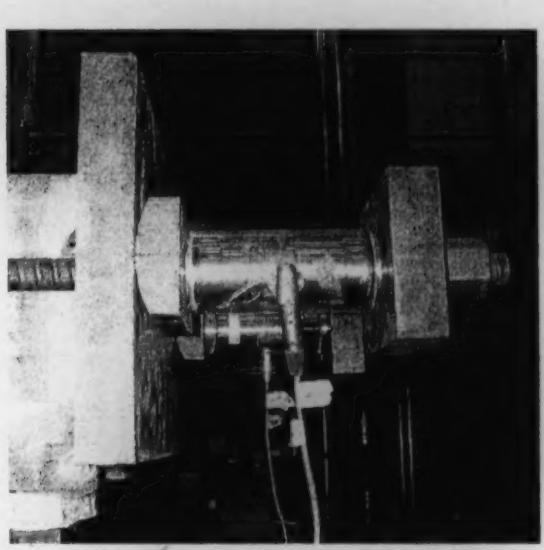

Load cells at the prestressing bars

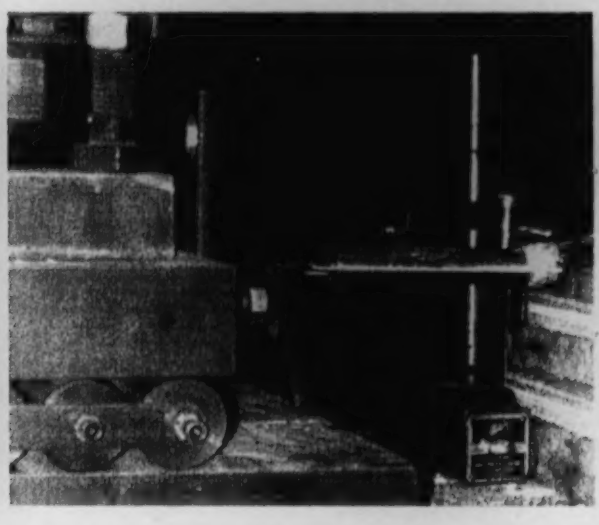

LVDTs were attached with each support to monitor translational movement

Figure 3.10 Instrumentations

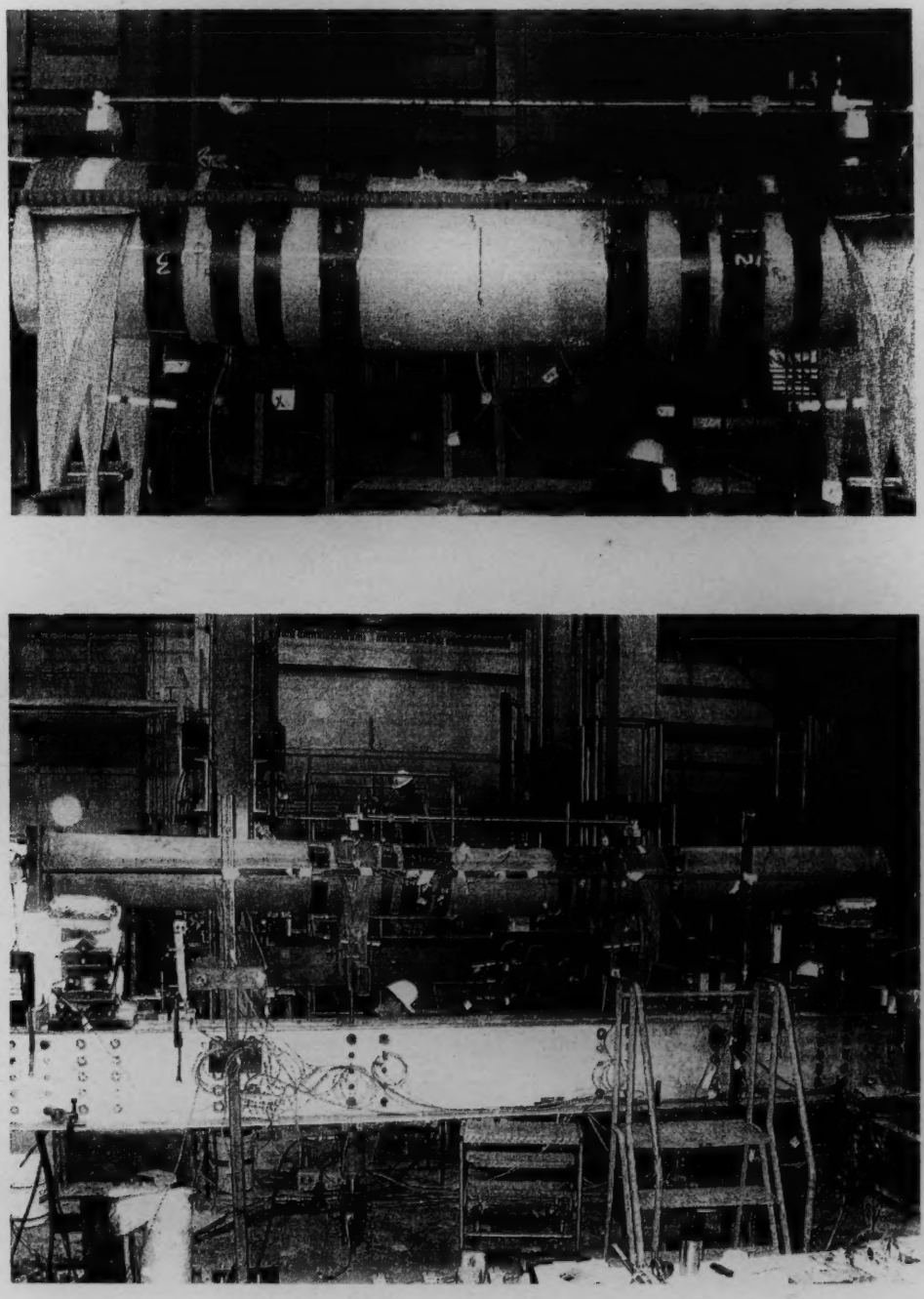

Figure 3.11 Steel collars in pre-wrinkle test

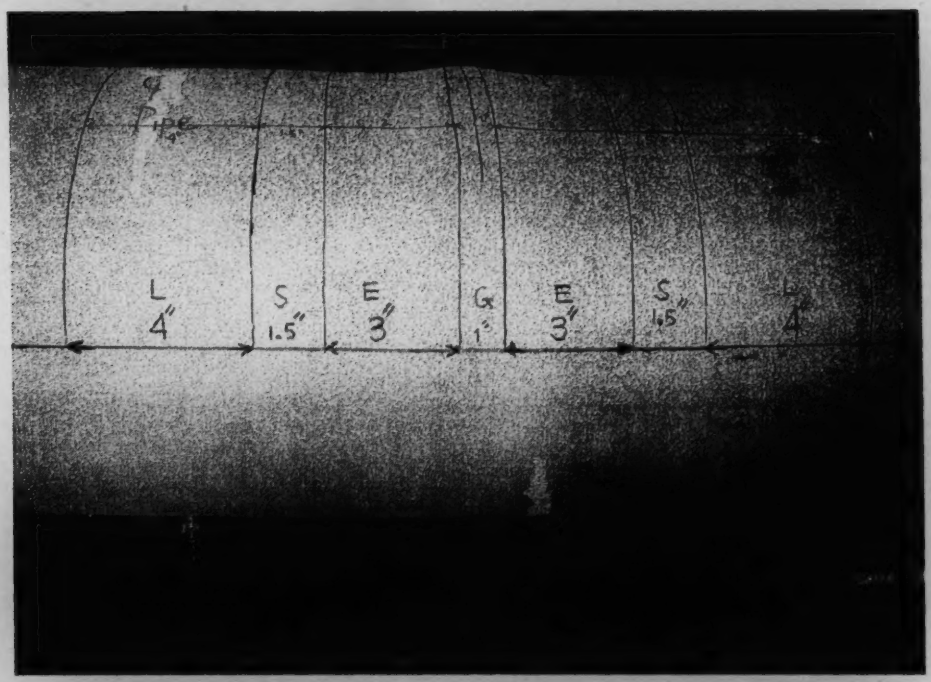

Figure 3.12 Marking on the pipe showing geometry of the sleeves in test-3

Figure 3.13 Marking on putty for middle sleeves in test-3

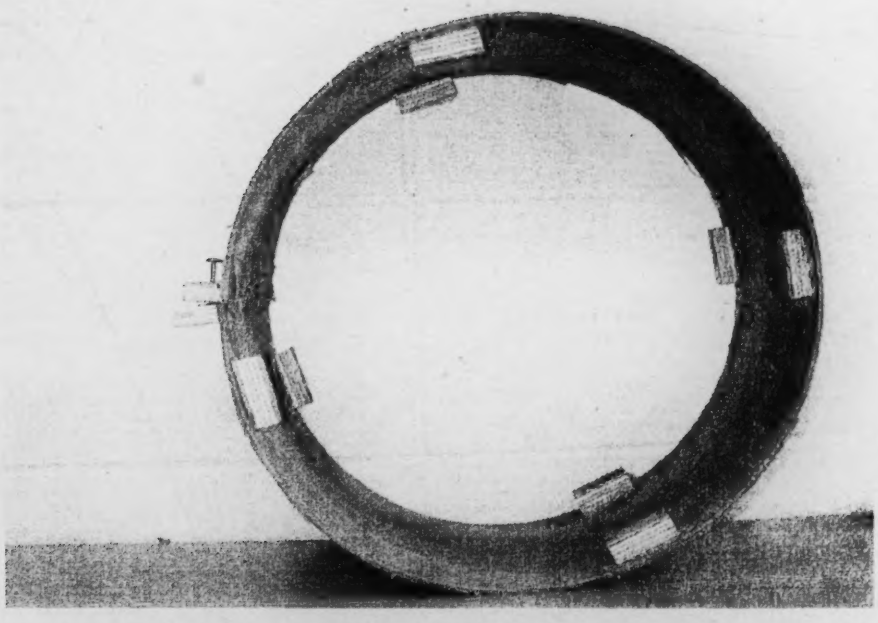

Figure 3.14 Formwork for removing air voids from epoxy putty

Figure 3.15 Strain gauge and demecs on the middle sleeve

4. EXPERIMENTAL RESULTS

4.1 OBJECTIVE

The main objective of the experimental program was to obtain laboratory results to analyze the behaviour of pipe specimens that can be compared with FE models. Most of the specimens failed by fibre fracture and inward buckling in the previous experimental program conducted by Youzwishen and Cheng (2001) so the aim was to achieve a design configuration that would overcome fibre fracture and inward buckling problems.

4.2 MATERIAL PROPERTIES

MBrace EG900 E-glass Reinforcement System was used for sleeve design. This type of glass fibre composite (GFRP) contains uniaxial glass fibre sheets. Typical physical properties of the system provided by the manufacturer have already been given in **Table 3-1**.

Three tests were conducted in this project. Test specimens were approximately 4070 mm long with an outside diameter of 323.9 mm and a wall thickness of 6.33 mm. This results in a diameter to thickness ratio (d/t) of approximately 52. All pipes were X60, with a nominal yield strength of 414 MPa. However from coupons test results obtained by Youzwishen and Cheng (2001), the average nominal yield strength was 523 MPa. The average modulus of elasticity (E) of coupons was 192,128 MPa. Since the same batch of pipes was used in this project, no further coupon tests were conducted to verify the actual material properties. Mechanical properties for NPS 12 pipes have already been given in **Table 2-6**.

Apart from material properties, geometrical configuration of the sleeves also significantly affects the behaviour of the repaired pipe. Geometrical properties like length and gap size

of sleeves can change the flexural behaviour and the failure mode of the pipe. The effects of different sleeve configurations will be discussed in Chapter 5.

For each test, different types of sleeve techniques were used. The performance of each sleeve configuration is based on the moment-curvature behaviour of the repaired pipe.

4.3 DATA CALCULATIONS

Moment-curvature behaviour is an essential quantitative scale to measure the performance of a repair technique. It shows not only the post-buckling capacity but also the ductility of the repaired pipe. These are the most important factors on which design and performance of the sleeve are based.

Moment is calculated at mid-length of the pipe where second order moment is the maximum due to the maximum vertical deflection of the pipe. The total mid-span moment (M_T) is the sum of flexural moment caused by point loads and the second order moment caused by axial load and vertical deflection of the pipe.

Moment was calculated by using the following expression:

(4.1) $$M_T = \frac{R_E + R_W}{2} \times \left(L_S + \frac{\Delta_E + \Delta_W}{2} \right) + P\Delta X_3$$

Where:

R_E and R_W are east and west reaction loads (kN).

L_S is the length of original shear span (m).

Δ_E and Δ_W are longitudinal movement of east and west reactions (m).

P is total axial load (kN).

ΔX_3 is vertical deflection of the pipe at mid length (m).

Two rotation meters were attached to the specimen at the location of point loads. The curvature was measured with the help of numerical values taken from rotation meters and using the following expression:

$$\Phi = \frac{(\theta_1 + \theta_2)}{L_{1-2}} \times \frac{\pi}{180} \times 10^6 \quad (4.2)$$

Where:

Φ is Global Curvature (micro radians/mm).

θ_1 and θ_2 are rotations measured by east and west sides RVDTs (degrees).

L_{1-2} is longitudinal distance between rotation meters (mm).

4.4 DISCUSSION OF EXPERIMENTS

Three tests were conducted in the I.F. Morrison Laboratory at the University of Alberta. Each test was conducted into two phases:

(i) Pre-repair buckling and

(ii) Post-repair failure.

The pre-repair buckling phase was conducted to produce local buckling in an unbuckled specimen so that it can be repaired by external sleeve(s). Procedures for performing both the phases are mentioned in detail in section 3.5.

Internal pressure, axial load and flexural bending were applied to the specimen as mentioned. Steel collars were snugged (as mentioned in section 3.5.2) in the pre-repair buckling test before applying flexural bending. The purpose of providing steel collars was to restrict the primary wrinkle to appear near the mid length of the pipe. There are two main reasons for restricting the position of the primary wrinkle. If the primary wrinkle appears near the mid length of the specimen, the position of the wrinkle will be closer to what has been incorporated in the finite element (FE) model. In the FE model imperfection is provided at the mid length of the pipe so the primary wrinkle appears at

that location. Moreover shear and constant moment span is not disturbed in the post-repair test if the wrinkle appears near the mid length of the pipe. Steel collars were snugged after internal pressure was applied. Imperfection would result in the pipe wall if the pressure had been applied prior to snugging the collars. Loose collars or hand tightened collars may not be effective in causing the wrinkle to appear near the mid length of the pipe.

In all three tests, the wrinkle appeared within 200 mm from the mid length of the pipe. Pre-repair tests were stopped when a wrinkle called the primary wrinkle was formed in the pipe and the wrinkle had a height sufficiently visible as shown in **Figure 4.1**.

When the primary wrinkle reached a sufficient height and moment capacity of the pipe started dropping, the pre-wrinkle test was stopped. The test specimen was unloaded so that FRP sleeves could be applied. It was not possible to apply FRP sleeves without unloading the specimen and removing all instruments from the pipe.

Test results and behaviour of each specimen are discussed in the following subsections.

4.4.1 Test-1

The primary wrinkle appeared at a distance of 160 mm west of the mid length of the pipe. The position of the primary wrinkle with respect to the mid length of the pipe for test-1 is shown in **Figures 4.1** and **4.2**. The specimen was unloaded and instrumentation was removed so that the sleeves could be applied. The sleeve region on the pipe was cleaned and marked as shown in **Figure 4.2**.

Mbrace primer was applied on the pipe at the sleeve location to provide a good bond between the pipe and the sleeves. Putty was placed on the top surface of the pipe at the location of the middle sleeve. Putty provided a smooth surface along the wrinkle crest and contact between the pipe surface and the middle sleeve.

A circular formwork (collar) made from cardboard was snugged on freshly applied putty to remove voids from the putty. Curing of putty was allowed for twenty-four hours.

FRP sheet was cut into desired sizes so that sleeves could be made. Symmetrical odd sleeves were applied to the pipe. Mbrace saturant was used as a matrix to apply the sleeves. FRP matrix was mixed and made according to manufacturer's specifications. Sleeve configuration used for this test is shown in **Figure 4.3**. The length of the middle sleeve was 150 mm (~0.5d). The length of side sleeves was 100 mm (~0.33d) and the side gap was 75 mm (0.25d). In order to provide more stiffness to the wrinkled region seven layers of FRP (sleeve to pipe stiffness ratio = 0.15) were wrapped around 100 mm centre of the middle sleeve. Five layers (sleeve to pipe stiffness ratio = 0.11) were wrapped around the remaining 50 mm on either side. The sleeves were allowed to cure for seven days.

The sleeve configuration for this test was selected from FEA on the basis of:

a. moment-curvature behaviour and
b. ductility.

When the sleeves were cured and became hard, a strain gauge, oriented in the hoop direction of the pipe was applied on the middle sleeve so that strain in the fibre could be monitored. The strain gauge was placed at the centre of the middle sleeve i.e. at the location of the wrinkle crest. In order to verify the results of the strain gauge, 2" (50mm)-demecs were also fixed on the middle sleeve as shown in **Figure 4.4.** Demecs were placed in both hoop and longitudinal directions. No significant differences were observed between the strain data obtained from demecs and strain gauges.

The specimen was reloaded after all the instrumentation had been done. **Figure 4.5** shows the assembly or test setup immediately before reloading. Fracture sounds were heard from the middle sleeve when load was applied even though no visible fracture was noticed initially. So it was presumed that either sub-surface fibre had fractured or debonding was occurring between fibre layers.

Increase in flexural moment capacity (referred to as post buckling capacity) of the pipe was noticed when it was loaded. The repaired pipe resisted a maximum moment capacity almost 90% of its original (un-buckled) capacity in the pre-wrinkle test. Global moment-curvature behaviour of the pipe in test-1 is shown in **Figure 4.6**.

Strain in the middle sleeve was monitored by strain gauges and demecs. Initially strain was noticed due to applied internal pressure. Strain in the fibre increased at a slower rate when the pipe was reloaded. When the wrinkle started growing faster, strain increased significantly. The middle sleeve was subjected to high strains developed by the growth of the primary wrinkle. **Figure 4.7** shows the strain in the fibre with respect to global curvature of the specimen. Fibre in the middle sleeve was intact until a strain value of 1.95%. When the strain in the fibre reached ultimate capacity, the sleeve fractured suddenly and moment capacity of the specimen dropped rapidly. The middle sleeve fractured suddenly when strain exceeded 1.95%. The fibre fracture is shown in **Figure 4.8**.

An inward secondary wrinkle was also observed along the edge of the middle sleeve in the hoop direction. Moment-curvature behaviour of the test was very close to the FEA except for the fibre fracture problem not incorporated into parametric studies. Failure mode for the pipe obtained from FEA is shown in **Figure 4.9**. Both FEA and test results give almost identical post buckling capacity as shown in **Figure 4.10**. The test was stopped when the pipe was no longer resisting the load and underwent large deflection. The specimen at the end of test is shown in **Figure 4.11**.

4.4.2 Test-2

Unlike test-1, the primary wrinkle appeared east of the mid length of the pipe. However its location was at a distance of 195 mm, which was not very far from the mid-length of the pipe. Unlike all the previous tests, unsymmetrical odd sleeve configuration was used

as shown in **Figure 4.12**. The length of the middle sleeve was 125 mm (~0.42d). Side sleeves of different length were used. A 125 mm (~0.42d) long sleeve was placed on the west side of the middle sleeve and a 100 mm (~0.33d) long sleeve on the east side. The gap between the middle and side sleeves was 75 mm (~0.25d). Ten layers of FRP (sleeves to pipe stiffness ratio =0.22) were wrapped around the pipe to provide more stiffness to the wrinkled area than that of test-1.

FRP sleeve configuration for this test was selected from parametric studies so that inward buckling could be avoided. Unsymmetrical lengths of side sleeves were chosen to allow a secondary wrinkle to appear in the sleeved region. Six strain gauges were installed on the middle sleeve to monitor fibre strain so that fibre fracture could be anticipated well before it would be visible. 2" (50 mm)-demecs were also fixed as shown in **Figure 4.13**.

The pipe was reloaded when the sleeves were cured and all instrumentation was done. Strain in the middle sleeve increased when load was applied. When strain reached 1.3%, the fibre started fracturing and mid-span moment started dropping. It was decided to place a steel collar on the centre of the middle sleeve i.e. on the location of wrinkle crest so that complete fibre fracture could be avoided and behaviour of the pipe could be observed in the absence of fibre fracture.

A steel collar 52 mm wide and 6.23 mm thick was snugged on the centre of the middle sleeve as shown in **Figure 4.14** to restrict the growth of the primary wrinkle. When the load was applied an increase in the moment was noticed. The test and FEA results are very close to each other as shown in **Figure 4.15,** except the gain in moment capacity followed by applying steel collar which was not applied in FEA. The moment then dropped followed by the ovalization that occurred in the gap between middle sleeve and west side sleeves. The specimen was unloaded. It was decided to observe the behaviour of the specimen at higher internal pressure. The specimen was unloaded and all instrumentation was removed.

An internal pressure of approximately 1950 psi (four times the pressure which was used during the tests and ~80% of SMYS) was applied and the pipe was reloaded. It was not possible to apply axial load due to the large deflection of the specimen and the stability problem of dywidag bars. Moment capacity of the pipe increased as shown in **Figure 4.16** and an outward secondary wrinkle appeared in the gap between the middle sleeve and west side sleeve as shown in **Figure 4.17**. The test was ended when jack stroke for point loads exhausted and it was not possible to apply more loads on the pipe. The deflection at the end of the test is shown in **Figure 4.18**. It may be concluded that at higher internal pressure like gas pipelines, this sleeve configuration might produce better results.

4.4.3 Test-3

The primary wrinkle appeared at a distance of 200 mm east of the mid-length of the pipe. Odd sleeve configuration has been used in all the full-scale tests conducted so far so it was decided to observe the behaviour of the pipe using the even sleeve configuration. Even sleeve configuration was used to observe the difference in behaviour of the pipe from odd sleeve configuration. Even sleeve configuration is more complex. Skill and precision are required to apply an even sleeve since the gap between two middle sleeves with respect to the centreline of wrinkle can affect the behaviour of the pipe significantly so the uniform gap between two middle sleeves needs accuracy. The sleeve configuration used in this test is shown in **Figure 4.19**.

The pipe surface was cleaned and marked for the sleeves. Primer and putty was applied as discussed in the previous subsections. Marking on the putty was made to facilitate the middle gap as shown in **Figure 4.20**.

The middle sleeves were placed at a distance of 12.7 mm (~0.04d) on both sides from the centre of the wrinkle. This resulted in a gap of 25 mm (~0.08d) between the middle sleeves. The length of the middle sleeves was 75 mm (~0.25d). Eleven layers of fibre

sheet (sleeve to pipe stiffness ratio = 0.24) were applied. Two side sleeves were also provided at a gap of 38 mm (~0.125d) from each middle sleeve. The length of the side sleeves was 100 mm (~0.33d).

Since the middle sleeves were not placed directly on the wrinkle crest, fibre fracture was not expected in this test. Five strain gauges were installed on the wrinkle region in the hoop direction as shown in **Figure 4.21**. One strain gauge was placed at the crest of the wrinkle i.e. in middle gap and two on each middle sleeve.

When all instrumentation was done, the pipe was reloaded. Even though no visible cracking was found, debonding and fracture sounds were heard from the sleeves when load was applied to the pipe. A significantly different behaviour was observed from the last two tests. The pipe was efficiently carrying the load until an outward secondary wrinkle appeared adjacent to the east load strip as shown in **Figure 4.22**. It seems that the cause of this wrinkle was a concentration of stresses at this location. More ductility would have been achieved if the load straps had not been present there. It is presumed that in the absence of load straps in the field, this configuration may perform better. The moment-curvature behaviour of the pipe is shown in **Figure 4.23**. It can be expected that pipe might be in serviceable condition for longer if this sleeve configuration is used. Even sleeves may produce better results i.e. more capacity, less deflection and no fibre fracture problem.

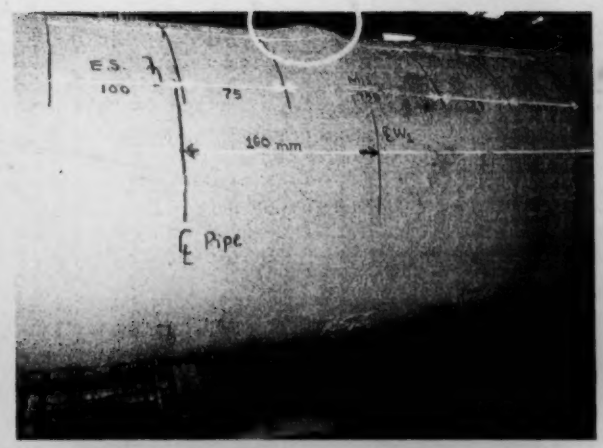

Test-1

Test-2

Test-3

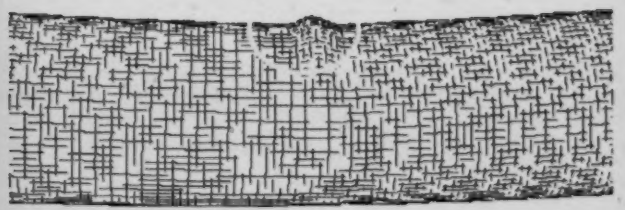

FEA model

Figure 4.1 Primary wrinkle

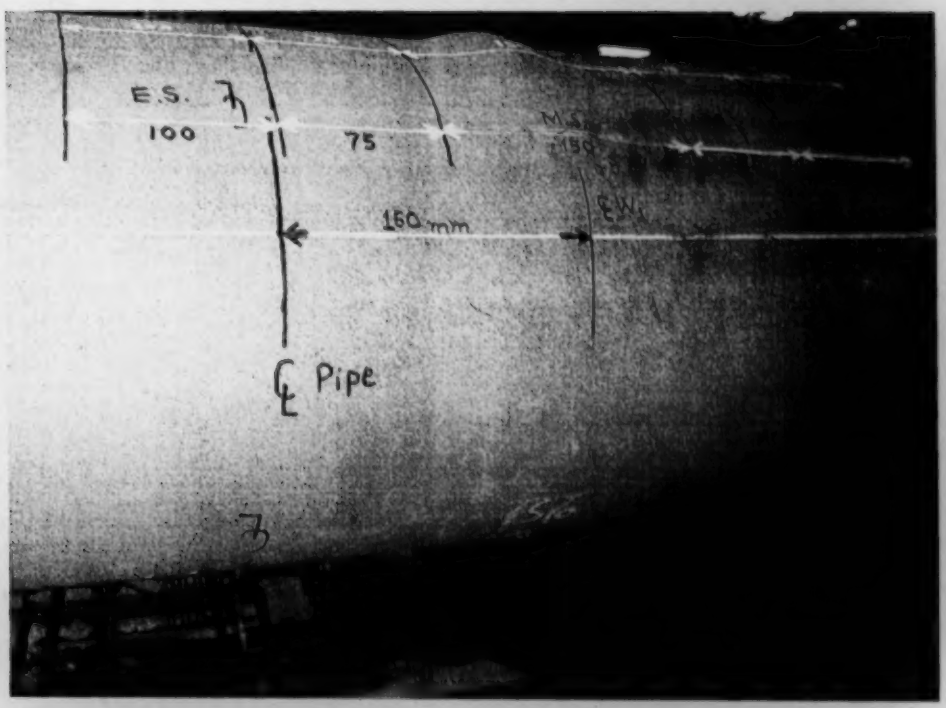

Figure 4.2 Location of primary wrinkle and sleeve marking for test-1

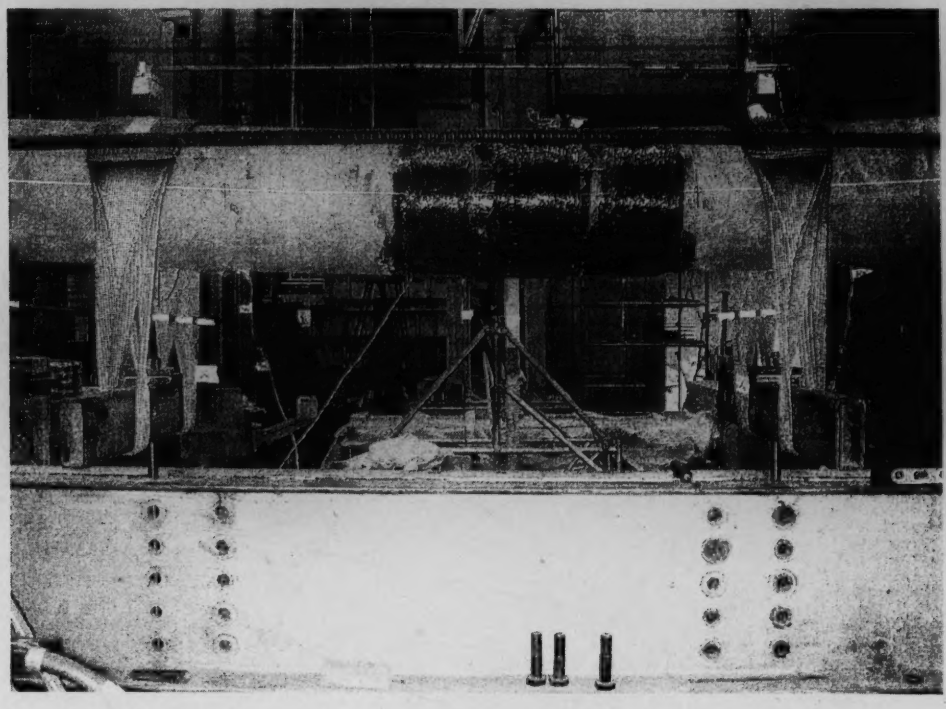

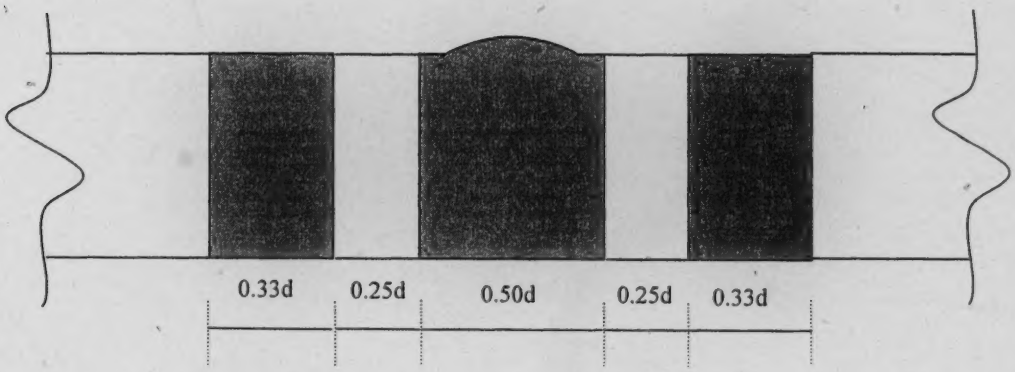

Figure 4.3 Odd sleeve configuration used in test-1

Figure 4.4 Demecs and strain gauge on the middle sleeve in test-1

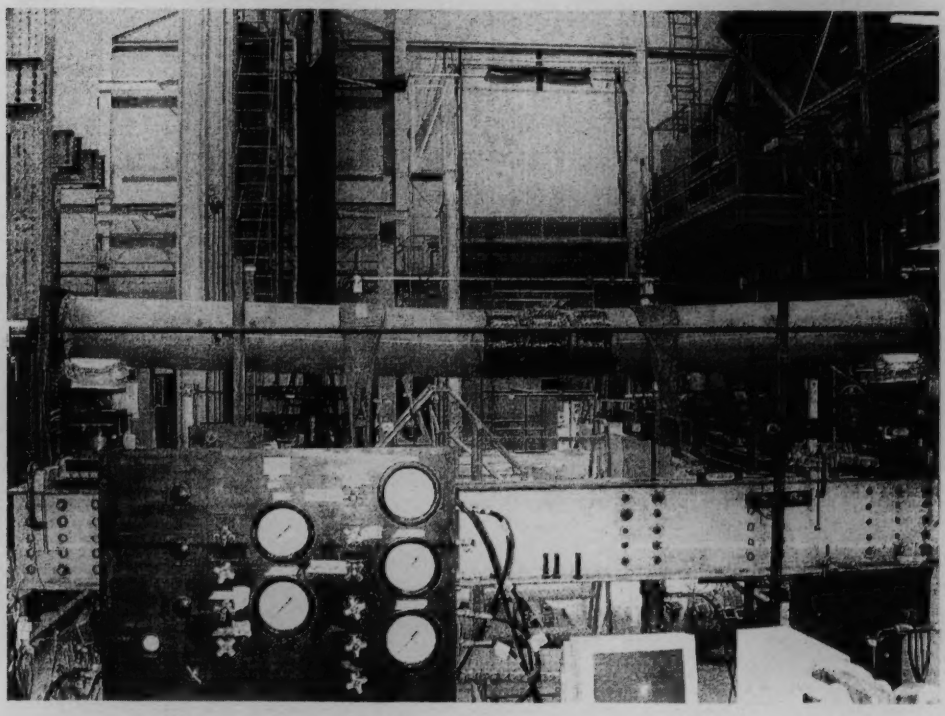

Figure 4.5 Reloading of the specimen for Post-repair test-1

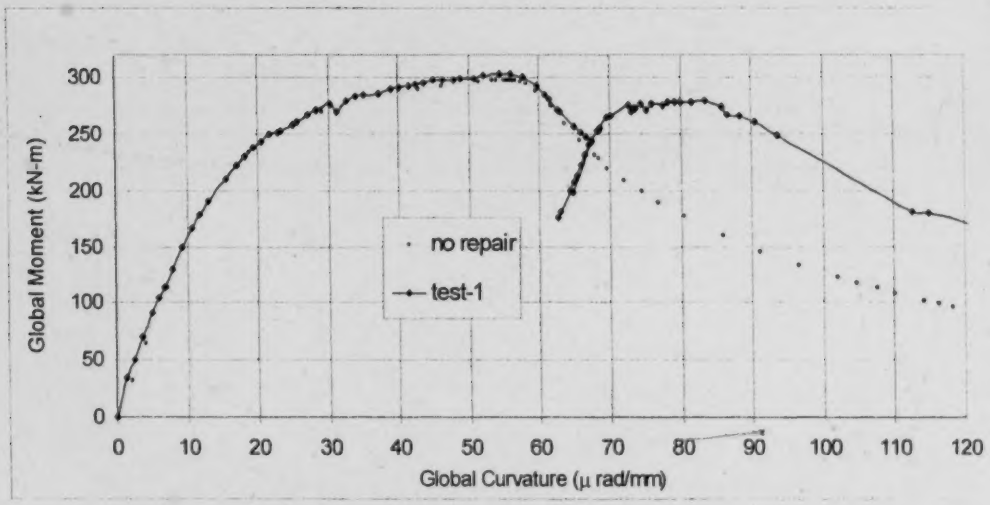

Figure 4.6 Moment-curvature behaviour of the specimen in test-1

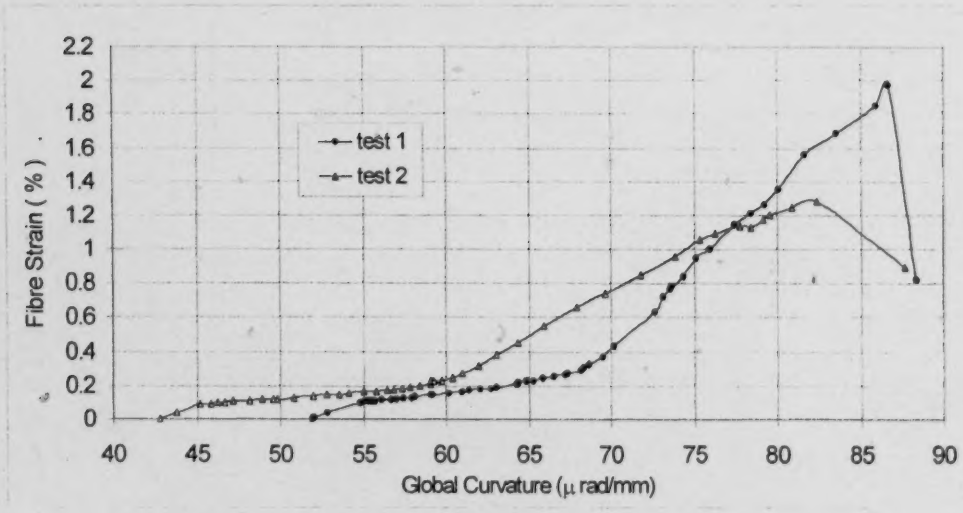

Figure 4.7 Strain in the middle sleeve at wrinkle crest

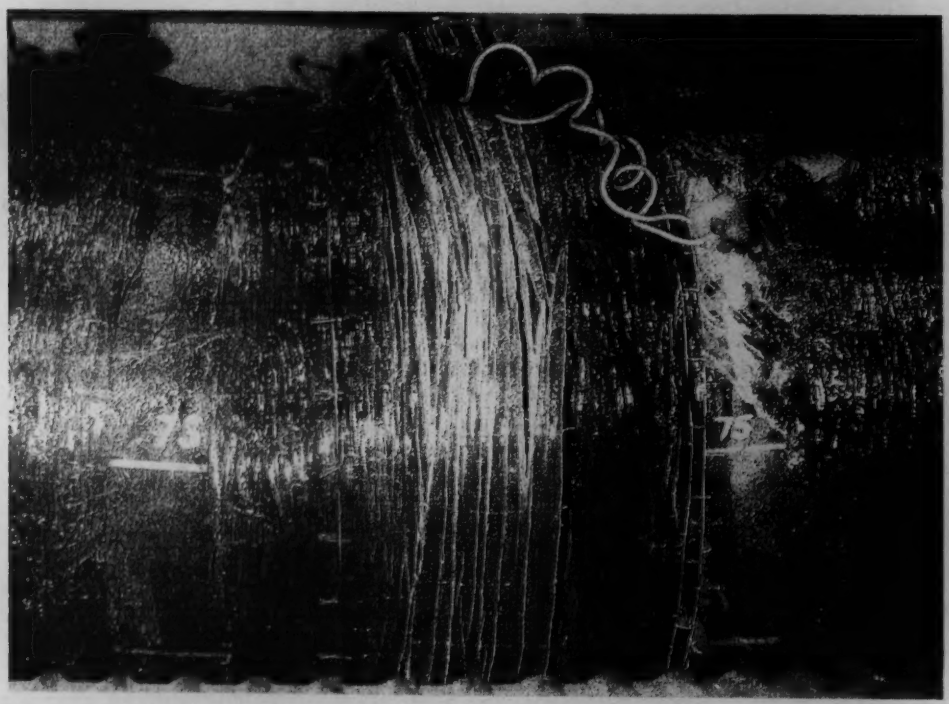

Figure 4.8 Fibre fracture at wrinkle crest in test-1

Figure 4.9 Failure mode of the pipe in FEA model for test-1

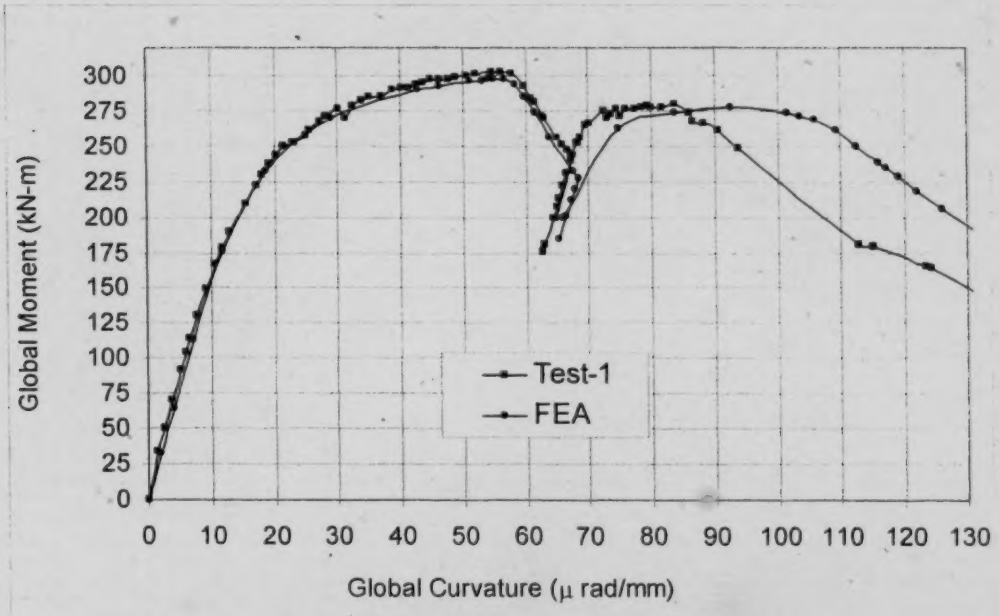

Figure 4.10 Comparison between test-1 and FEA results

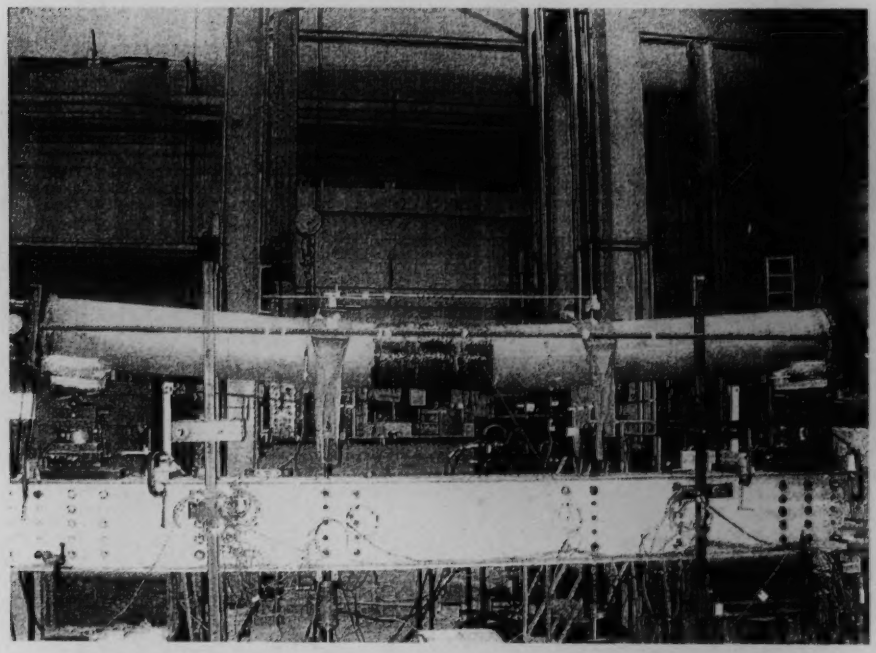

Figure 4.11 Deflection of the specimen at the end of test-1

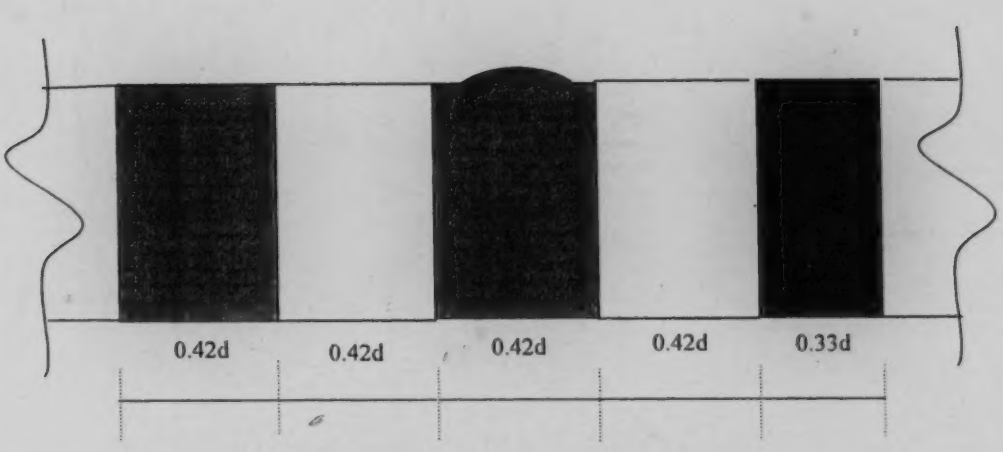

Figure 4.12 Unsymmetrical odd sleeve geometry used in test-2

Figure 4.13 Strain gauges and demecs on the middle sleeve in test-2

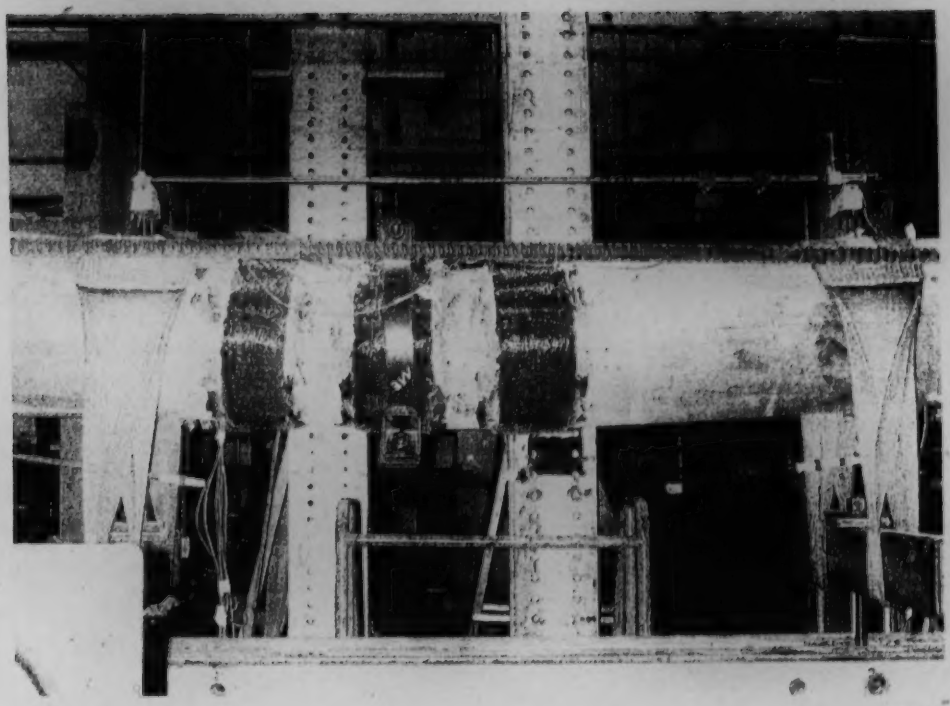

Figure 4.14 Steel collar was applied on the middle sleeve in test-2

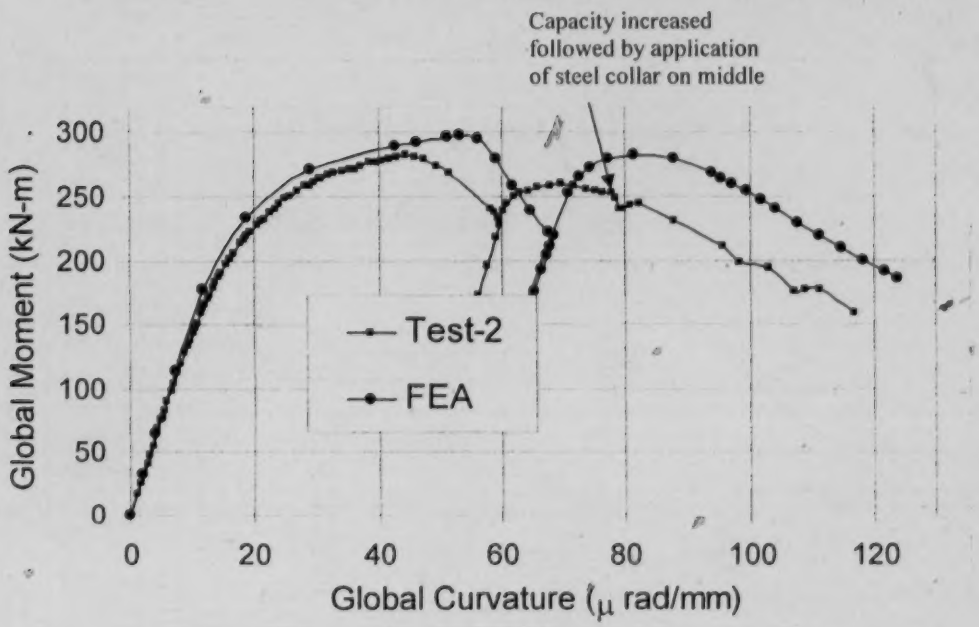

Figure 4.15 Moment-curvature behaviour in test-2

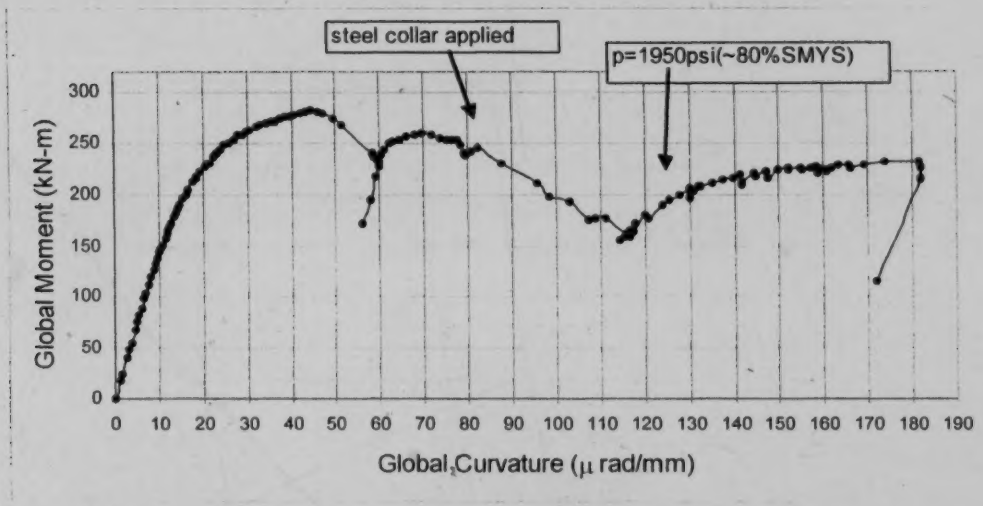

Figure 4.16 Moment-curvature behaviour at higher internal pressure in test-2

Figure 4.17 Secondary wrinkle in test-2 and FEA

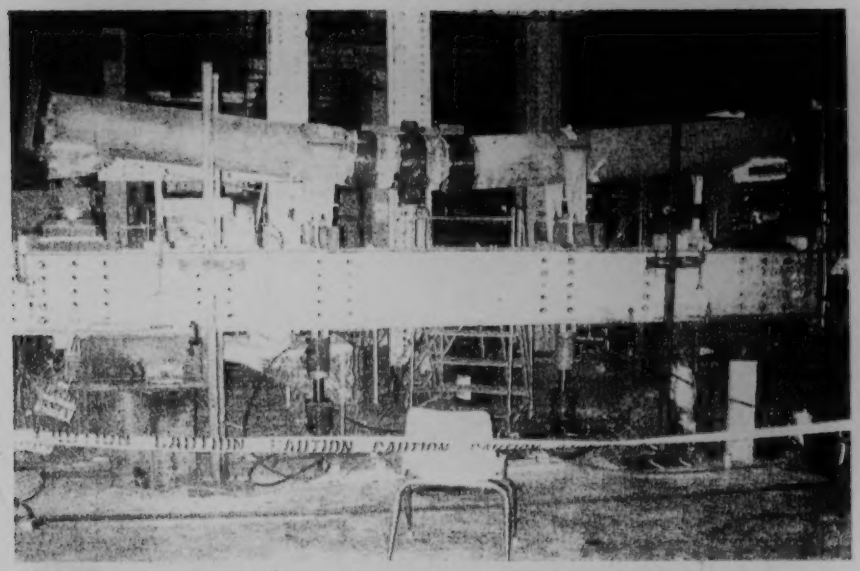

Figure 4.18 Deflection of the specimen at the end of test-2

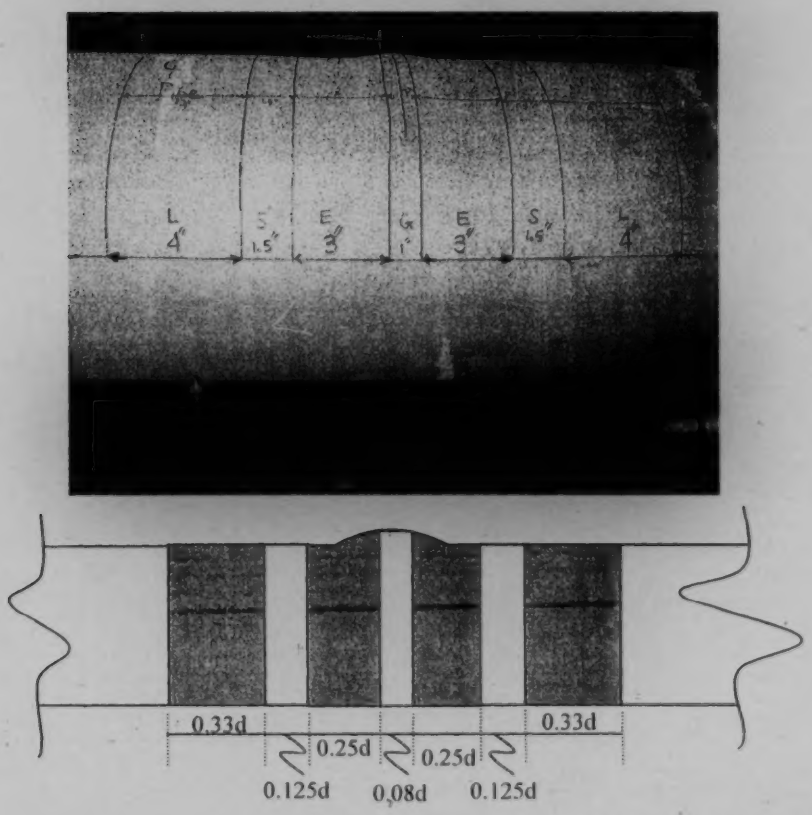

Figure 4.19 Sleeve configuration and marking on the specimen for test-3

Figure 4.20 Marking on epoxy putty for the middle sleeve in test- 3

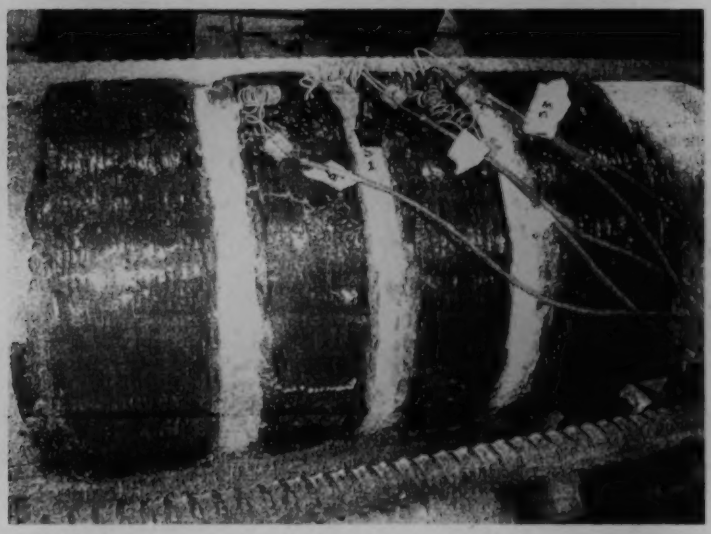

Figure 4.21 Strain gauges on the specimen and the middle sleeves in test-3

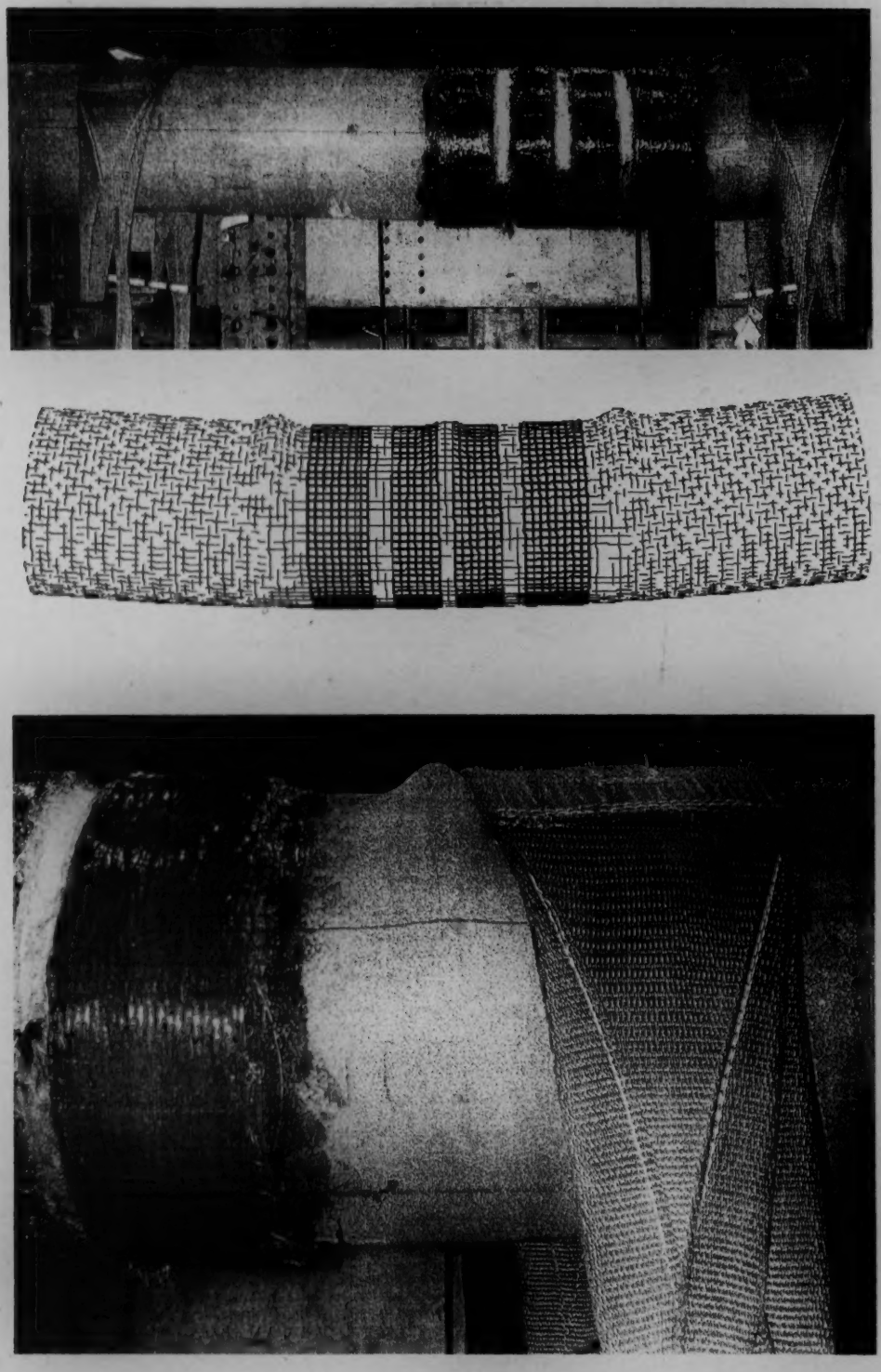

Figure 4.22 Secondary wrinkle in test-3 and FE model

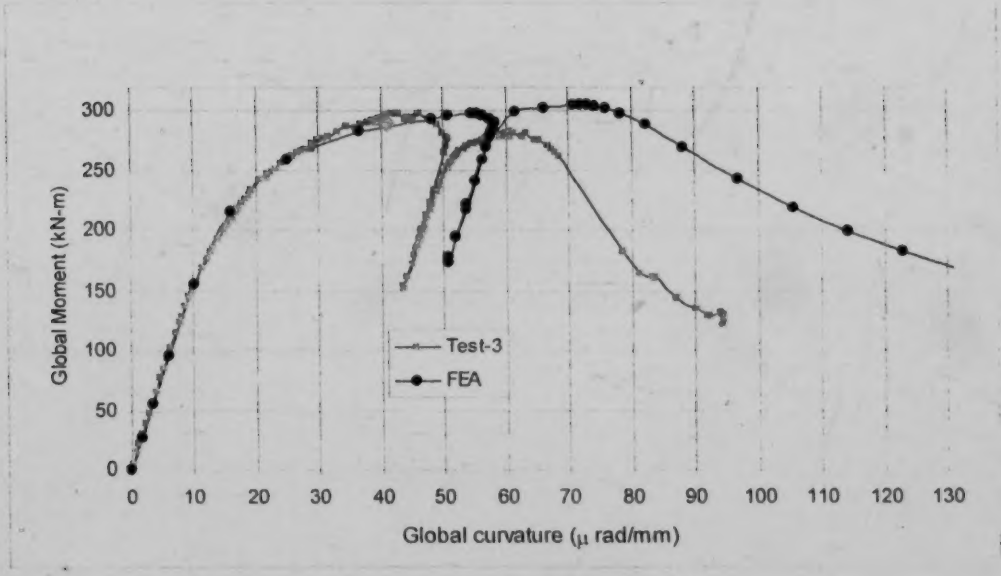

Figure 4.23 Moment-curvature behaviour in test-3

5. FINITE ELEMENT ANALYSIS

5.1 GENERAL

Finite element analysis (FEA) helps to develop an understanding of the post-buckling behaviour of a wrinkled pipe that has been repaired. This is a very economical and efficient method of studying the behaviour of a wrinkled pipe under different kinds of loading.

In this research program, the main objective of using FEA is to develop an optimum sleeve design based on the post buckling capacity and mode of failure of the repaired pipe. Post buckling or secondary moment capacity is the maximum flexural moment a locally buckled pipe can resist after repair. We'll use the term "primary moment" for the flexural moment capacity of an un-repaired pipe.

Since fracture of the middle sleeve was observed during most of the experiments, it became necessary for the sleeve to be designed so that fracture can be avoided. Integrity of the middle sleeve is a major factor of consideration for sleeve design in the case of single or odd sleeve configurations.

The three major factors contributing to optimum sleeve design are:

(i) Post buckling capacity of the pipe,
(ii) Mode of failure which allows subsequent or sequential repair,
(iii) Integrity of the sleeve(s).

Initially FEA in this research project was conducted using the commercially available FEA package ABAQUS/Standard Version 5.8 (Hibbitt, Karlsson and Sorensn, 1999). Later on, a new Version 6.2 (Hibbitt, Karlsson and Sorensn, 2002), was also used.

5.2 FINITE ELEMENT MODEL

The length of the F.E. model was 54" (~1370 mm). This was the length of the constant moment region between two load straps in the experimental program. Since the pipe is longitudinally symmetrical, half model size was used as shown in **Figure 5.1**. Half model size saves disk space and computer processing time. Symmetry had successfully been used in previous studies (Youzwishen and Cheng (2001), Zhou and Murray (1993)). NPS 12 pipes, which were used in the experimental program, possessed a d/t of approximately 52. The same d/t was incorporated into the F.E. model.

5.2.1 Mesh and Element Selection

The mesh of a F.E. model plays a vital role in predicting the behaviour of the model. Even though finer mesh takes more computer processing time, it gives more realistic model results. A finer mesh also allows more variation in geometrical parameters of the sleeve design.

For the model used in this project the element size in the circumferential and longitudinal directions is 12.7 mm x 12.7 mm. This results in a mesh of 40x108 elements. Two types of elements have been used in the model. Finite strain four-node, three-dimensional, and doubly curved elements (S4R) have been used to model the pipe wall. Each node has six degrees of freedom, three translational and three rotational. For the pipe subjected to large deformations and displacements, S4R elements had successfully been used in previous studies (Youzwishen and Cheng, 2001). Three-node, flat, small strain elements (STRI3) have been used to model the pipe end plates. STRI3 are thin shell elements.

5.2.2 Boundary Conditions

Since half model size is used in FEA, appropriate boundary conditions are required where the plane of symmetry intersects the pipe. Intersection of the symmetry plane with the top and bottom of the pipe is shown in **Figure 5.2**. Symmetry eliminates the possibility of out

of plane buckling. In order to apply symmetry, nodal displacements and rotations are not allowed on the line of the symmetry.

A pin-roller type boundary condition is applied to the pipe as shown in **Figure 5.2**. Both ends of the pipe are restrained in the vertical direction. Horizontal translation is allowed for one end. In-plane rotation is allowed for both ends so that specified rotation can be applied in order to achieve flexural bending in the pipe. Out of plane movements at the reactions are restrained.

5.2.3 Imperfection

The diameter of the pipe is assumed to be imperfect. An imperfection pattern is applied by creating a uniform bulge along the circumference at the mid-length of the pipe model. The maximum bulge height reaches 0.1 mm. This type of initial imperfection had been successfully used in the previous F.E.A. (Youzwishen and Cheng, 2001, Yoosef-Ghodsi and Murray, 1999).

5.2.4 Loading Conditions

Norman wells pipeline is subjected to external loads mentioned in detail in section 2.2. In order to simulate loading conditions in the field, three types of loads are applied to the FE model described in the following subsections.

5.2.4.1 Internal Pressure

When the pipe is in operation, the pipe wall is subjected to fluid pressure. A pressure of 3.3 MPa (3300 kPa), which corresponds to 20% of SMYS in the hoop direction, was applied to the pipe elements as representative of internal fluid pressure in the pipe during operation.

5.2.4.2 Axial Loads

Axial loads are generated by temperature differential, Poisson's effect, and the soil movement effect. The soil movement effect was neglected in the laboratory tests.

By using equation 2.1, longitudinal compressive stresses due to the temperature differential effect (σ_α) were calculated to be –108 MPa ($200000*12x10^{-6}*45$).

(2.1) $$\sigma_\alpha = -E \cdot \alpha \cdot \Delta T$$

Tensile stresses due to Poisson's effect (σ_v) were calculated to be +24.8 MPa using equation 2.2.

(2.2) $$\sigma_v = \nu\sigma_h = \nu\left(\frac{pd_i}{2000\,t}\right)$$

In laboratory tests, an additional axial load was generated by the close vessel effect of the pipe. Rigid end plates were welded to the specimens to retain water and apply internal pressure. Longitudinal tensile stresses originated in the pipe wall when fluid pressure acted on the end plates. Since the pipeline in the field is a continuous pressure vessel, the additional tensile loading is not present and, therefore, compressive stresses are not generated. Compressive stresses, generated by the closed vessel effect (σ_l), were calculated using equation 5.1.

(5.1) $$\sigma_l = \frac{pd_i}{4000\,t}$$

where:

p = internal pressure of fluid (kPa)

d_i = inside diameter of the pipe (mm)

t = wall thickness of the pipe (mm)

Total stresses (σ_1) were calculated to be –41.33 MPa.

A total pressure of –9.93 MPa, caused by net axial load, was applied to the pipe model through cap elements at pipe ends. It was calculated by using equation 5.2.

$$p_{end} = (\sigma_\alpha + \sigma_v + \sigma_1) \times (\frac{4t}{d}) \quad (5.2)$$

5.2.4.3 Curvature

As mentioned in section 2.2.3, due to several weathering effects such as soil consolidation, frost heave, undulation, inclined movement, etc., differential soil settlement occurs along the pipe length, which causes flexural bending in the pipe. Curvature or flexural bending in the pipe was provided by two load straps in the experimental program as mentioned in section 3.5.1.3. In the FE model, in-plane rotations of reaction point were prescribed at the pipe ends to simulate curvature in the field.

5.2.5 Sleeve Application

A procedure similar to laboratory tests was followed in FEA. Axial load, internal pressure and curvature were applied to the model to produce the wrinkle in the plain pipe. When the primary wrinkle appeared in the FE model, the pipe was unloaded and external sleeves were applied. S4R elements of size 12.7 mm x 12.7 mm were used for the FRP sleeve. Pipe and sleeve elements shared the same nodes. Sleeves were modelled as a second layer of elements attached to the pipe model.

5.2.6 Analysis Procedure

FEA was conducted in two major phases similar to the laboratory tests, i.e. the pre-wrinkle test to produce a buckle in the plane pipe and the post-repair test after applying

the sleeve(s). The procedure in FEA was divided into 8 or 16 steps depending on the type of the repair technique used. Analysis for sequential sleeve repair was completed in 16-steps whereas all other (single, odd and even sleeves) were completed in 8-steps.

In the first step the sleeve elements were removed. Internal (fluid) pressure and axial loads were applied in the second and the third steps respectively. In the fourth step, rotations were applied to the pipe ends to provide curvature to the pipe. A primary wrinkle appears in the pipe at the end of the fourth step. The loads were removed in the fifth and the sixth steps in a reverse sequence as were done in the experiments, so that sleeves could be applied. The first phase was completed in six steps.

Second phase of analysis begins with the seventh step in which the sleeve elements, internal pressure and axial loads were applied. End rotations were applied in the eighth step to observe the behaviour of the pipe after the rehabilitation. Applied rotation for the repaired pipe was more (approximately two times) than that of the plain pipe used in the fourth step.

5.3 SLEEVE GEOMETRY OR CONFIGURATION

Single and multiple sleeves can be used to repair the wrinkled pipe. In order to identify different sleeve patterns, they are divided into three main configurations on the basis of the number of sleeves used in a particular repair.

5.3.1 Single Sleeve Configuration (SS)

When only one sleeve is used to repair a wrinkled pipe, it is referred to as a single sleeve. The sleeve is evenly placed on the centre of the wrinkle along the length of the pipe as shown in **Figure 5.3**.

5.3.2 Odd Sleeve Configuration (OS)

When odd numbers of sleeve are used, mostly three, it is referred to as odd sleeve configuration. One sleeve referred to as the middle sleeve is placed evenly on the centre of wrinkle just like single sleeve and two sleeves referred to as side sleeves are placed along the length of the pipe at a certain distance on the both sides of the middle sleeve as shown in **Figure 5.4**. The distance between middle and side sleeves is called the gap or side gap.

5.3.3 Even Sleeve Configuration (ES)

When number of sleeves is even, mostly four, it is referred to as even sleeve configuration as shown in **Figure 5.5**. Two sleeves are placed at an equal distance from the centre of the wrinkle and are called middle sleeves. The distance between two middle sleeves is called the middle gap. Two sleeves are placed at a certain distance from middle sleeves along the length of the pipe and are called side sleeves. The spacing or distance between a side sleeve and adjacent middle sleeve is called the gap or side gap. Until the word "middle" is used with the term "gap", it should be referred to as "side gap".

If only two middle sleeves are used, it is called double sleeve configuration (DS). Basically double and even sleeves are the same; the different names have been use to distinguish them from each other.

The following abbreviations are used in this chapter:

SS = Single Sleeve Configuration
OS = Odd Sleeve Configuration
ES = Even Sleeve Configuration
DS = Double Sleeve Configuration
MS = Length of Middle Sleeve(s)
SSL = Length of Side Sleeves
MG = Middle Gap Size

GS = Side Gap Size

ρ = Stiffness Ratio ($E_s t_s / E_p t_p$)

5.4 PARAMETERS

It was revealed from the previous studies that certain parameters of a particular sleeve configuration can impose a major effect on the post buckling capacity, ductility and failure mode of the repaired pipe.

Those parameters are:

- Length of middle sleeve(s)
- Gap sizes between the sleeves
- Thickness and stiffness of the sleeve(s)

The length of the sleeve(s) and the gap sizes are measured along the length of the pipe. It has been observed from FEA that the length of side sleeves does not have significant effect on post buckling behaviour of the pipe. Therefore the length of the side sleeves is kept constant for all cases. It should be remembered that the length of side sleeves are 0.33d in the parametric studies until otherwise specifically mentioned in the following sections. The effect of varying length of the middle sleeve and side sleeve will be discussed in the following sub-sections.

The distance or spacing between two adjacent sleeves along the pipe length is called gap size. In the experimental program, glass fibre reinforced polymer (GFRP) sheets were used in various layers to make a sleeve. Thickness of the sleeve is the total thickness of all the layers present in that particular sleeve. In FEA, thickness of the sleeve is mentioned in terms of thickness of the pipe (t_p).

The stiffness of the sleeve is the product of the amount of material present in the sleeve and the type of the material used, i.e. thickness of the sleeve and tensile modulus of

elasticity of FRP (E_st_s). It is a function of sleeve thickness provided the modulus of elasticity remains the same. Stiffness has been calculated in terms of the ratio between the stiffness of sleeve to the stiffness of the pipe (E_st_s/E_pt_p). For a constant length, width, and tensile modulus of elasticity of a sleeve, the more thicker the sleeve, the stiffer is the sleeve. Since stiffness of the pipe (E_pt_p) is the same for all FE models, the higher the stiffness of the sleeve, the higher the stiffness ratio (E_st_s/E_pt_p). In other words stiffness ratio is a function of sleeve thickness (t_s) for all configured FE models. Stiffness ratio is denoted by symbol "ρ ".

The performance of a sleeve may be judged by post buckling capacity, ductility, and mode of failure of the pipe. The effect of length and gap size of the sleeves on the behaviour of the pipe for all sleeve configurations is discussed in the following sub-sections. The effect of sleeve stiffness and thickness will be discussed in section 5.5.

5.4.1 Single Sleeve

The length of sleeve(s) is discussed in terms of diameter (d) of the pipe. In order to observe effect of varying sleeve length on the post buckling capacity of the pipe, four different sleeve lengths of 0.42d, 0.50d, 0.58d and 0.66d were modelled. A sleeve length shorter than 0.50d may not provide reasonable strength to the pipe and may cause an inward buckling in the pipe.

The moment-curvature behaviour of a single sleeve shows that length of the sleeve does not significantly affect the post buckling moment capacity of the pipe provided a constant stiffness ratio is used. As shown in **Figure 5.6**, the post buckling capacity remains almost the same for different sleeve lengths. A single sleeve stops the growth of the primary wrinkle effectively. However, as indicated from the previous studies, a secondary wrinkle is formed at the edge of the sleeve, at a rate of growth normally faster than the primary wrinkle. A similar mode of outward (bulge) buckling was observed for single sleeves having lengths of 0.50d, 0.58d and 0.67d. A mode of inward buckling was found for the sleeve length of 0.33d.

5.4.2 Odd Sleeves

In order to observe the effect of varying middle sleeve length on the behaviour of the pipe, 0.33d and 0.50d long middle sleeves were modelled with a constant stiffness ratio of 0.30. The length of the sleeves was chosen keeping the length of the primary wrinkle in mind. Since the wrinkle wave-length is approximately 0.28d to 0.31d, anything shorter than a 0.33d sleeve may not be able to cover the full length of the wrinkle. Post buckling capacity increases when the length of the middle sleeve is increased as shown in **Figure 5.7**, post buckling moment capacity for a 0.50d sleeve is little more than that of a 0.33d sleeve of the same gap size and stiffness ratio. This means that the longer sleeve provides more strength to the pipe.

In order to observe the effect of varying gap sizes on the behaviour of the pipe, 0.33d and 0.50d long middle sleeves were modelled with varying gap sizes. The stiffness ratio was kept constant (0.30). It is observed for both 0.33d and 0.50d sleeves that the post buckling capacity of the pipe decreases when the gap is increased from 0.08d to 0.33d or vice versa as shown in **Figure 5.8**. Smaller gaps provide more strength to the sleeved region and enable the pipe to resist more loads. A gap longer than 0.33d results in almost the same post buckling capacity. This happens because a 0.33d or longer gap disregards the effectiveness of side sleeves and causes the sleeves to act as a single sleeve. A 0.50d single sleeve is compared with an odd sleeves configuration having a middle sleeve of 0.50d and side sleeves of 0.33d. **Figure 5.9** shows that a gap longer than 0.33d in an odd sleeve gives similar moment-curvature behaviour to a single sleeve. It can be concluded that the post buckling capacity of a repaired pipe may increase when the gap is reduced provided all other parameters remain the same for an odd sleeve configuration.

The sleeve thickness has significant impact on the post buckling capacity and the ductility of a repaired pipe. The effect of varying thickness was analyzed on a 0.33d long middle sleeve with a gap size of 0.08d. The buckling capacity and ductility increase when the thickness of the sleeves is increased as shown in **Figure 5.10**. This is because of an increase in fibre stiffness in the global hoop direction. The effect of sleeve stiffness is

discussed in detail in 5.5.2. The growth of the primary wrinkle continues if less than $0.77t_p$ middle sleeve is used. Due to the fibre fracture problem during the experiments, it is recommended that a sleeve thickness of more than $0.77t_p$ be provided.

We can summarize the above discussions. When odd sleeve configuration is used to repair a wrinkled pipe, the post buckling capacity of the pipe increases if length and thickness of the middle sleeve are increased. Smaller gaps provide more capacity than longer gaps. Gap sizes should be kept shorter than 0.33d otherwise odd sleeves may produce the effect of a single sleeve.

5.4.3 Even Sleeve

The length of middle sleeves has a significant effect on the behaviour of the pipe. In order to analyze this effect, gap sizes, stiffness and thickness of the sleeves were kept constant whereas sleeve length was varied, in which 0.08d, 0.17d, and 0.25d long middle sleeves were modelled. Middle and side gaps were kept at 0.08d and 0.17d respectively and the stiffness ratio was 0.30. The length of side sleeves was kept constant at 0.33d.

It is observed that the post buckling capacity and the ductility of the pipe increase when the length of the middle sleeves is increased as shown in **Figure 5.11**. Longer middle sleeves may increase the stiffness of the sleeved region and provide sufficient support to the wrinkled region to resist more bending moment. Smaller sleeves (0.08d) may not be able to cover the full length of the wrinkled surface and stop the growth of the primary wrinkle.

In order to analyze the effect of varying side gap sizes, length, stiffness and size of the middle gap of the sleeves were kept constant. Effect of side gap sizes was analyzed for three sets of middle sleeve length.

In the first set of analysis, 0.08d middle sleeves were modelled. Side sleeves were 0.33d, the middle gap was 0.08d and the stiffness ratio was 0.30. Side gap sizes were varied, in

which 0.08d, 0.17d, 0.25d, and 0.33d side gaps were provided. It is observed that varying gap sizes has a negligible effect when 0.08d long middle sleeves are used. Moment capacity does not vary significantly when side gap sizes are varied as shown in **Figure 5.12**. Even though the side gap sizes have impact on the behaviour of the pipe, a 0.08d long middle sleeve may not improve post buckling capacity for any gap size.

In the second set of analyses, 0.17d middle sleeves were modelled with all other parameters kept similar to the first set of analysis. It was observed that side gap sizes have a significant effect on the post buckling capacity and ductility of the pipe. Post buckling capacity and ductility increase when gap size decreases or vice versa as shown in **Figure 5.13**.

In the third set of analysis, 0.25d middle sleeves were modelled with all other parameters kept similar to the first and second sets of analysis. It was observed that the post buckling capacity and the ductility of the pipe increase if side gap sizes are decreased. Maximum post buckling capacity is achieved when the side gap is 0.08d as shown in **Figure 5.14**. Post buckling capacity curves for all three sets of analysis are shown in **Figure 5.15**. It may be concluded that gap size is effective only when 0.17d or 0.25d middle sleeves are provided. Post buckling capacity and ductility of the repaired pipe increase when gap sizes are decreased or vice versa provided the length of the middle sleeves is 0.17d or greater. Since 0.08d middle sleeves may not significantly improve flexural capacity for any gap size, it is recommended that at least 0.17d middle sleeves be provided to obtain better repair results.

The location of the secondary wrinkle depends largely on gap size. If the gap between side sleeves and middle sleeves is increased to more than 0.17d, there are more chances for a secondary wrinkle to appear in the gaps (i.e. within the sleeved region). This will be discussed in detail in section 5.5.3.

The gap size between two middle sleeves (referred to as the middle gap) also has a significant effect on the post buckling capacity and failure mode of the wrinkled pipe.

Therefore in addition to side gap sizes, even sleeve configuration was also analyzed on the basis of the middle gap.

Since the length of the primary wrinkle is approximately 0.28d to 0.31d, a middle gap of more than 0.17d may not be effective because two middle sleeves will have to be placed too far from each other to stop the growth of the primary wrinkle. Therefore only two sets of middle gap sizes are considered for the analysis i.e. 0.08d and 0.17d.

In the first set of analysis, a 0.17d middle gap was provided. All other parameters except the side gap sizes were kept constant. Lengths of middle and side sleeves were 0.25d and 0.33d respectively and the stiffness ratio was 0.30. Side gap sizes were varied. It was observed that there was no significant change in the behaviour of the pipe when the side gaps were varied and the post buckling capacity is low, as shown in **Figure 5.16**. This is because of the inability of the middle sleeves to stop the growth of the primary wrinkle. Even though lower post buckling capacity is achieved, it is still more than if the pipe was not repaired. The secondary wrinkle does not appear when the middle gap is 0.17d and the primary wrinkle continues to grow. Therefore it is recommended that a middle gap longer than 0.08d should not be used.

In the second set of analysis, middle gap size was reduced to 0.08d and all other parameters were kept the same as mentioned for the first set. Side gap sizes were varied. It is observed that contrary to the results of the 0.17d middle gap, post buckling capacity and ductility vary significantly when side gap sizes are varied as shown in **Figure 5.14**. This means that a middle gap longer than 0.08d may disregard the effect of varying side gap sizes.

The effect of the length of the side sleeves on the post buckling capacity was also analyzed. 0.25d, 0.33d and 0.42d side sleeves were modelled. The lengths of the middle sleeves and the middle gap were kept constant at 0.25d and 0.08d respectively. Two sets of 0.08d and 0.25d long side gap sizes were chosen. For each set of side gap, the length of side sleeves was varied. It is observed that the effect of varying side sleeve length on

the post buckling capacity of the pipe is negligible. 0.25d, 0.33d and 0.42d long side sleeves provided almost the same post buckling capacity if all other parameters remain same as shown in **Figure 5.17**. It seems that there is no significant difference between using 0.25d, 0.33d and 0.42d long side sleeves when all other factors are same. However, 0.33d long side sleeves are used in most of the multiple sleeve models in FEA.

5.5 SLEEVE STIFFNESS

An effective and optimum sleeve design is the one which enables the wrinkled pipe to resist secondary (post buckling) moment capacity approximately equal to the primary moment, provides more ductility to the pipe and enables the pipe to fail in an outward secondary wrinkle. The higher the post buckling capacity and the ductility of a repaired pipe, the longer is the service life of the pipe. Mode of failure of the repaired pipe is important because it might be possible to repair the pipe more than one time if an outward secondary wrinkle appears. The repair after the appearance of a secondary wrinkle is referred here to as a sequential sleeve repair.

In the following subsections we will discuss the effect of varying sleeve stiffness on the post buckling capacity and the failure mode of the pipe.

5.5.1 Single Sleeve

Initially five single sleeves of different length were modelled. Stiffness of each sleeve was varied to observe its effect on the post buckling behaviour of the pipe. 0.33d, 0.42d, 0.50d, 0.58d, and 0.67d long single sleeves were analyzed with varying stiffness ratios for each particular length of the sleeve. It is observed that a sleeve shorter than 0.42d mostly fails in inward buckling which does not allow any further repair of the pipe by using external sleeves. A 0.33d long sleeve with an inward buckle is shown in **Figure 5.18**. Therefore it is suggested that 0.50d or longer single sleeve be used to avoid inward buckling.

A 0.50d long single sleeve was modelled with varying stiffness ratios (0.11 to 0.54). The post buckling capacity of the pipe is the minimum for a stiffness ratio of 0.11 and reaches a maximum value at a stiffness ratio of 0.37 as shown in **Figure 5.19**. When stiffness of the sleeve is increased, the post buckling capacity of the pipe also increases. But the increase is neither constant nor consistent. The post buckling capacity remains almost the same for a stiffness ratio of more than 0.37.

Similar procedure is adopted for a 0.58d long sleeve. The results were almost identical to those of the 0.50d sleeve i.e. the post buckling capacity increases when the stiffness ratio is increased to 0.37 and then remains almost the same for a stiffness ratio of more than 0.37. The results obtained for 0.50d and 0.58d sleeves are plotted in **Figure 5.20**. The post buckling behaviour of the pipe repaired with 0.50d and 0.58d sleeves varies significantly when the stiffness ratio varies from 0.11 to 0.37 but remains the same for stiffness ratios greater than 0.37. It is also evident from **Figure 5.20** that a sleeve length of 0.50d or greater may produce almost the same post buckling capacity. It was also observed that a single sleeve can hardly produce a secondary moment capacity equal to the primary moment capacity.

Stiffness ratio has a significant effect on the failure mode of the pipe. A 0.50d single sleeve with varying stiffness ratios (0.11 to 0.53) was modelled. For stiffness ratios of less than 0.30, the growth of the primary wrinkle may not be stopped. Failure mode of a 0.50d sleeve with a stiffness ratio of 0.11 is shown in **Figure 5.21**. It seems that the primary wrinkle continues increasing. The growth of the primary wrinkle may be stopped when stiffness ratios of more than 0.30 are used. Even though a stiffness ratio of more than 0.30 stops the growth of the primary wrinkle, there is possibility of inward buckling if the stiffness ratio is less than 0.41. When the stiffness ratio is increased to 0.41, outward secondary wrinkle appears as shown in **Figure 5.22**.

It can be concluded that stiffness ratio and sleeve length play a vital role in achieving optimum sleeve design. Most of the repair techniques on the basis of FEA suggest that multiple sleeve design be preferred over a single sleeve. A single sleeve is desired due to

its simplicity and easiness in application, a 0.50d single sleeve with a stiffness ratio of 0.41 seems to be the optimum sleeve design as far as the post buckling capacity and the mode of failure of the pipe is concerned.

5.5.2 Odd Sleeve

For an odd sleeve configuration the post buckling capacity depends on the length of the middle sleeve, stiffness ratio and side gap size. The effect of varying length and gap sizes has already been discussed in section 5.4.2. In order to analyze the effect of the stiffness ratio on the post buckling capacity of the pipe, odd sleeves having a middle sleeve length of 0.33d and 0.50d were modelled and stiffness ratios were varied.

In the first analysis, the length of middle and side sleeves was 0.33d and gap size was kept constant at 0.17d while the stiffness ratio was varied from 0.11 to 0.45. The post buckling capacity of the pipe increases when the stiffness ratio is increased as shown in **Figure 5.23**. The stiffness ratio of 0.45 provides maximum post buckling capacity and ductility.

In the second analysis, the length of the middle sleeve was increased to 0.50d while gap size and side sleeve length were kept unchanged. The stiffness ratio was varied from 0.11 to 0.37. The post buckling capacity increases significantly when the stiffness ratio is increased from 0.11 to 0.24 as shown in **Figure 5.24**.

It can be concluded for odd sleeve configuration that the post buckling capacity of a repaired pipe increases when the stiffness ratio is increased.

In order to elaborate on the combined effect of varying stiffness and the length of the middle sleeve, three curves are plotted in **Figure 5.25**. Each curve represents a fixed sleeve length and varying stiffness ratio. Gap size and the length of side sleeves are 0.17d and 0.33d respectively. It seems that there is a trade off between the stiffness ratio and the length of the middle sleeve. If the length of middle sleeve is increased, maximum post

buckling capacity is achieved at a lower stiffness ratio or vice versa. A 0.33d middle sleeve needs a stiffness ratio of 0.42 to resist the post buckling capacity equal to the primary moment capacity. Whereas a 0.42d middle sleeve needs a stiffness of 0.30, a 0.50d sleeve needs a stiffness ratio of 0.22 to resist the same amount of post buckling capacity. This means if we provide longer middle sleeves then we may achieve higher post buckling capacity at lower stiffness ratio or vice versa.

In order to investigate the combined effect of varying stiffness and gap size, two curves are plotted in **Figure 5.26**. Each curve represents a constant sleeve length of 0.33d. Two different gap sizes of 0.17d and 0.33d are provided and stiffness ratios are varied for each curve. For a 0.17d gap, the secondary moment equal to the primary moment capacity is achieved when the stiffness ratio is about 0.42 as shown in **Figure 5.26**. The same capacity is achieved for a gap size of 0.33d when the stiffness ratio is 0.62. This shows that if we increase the gap size, we will have to provide a stiffer sleeve in order to achieve the secondary moment equal to the primary moment.

So increasing the stiffness ratio and the length of the middle sleeve and reducing the gap size may contribute towards increasing secondary moment provided other factors remain the same. For most of the odd sleeve designs, there is no significant change in secondary moment if the stiffness ratio is more than 0.45.

The location of the secondary wrinkle largely depends on the gap size whereas the type of the wrinkle depends largely on the stiffness ratio. In most of the cases for lower stiffness ratios, the growth of the primary wrinkle cannot be stopped and the secondary wrinkle may not appear.

In order to observe the effect of the stiffness ratio on the failure mode of the pipe, two sets of sleeve geometry were modelled with all parameters kept constant except the stiffness ratio. In the first set of analysis, the length of sleeves was 0.33d and gap size was 0.17d. Stiffness ratio was varied from 0.11 to 0.50. It was observed that for lower stiffness ratio, the growth of the primary wrinkle cannot be stopped and the secondary

wrinkle does not appear. The primary wrinkle continued growing when a stiffness ratio was 0.26 or less as shown in **Figure 5.27**. Failure mode changes to inward buckling for a stiffness ratio of 0.26 to 0.42. When the stiffness ratio is increased to 0.50, the secondary wrinkle appears outside the sleeved region as shown in **Figure 5.28**. Because of the shorter gap size of 0.17d, the secondary wrinkle appears outside the sleeved region. An outward secondary wrinkle within sleeved region might have appeared if the gap size would have been increased to 0.25d or 0.33d. It should be remembered that a gap size of more than 0.33d is not used because it has already been mentioned that it would cause the odd sleeve to act as a single sleeve. Since inward buckling may occur if we use a stiffness ratio of less than 0.50, it is recommended that a stiffness ratio of 0.50 be used for a 0.33d long middle sleeve with a gap size of 0.17d.

In the second set of analysis, the length of the middle sleeve was increased to 0.50d and all other parameters were kept the same as mentioned in the preceding paragraph. For a stiffness ratio of less than 0.20, the primary wrinkle continues to grow as shown in **Figure 5.29**. When the stiffness ratio is increased to 0.30, an outward secondary wrinkle appears outside the sleeved region as shown in **Figure 5.30**. The sleeved region is referred to as the portion of the pipe length strengthened by the sleeves.

The location of the outward secondary wrinkle is governed by gap size. For a 0.33d middle sleeve with a gap size of 0.17d, the secondary wrinkle appears outside the sleeved region when the stiffness ratio is 0.50 or more as shown in **Figure 5.28**. For almost similar conditions, when the gap size is increased to 0.33d, the secondary wrinkle appears within the sleeved region as shown in **Figure 5.31**. Gap sizes of 0.25d or longer allow the secondary wrinkle to appear within the sleeved region. If gap sizes are 0.17d or shorter, the secondary wrinkle appears outside the sleeved region.

Based on FEA for odd sleeve configurations, a 0.42d long middle sleeve, with 0.33d long side sleeves, a gap size of 0.17d and a stiffness ratio of 0.37, is an optimum design configuration. Alternatively a 0.50d long middle sleeve, with 0.33d long side sleeves, 0.17d long gaps and a stiffness ratio of 0.30 is also an optimum sleeve design.

5.5.3 Even Sleeve

In order to analyze the effect of the stiffness ratio on the post buckling behaviour of the pipe, the length of sleeves and middle gap are kept constant while the stiffness ratio is varied. It has already been mentioned in subsection 5.4.3 that a middle gap of more than 0.08d may not significantly improve the flexural capacity of the pipe. Therefore the middle gap is kept constant (0.08d) for all the analyses in this subsection. The length of the side sleeves is 0.33d, also kept constant for all the analyses in this subsection. The length of the middle sleeves is 0.25d since less than 0.25d long middle sleeves may not provide sufficient moment capacity, which has already been discussed in subsection 5.4.3. Middle sleeves of more than 0.25d are not efficient since they provide similar capacity as 0.25d sleeves do. The stiffness ratio is varied from 0.15 to 0.54.

The post buckling capacity of the pipe increases when the stiffness ratio is increased as shown in **Figure 5.32**. It is observed that a secondary moment equal to the primary moment is achieved when the stiffness ratio is 0.30. There is no significant increase in the post buckling capacity if the stiffness ratio is increased from 0.30 to 0.54. It can be concluded that for this particular geometry of the sleeve, a stiffness ratio of 0.30 is reasonable.

In order to analyze the combined effect of varying gap sizes and the stiffness ratio, three curves are plotted as shown in **Figure 5.33**. Each curve represents a side gap of 0.17d, 0.25d and 0.33d whereas the length of the sleeves is the same for all the curves. The stiffness ratio is varied from 0.11 to 0.45. It is observed that for each gap size, the post buckling capacity increases when the stiffness ratio is increased. For the specific stiffness ratio, there is no significant difference in the secondary moment when different gap sizes are used. So it can be concluded that by increasing the stiffness ratio, the post buckling capacity can be increased whereas the ductility can be increased by decreasing the gap sizes as discussed in section 5.4.3 and shown in **Figure 5.14**.

The effect of the stiffness ratio on the failure mode of the pipe is also analyzed. The length of the sleeves, middle and side gaps are kept constant while the stiffness ratio is varied. The lengths of the middle and side sleeves are 0.25d and 0.33d respectively. The middle and the side gap sizes are 0.08d and 0.17d respectively. The stiffness ratio is varied from 0.11 to 0.54. It is observed that when the stiffness ratio is less than 0.30, the growth of the primary wrinkle may not be stopped and the secondary wrinkle may not appear as shown in **Figure 5.34**.

The secondary wrinkle appears when the stiffness ratio is 0.30 or greater. The location of the secondary wrinkle depends on the gap size. If the gap size is 0.17d or less, the secondary wrinkle appears outside the sleeved region provided the stiffness ratio is 0.30 or greater as shown in **Figure 5.35**. For the same sleeve configuration if the gap size is increased to 0.33d, the secondary wrinkle appears within the sleeved region as shown in **Figure 5.36**. When the secondary wrinkle appears outside the sleeved region, it seems convenient to apply sequential sleeves and the service life of the pipe can be increased.

On the basis of post buckling capacity and the failure mode of the repaired pipe, 0.25d long middle sleeves, with side sleeves of 0.33d, side and middle gaps of 0.17d and 0.08d respectively and a stiffness ratio of 0.37 seems to be an optimum sleeve design. Alternatively 0.25d long middle sleeves, with side sleeves of 0.33d, side and middle gaps of 0.25d and 0.08d respectively and a stiffness ratio of 0.45 seems to be an optimum sleeve design.

5.6 COMPARISON

In the preceding sections, the performance of each sleeve configuration with varying parameters has been discussed individually. In the following subsections, comparison among all sleeve configurations will be discussed.

5.6.1 Comparison between Even and Odd Sleeve Configurations

Even though both even and odd sleeves are considered multiple sleeve configurations, geometrically and technically both are significantly different from each other. However comparison of their performance is made on the basis of the post buckling capacity and the ductility of the repaired pipe. The same geometrical and material properties are used when they are compared with each other. Two sets of analyses are made.

In the first analysis, the side gap was 0.25d. The middle gap for even sleeve configuration was 0.08d. The stiffness ratio was 0.30 and the length of the side sleeves was 0.33d. The length of each middle sleeve was 0.25d for even sleeve configuration. A 0.50d long middle sleeve was modelled for odd sleeve configuration. For both even and odd sleeve configurations, the same amount of sleeve material was used. The comparison is based on the same amount of FRP materials used either by using two 0.25d long even middle sleeves or one 0.50d long odd middle sleeve, whereas side sleeves are 0.33d long and the same stiffness ratio of 0.30 for both configurations is used. Even though post buckling capacity for both sleeve configurations is not significantly different, an even sleeve configuration provides more ductility than that of an odd sleeve configuration as shown in **Figure 5.37**.

In the second analysis, the side gap was reduced to 0.17d whereas all other parameters were kept the same as discussed in the preceding paragraph. Even sleeve configuration provides more ductility than odd sleeve configuration as shown in **Figure 5.38**. Therefore it can be concluded that even though both even and odd sleeve configurations provide almost the same post buckling capacity for the given parameters, an even sleeve provides more ductile behaviour than an odd sleeve. The ductility of the pipe increases when the side gap sizes are decreased.

Odd sleeve configuration is susceptible to inward buckling especially for low or moderate internal (fluid) pressure. Fibre fracture is another problem in odd sleeves. It happens because the middle sleeve is placed directly on the crest of the primary wrinkle and

subjected to very high strains. These are a few disadvantages of using an odd sleeve configuration. The main advantage of using odd sleeve is its simplicity and ability to stop the primary wrinkle directly.

Even sleeve configuration is less likely to be susceptible to fibre fracture and inward buckling problems. It is also more likely to provide opportunity for sequential repairs. These advantages make even sleeves more attractive than odd sleeves. Even sleeve configuration requires more technical skill because accuracy is required for providing the middle gap.

5.6.2 Comparison between Even and Double Sleeve Configurations

Even and double sleeve configurations are basically the same. In the case of double sleeves, the side sleeves are not provided and only two middle sleeves are evenly applied to the wrinkled pipe.

Comparison is based on the same size of middle sleeves and the middle gap. The length of the middle sleeves was 0.25d, the middle gap was 0.08d and the stiffness ratio was 0.30. The side gap was 0.25d for even sleeves. Due to the side sleeves, more GFRP materials are used in the case of even sleeves. Both configurations provide almost the same post buckling capacity; however even sleeves provide more ductile behaviour than double sleeves as shown in **Figure 5.39**.

5.6.3 Comparison between Single and Odd Sleeve Configurations

Single and odd sleeve configurations are compared on the basis of the same length and stiffness of the middle sleeve. Since side sleeves and gap size do not exist in single sleeves, only the stiffness ratio and length of the middle sleeve were kept identical to compare these two configurations. The length of the middle sleeve was 0.50d and the stiffness ratio was 0.30. For odd sleeve configuration, the length of the side sleeves was 0.33d and the side gap size was 0.25d. Similar types of moment-curvature behaviour were observed. Odd sleeve configuration provides more post buckling capacity and

ductility than a single sleeve, though the difference is not very significant as shown in **Figure 5.40**. In the case of a single sleeve either inward buckling or a secondary wrinkle appeared adjacent to the sleeve edges depending on the length and stiffness of the middle sleeve, whereas the location of the secondary wrinkle can be manoeuvred by varying gap sizes in odd sleeve configuration. A single sleeve of 0.50d or longer may produce an outward secondary buckle adjacent to the sleeve but a less than 0.5d long sleeve is not recommended because it might produce an inward buckle. The odd sleeve seems to be a better design than the single sleeve since it gives more ductility, strength and variation in the mode of failure than a single sleeve.

5.6.4 Overall Comparison

In order to compare the performance of all different configurations, the stiffness ratio was kept constant at 0.30. For odd and even sleeve configurations, the length of the side sleeves was 0.33d and the side gap was 0.25d. The length of the middle sleeve was 0.50d for single and odd sleeves. For even and double sleeves, each middle sleeve was 0.25d and the middle gap was 0.08d. The moment-curvature behaviour of double, single and odd sleeve configurations is almost the same, whereas even sleeves provide slightly more post buckling capacity and ductility than all other configurations as shown in **Figure 5.41.** However the failure modes are different for each sleeve configuration, already discussed in the preceding sections. The failure mode and the ductility make the even sleeves more advantageous than other configurations.

5.7 SEQUENTIAL SLEEVE REPAIR

FEA and experimental results reveal that flexural capacity of a buckled pipe increases when the sleeves are applied but eventually it drops followed by either appearance of a secondary wrinkle or further growth of the primary wrinkle. To ensure a longer service life, it is necessary to design a sleeve configuration that may not only strengthen the wrinkled pipe but also provide a possibility of repair when the secondary wrinkle

appears. When the pipe is repaired two or more times, it is referred to as sequential sleeve repair.

When an outward secondary wrinkle appears, it is possible to repair the pipe again by applying sleeves on the secondary wrinkle. The pipe may resist external loads again after being repaired a second time. This is possible for most of cases when the secondary wrinkle appears outside the sleeved region so that sufficient space is available to apply the sleeves.

Sequential sleeve repair was also modelled and analyzed. The unbuckled pipe model was loaded until the primary wrinkle appeared. 0.25d double sleeves were applied to the wrinkled pipe with a middle gap of 0.08d and a stiffness ratio of 0.37. The sleeves were supposed to stop the growth of the primary wrinkle and provide the post buckling capacity almost equal to the primary moment. The pipe was reloaded when the sleeves had been applied. The pipe started resisting external loads again until a secondary wrinkle appeared along the edges of the sleeves as shown in **Figure 5.42**.

Then 0.33d long sleeves were applied to the secondary wrinkle and the pipe was reloaded. The pipe started resisting the loads again until another (tertiary) wrinkle appeared in the pipe wall as shown in **Figure 5.43**. The pipe was unloaded and the sleeves were applied again as shown in **Figure 5.44**. In this way the pipe can be repaired several times and its service life can be increased. The first repair acts as an even sleeve configuration because sleeves are applied having a gap between them, whereas the second repair acts as an odd sleeve because the sleeves are placed directly on the wrinkle crest.

The moment-curvature behaviour is shown in **Figure 5.45**. It is observed that the pipe achieves almost the same moment capacity after every repair, and the repair has also provided stable post buckling behaviour.

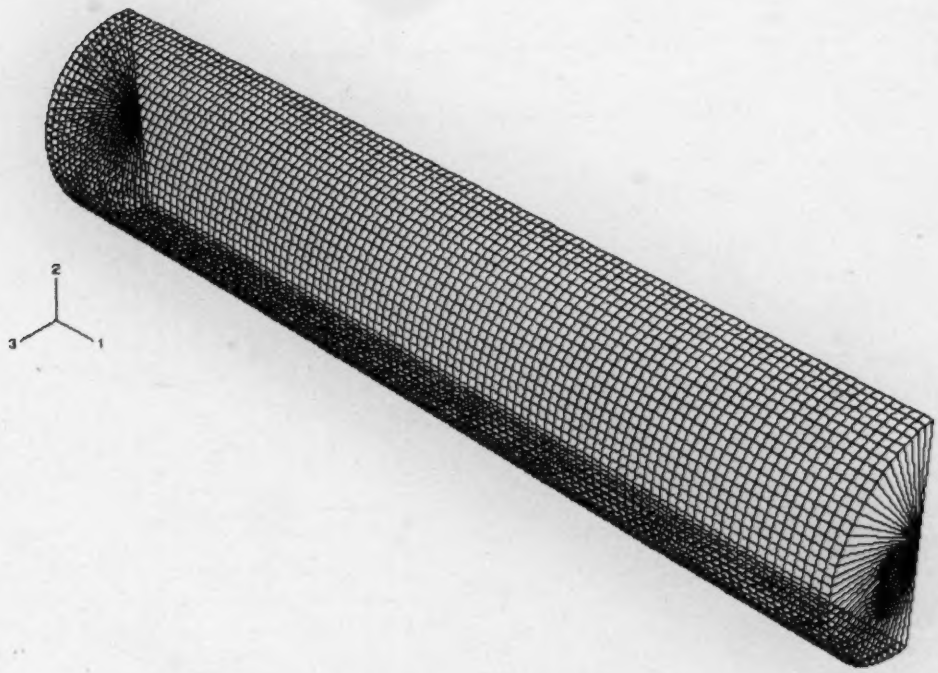

Figure 5.1 Finite Element Model of the pipe

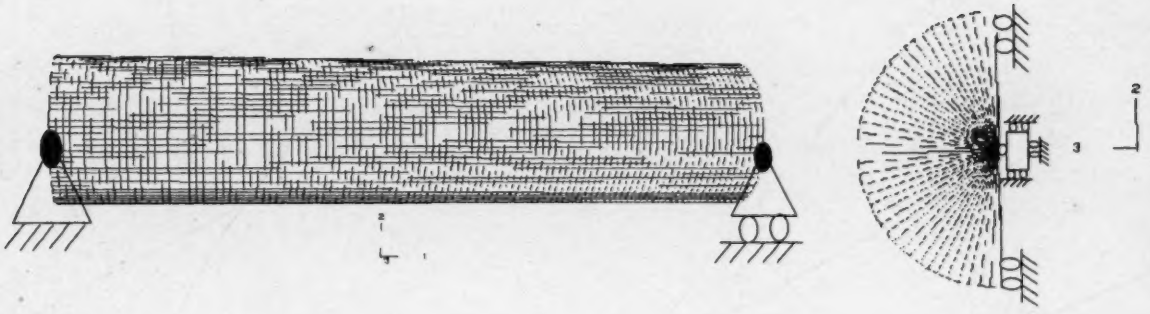

Figure 5.2 Boundary conditions

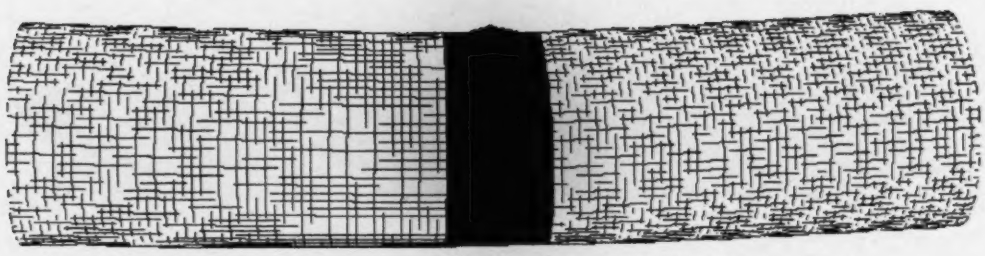

Figure 5.3 Single sleeve configuration

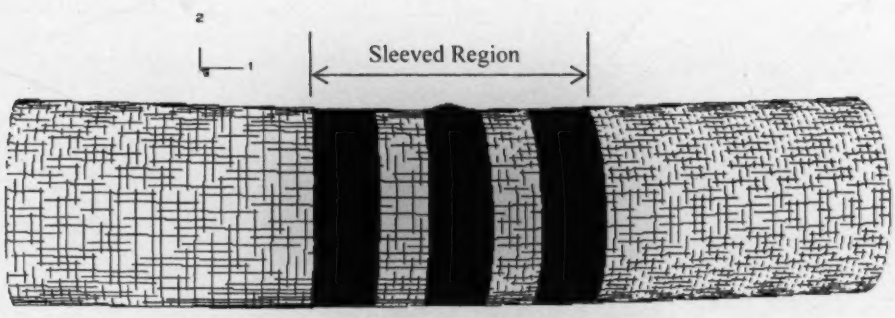

Figure 5.4 Odd sleeve configuration

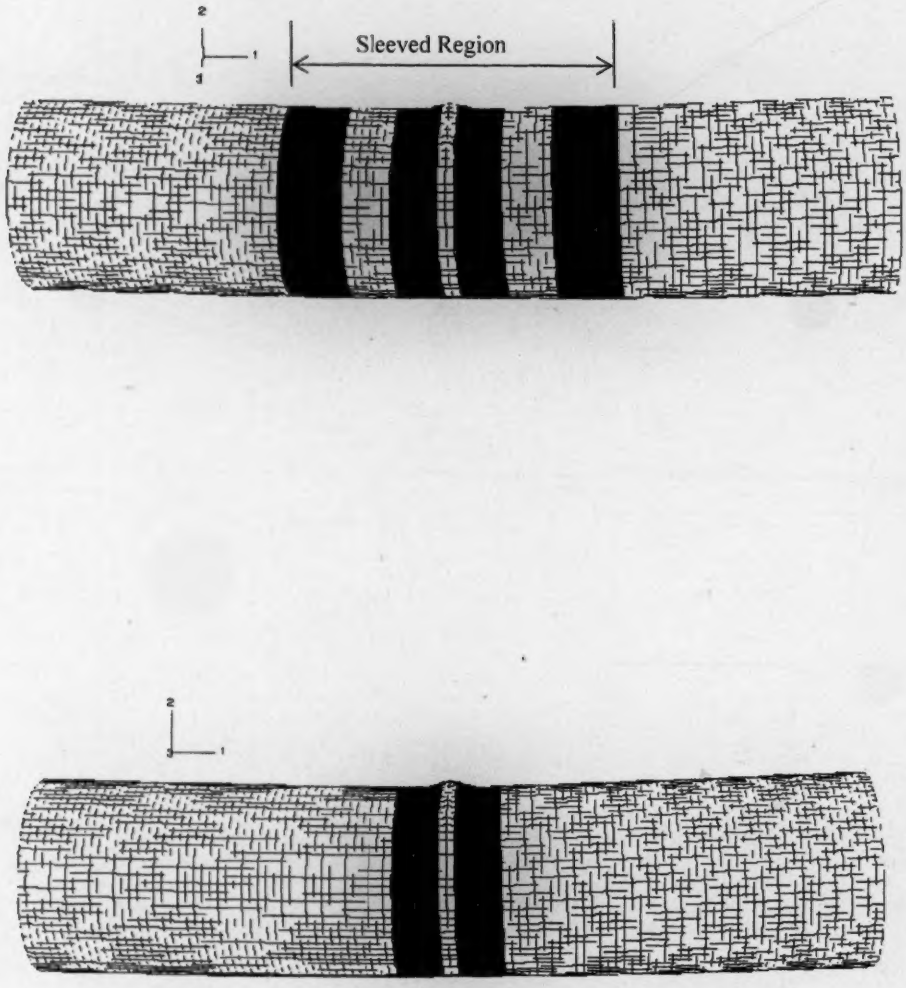

Figure 5.5 Even sleeve configuration

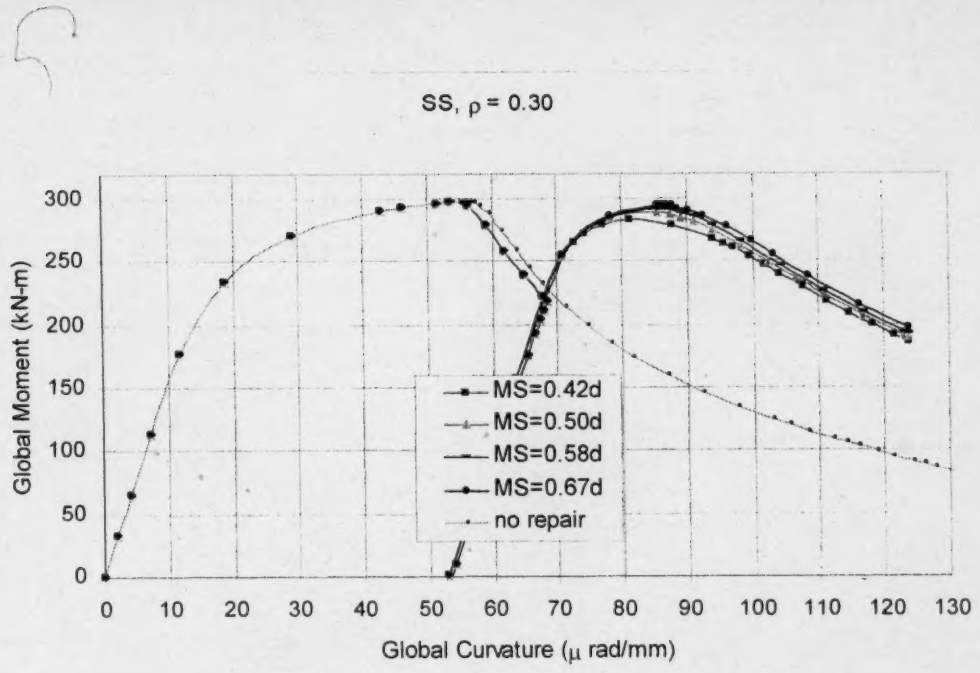

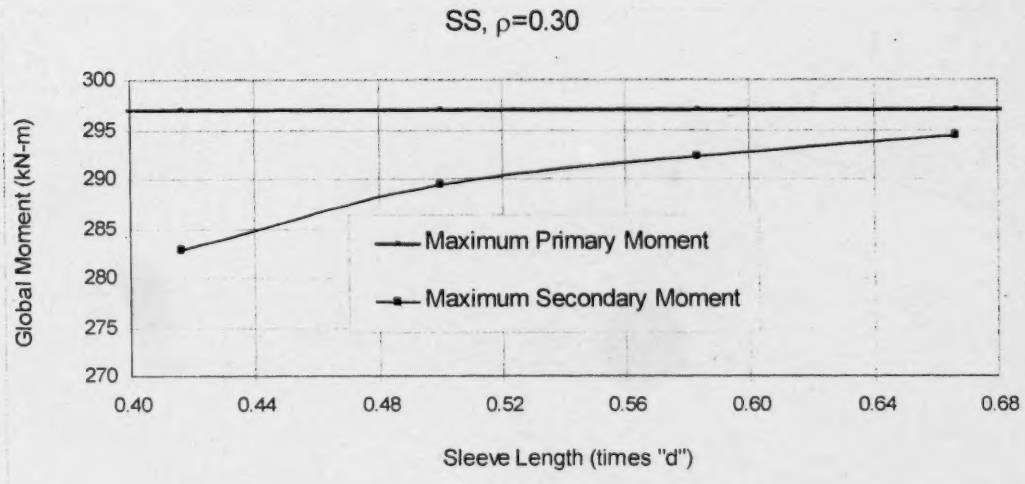

Figure 5.6 The effect of varying sleeve length for single sleeve

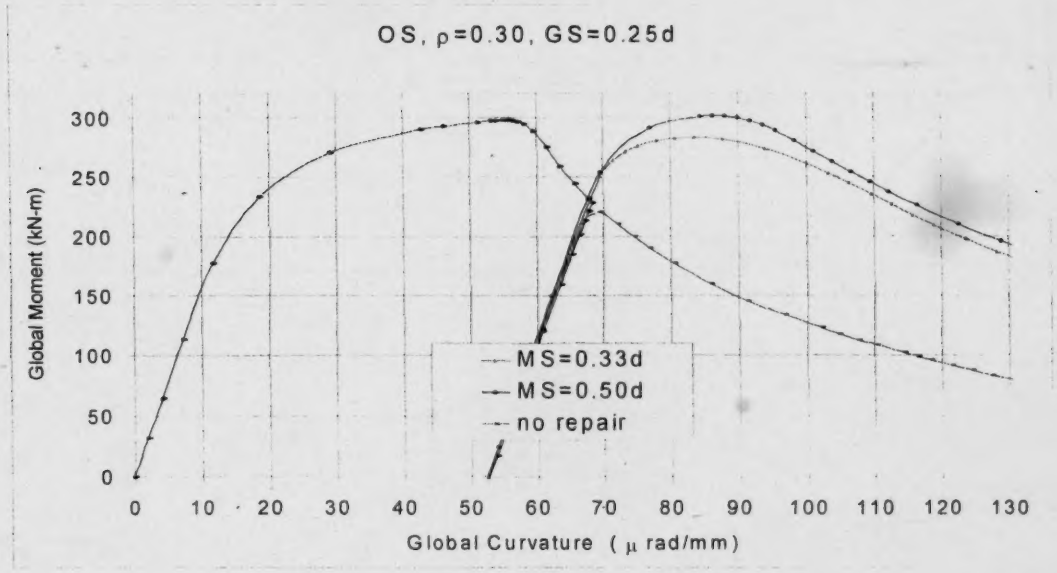

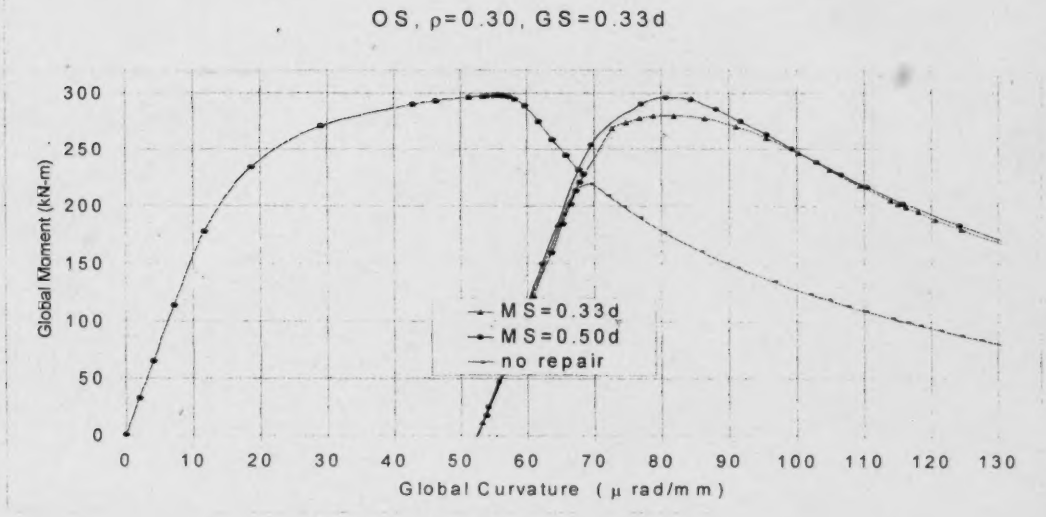

Figure 5.7 The effect of varying middle sleeve length for odd sleeve configuration

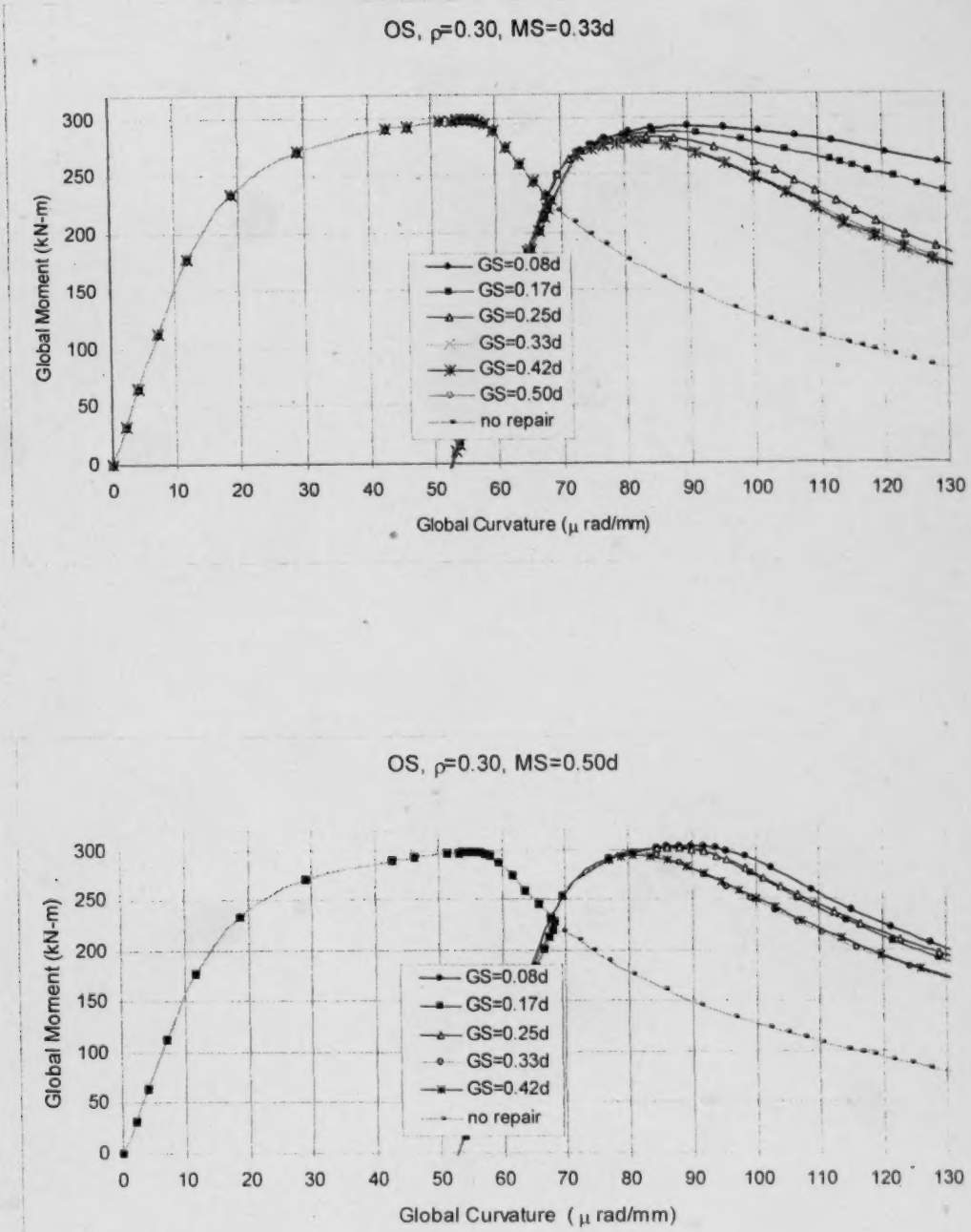

Figure 5.8 The Effect of varying gap size for odd sleeve configuration

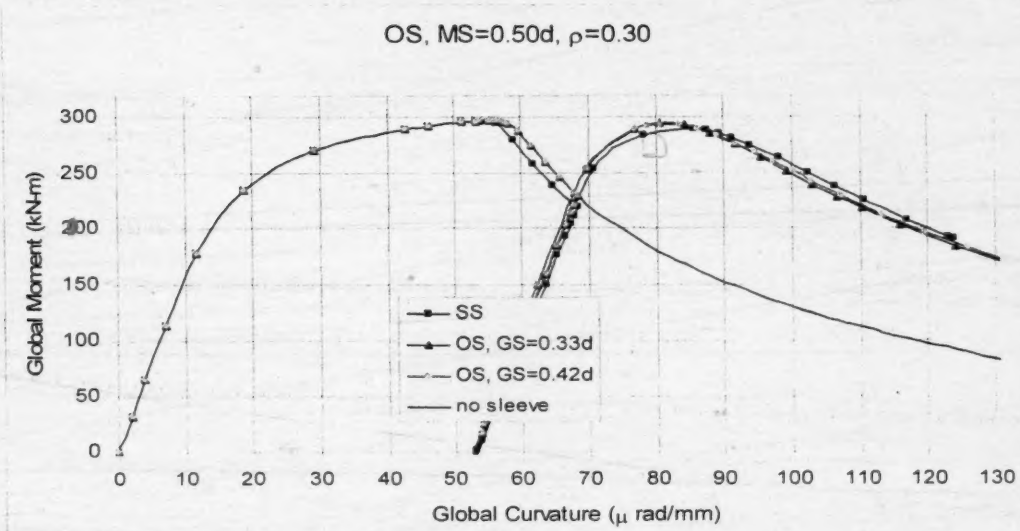

Figure 5.9 The effect of wider gaps for odd sleeve configuration

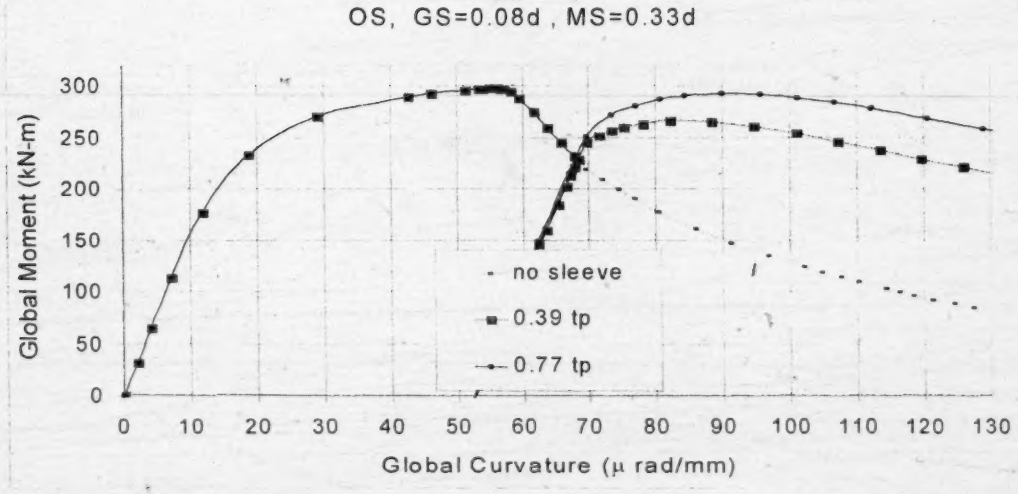

Figure 5.10 The effect of varying thickness of odd sleeve configuration

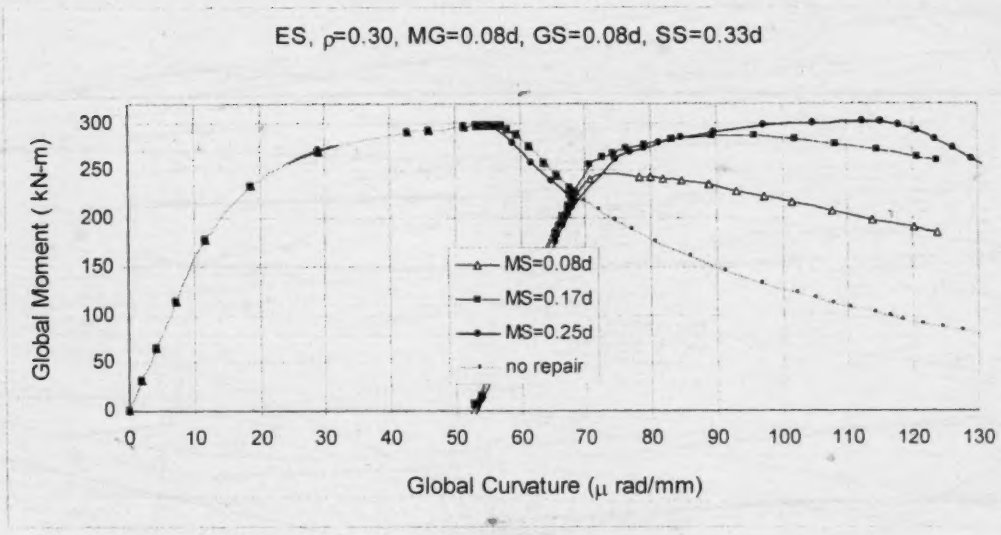

Figure 5.11 The effect of varying length of middle sleeves for even sleeve configruation

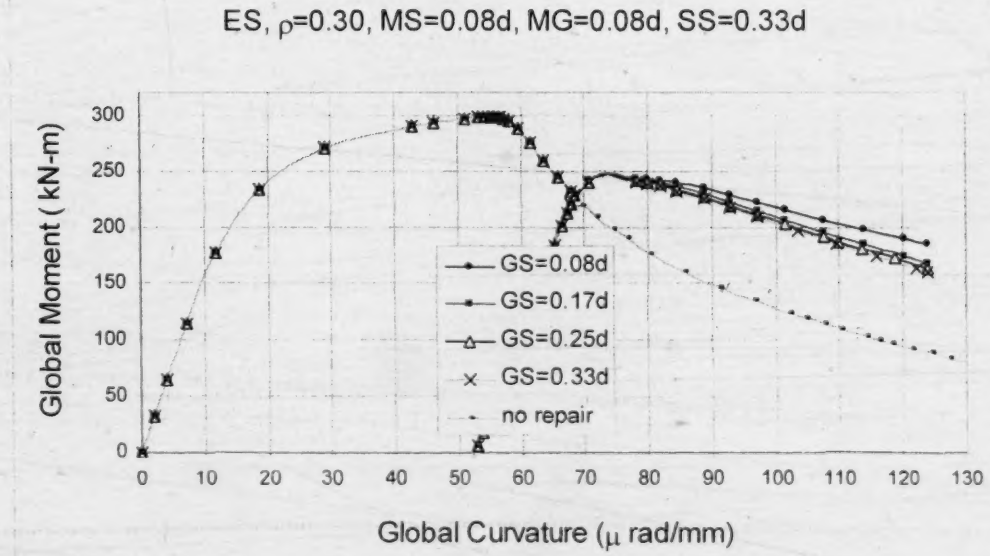

Figure 5.12 The effect of varying side gap sizes for even sleeve configuration

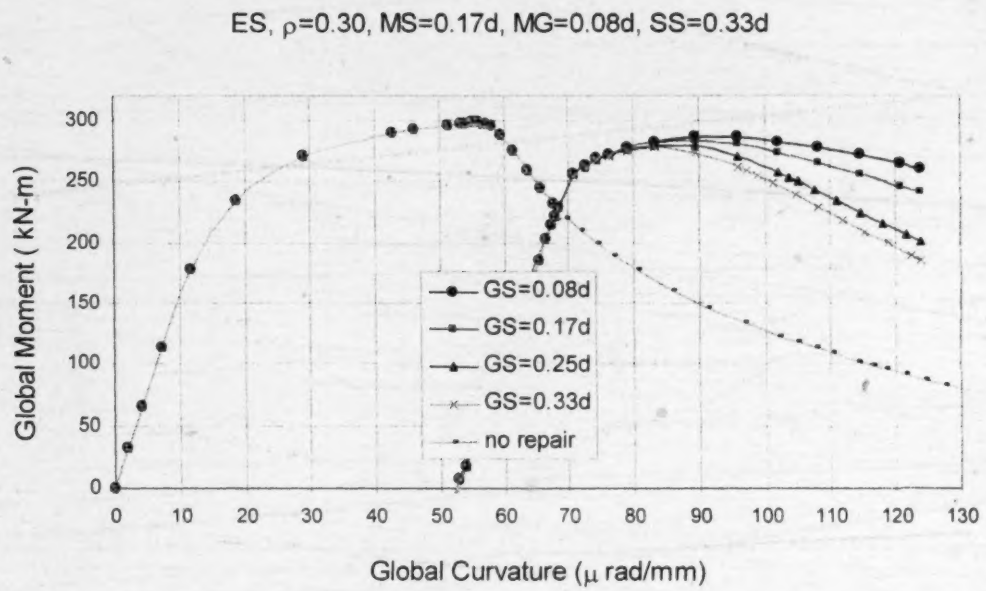

Figure 5.13 The effect of varying side gap sizes for even sleeve configuration

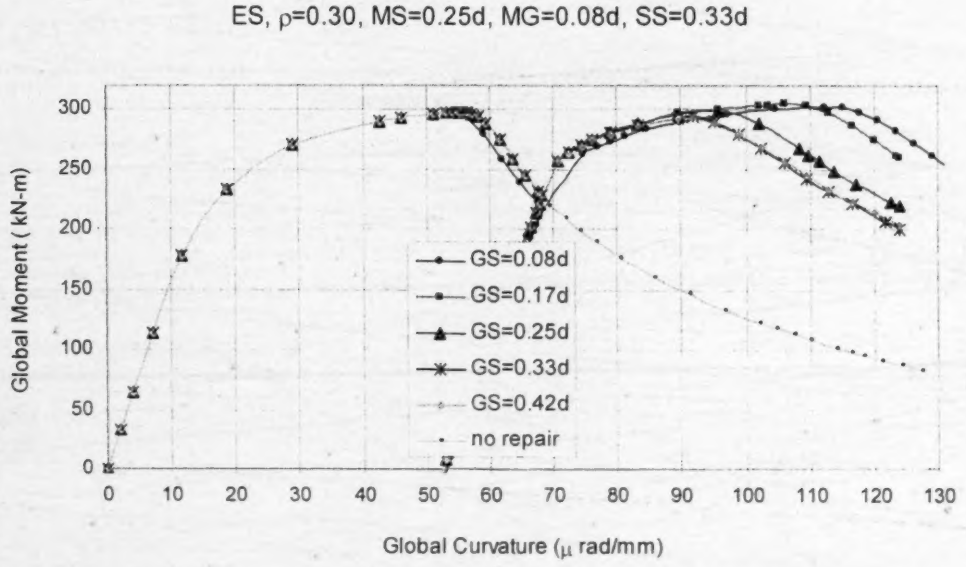

Figure 5.14 The effect of varying side gap sizes for even sleeve configuration

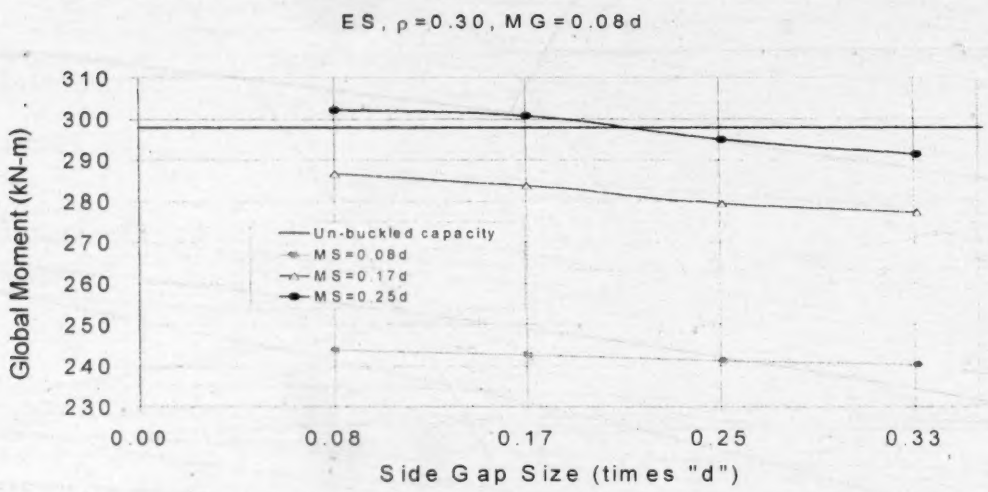

Figure 5.15 The effect of varying side gap sizes for even sleeve configuration

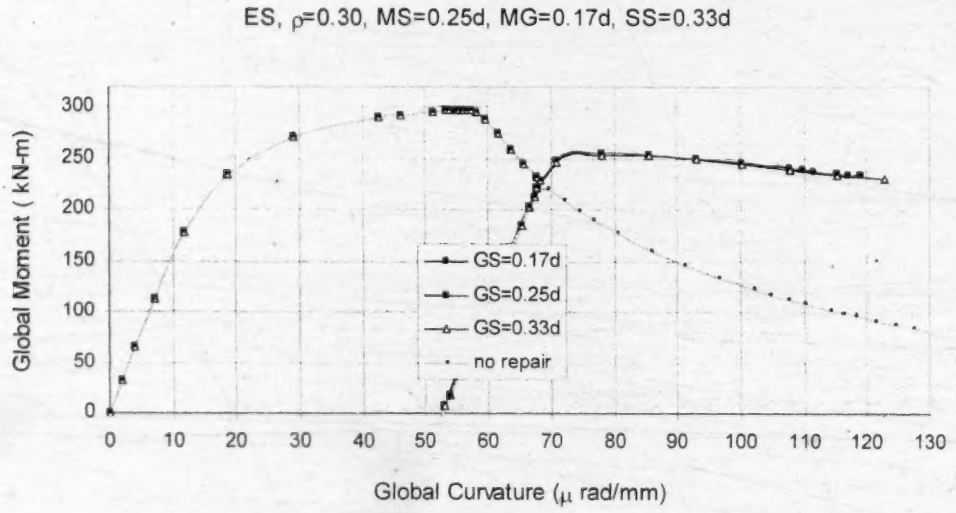

Figure 5.16 The effect of varying side gap sizes for even sleeve configuration

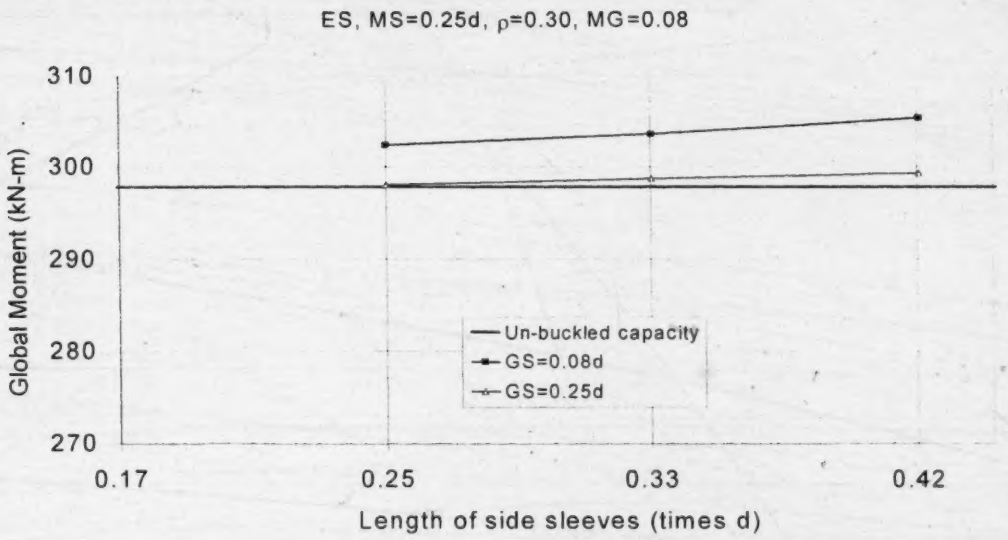

Figure 5.17 The effect of side sleeve length for even sleeve configuration

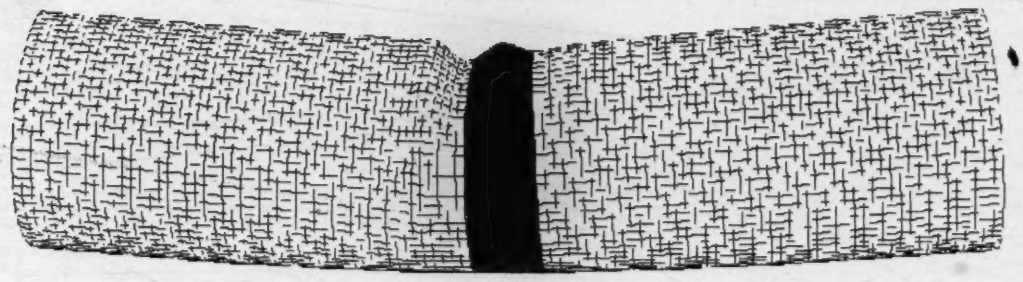

Figure 5.18 Inward buckling in a 0.33d single sleeve

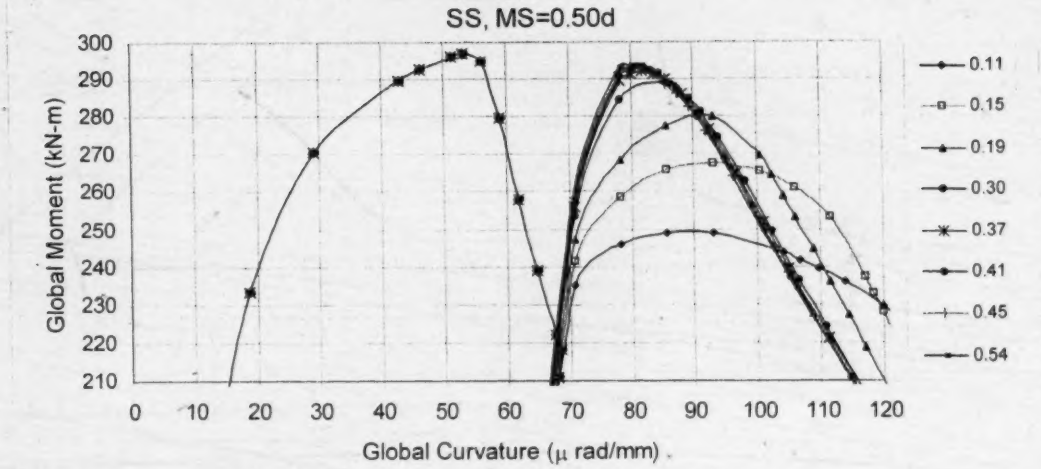

Figure 5.19 The effect of varying stiffness ratios (E_st_s/E_pt_p) for single sleeve

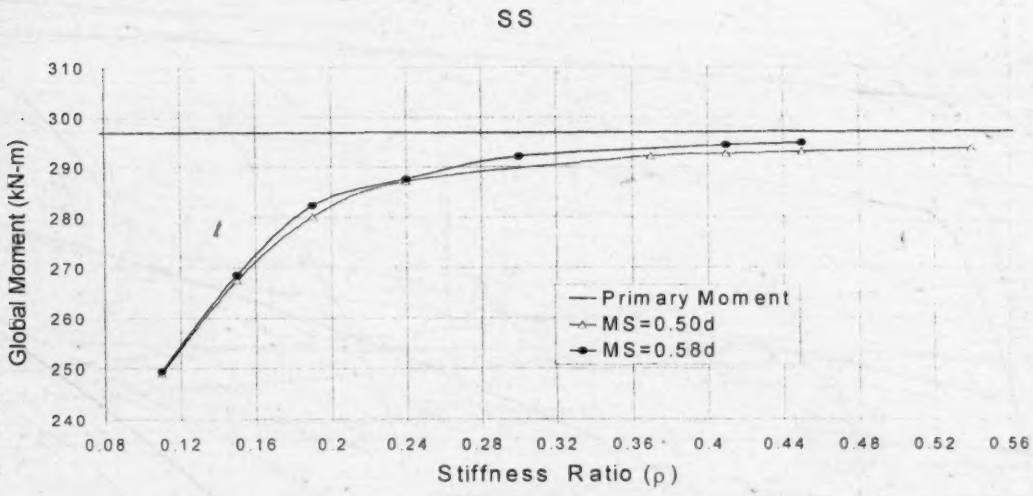

Figure 5.20 The effect of varying stiffness ratios (E_st_s/E_pt_p) for single sleeve

Figure 5.21 Failure mode of a 0.50d single sleeve ($\rho = 0.11$)

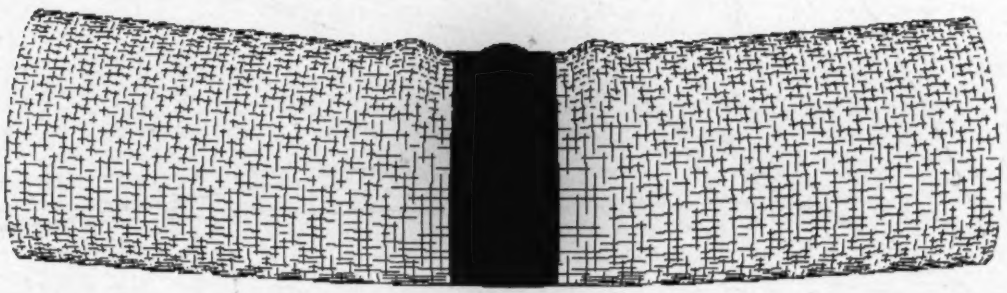

Figure 5.22 Failure mode of a 0.50d single sleeve ($\rho = 0.41$)

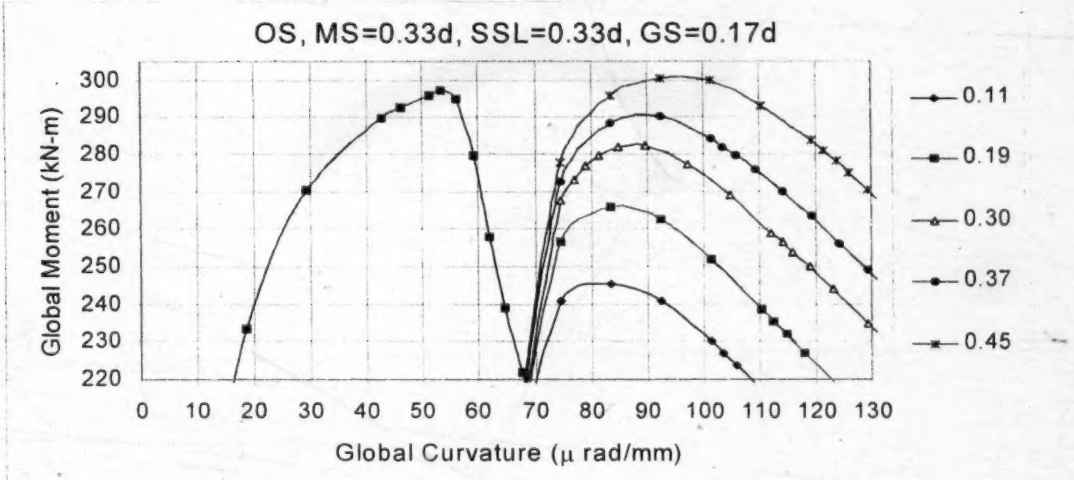

Figure 5.23 The effect of varying stiffness ratios (ρ) for odd sleeve configuration

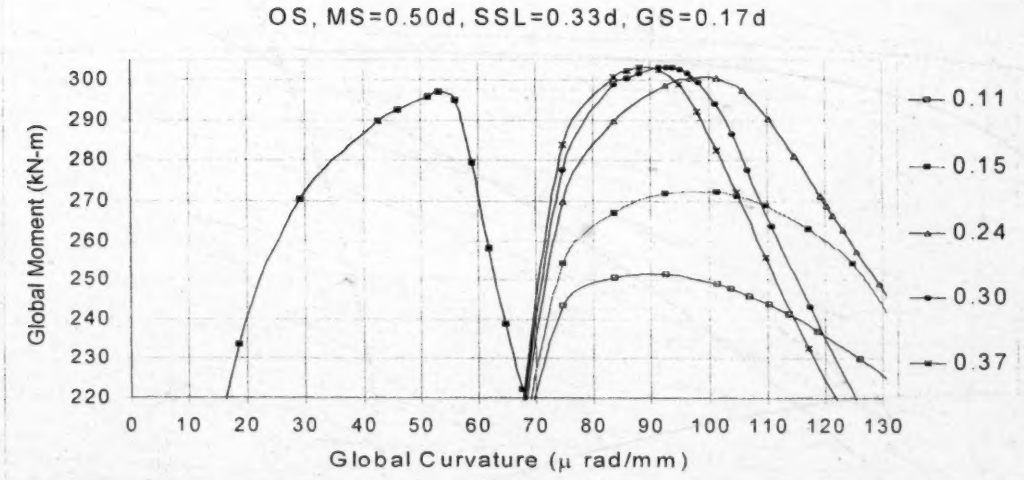

Figure 5.24 The effect of varying stiffness ratios (ρ) for odd sleeve configuration

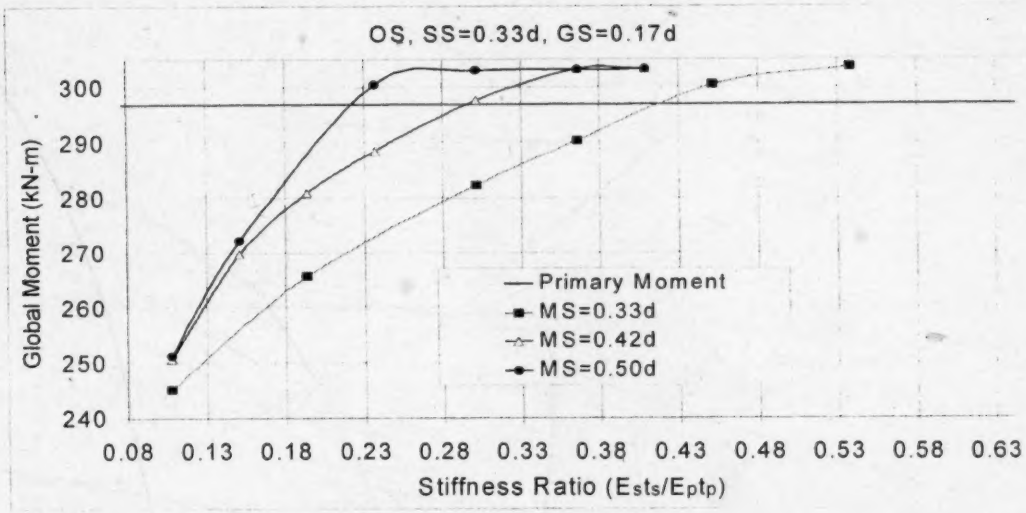

Figure 5.25 Combined effect of varying middle sleeve length and stiffness ratios for odd sleeve configuration

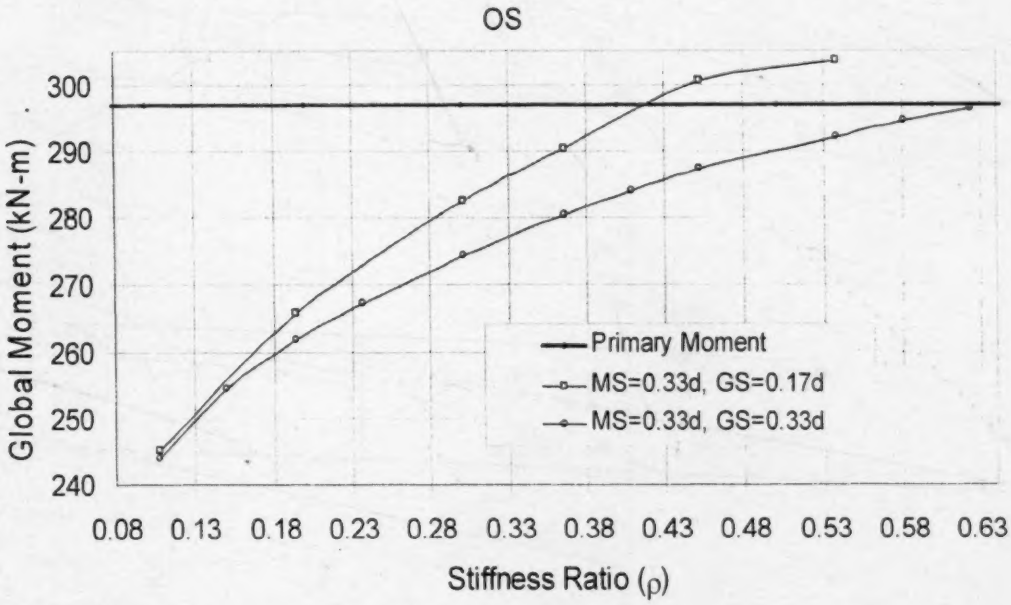

Figure 5.26 Combined effect of varying gap sizes and stiffness ratios for odd sleeve configuration

OS, MS=0.33d, ρ=0.11, GS=0.17d

Figure 5.27 The growth of the primary wrinkle for lower stiffness ratios

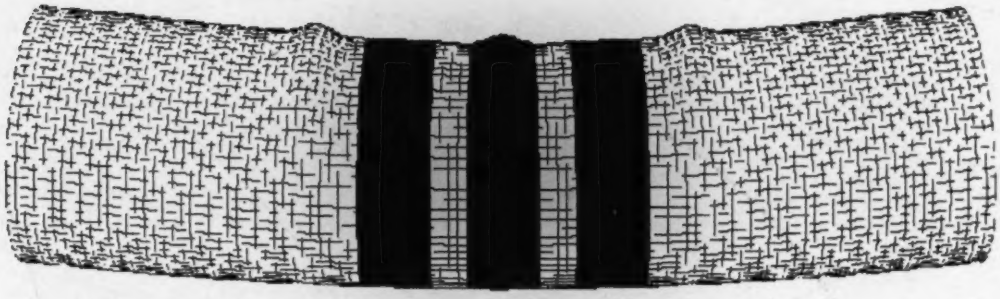

OS, MS=0.33d, ρ=0.50, GS=0.17d

Figure 5.28 Secondary wrinkle outside sleeved region for shorter gap sizes

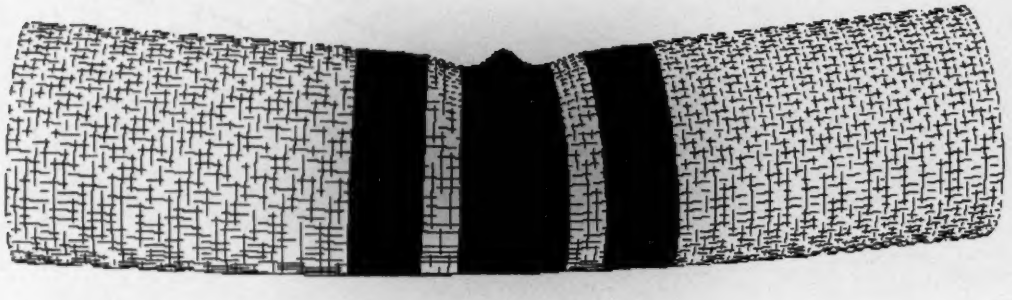

OS, MS=0.50d, ρ=0.15, GS=0.17d

Figure 5.29 The growth of the primary wrinkle

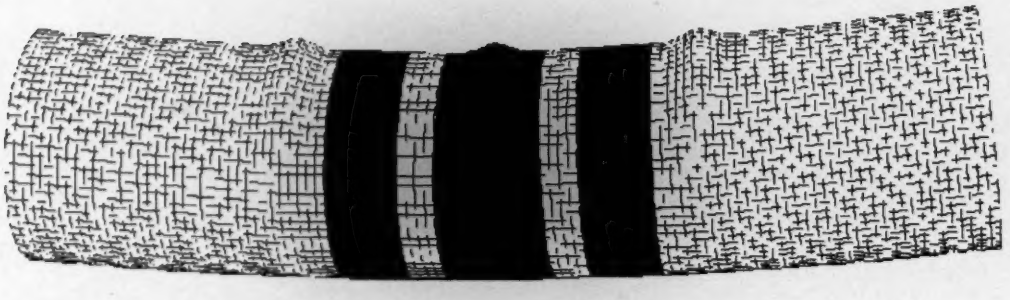

OS, MS=0.50d, ρ=0.30, GS=0.17d

Figure 5.30 Secondary wrinkle outside sleeved region

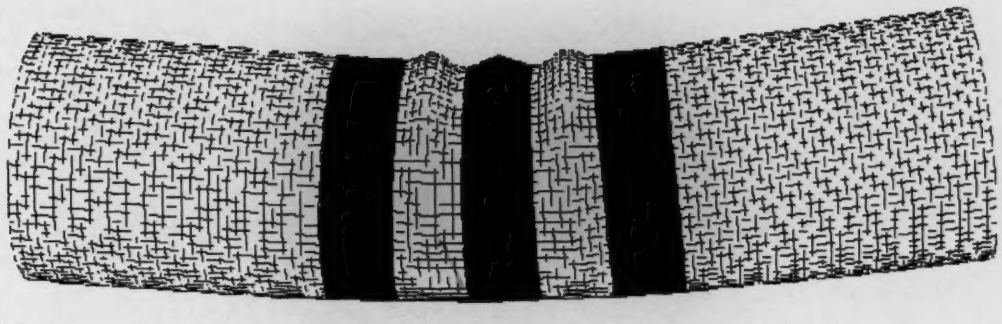

OS, MS=0.33d, ρ=0.54, GS=0.33d

Figure 5.31 Secondary wrinkle within sleeved region for longer gap sizes

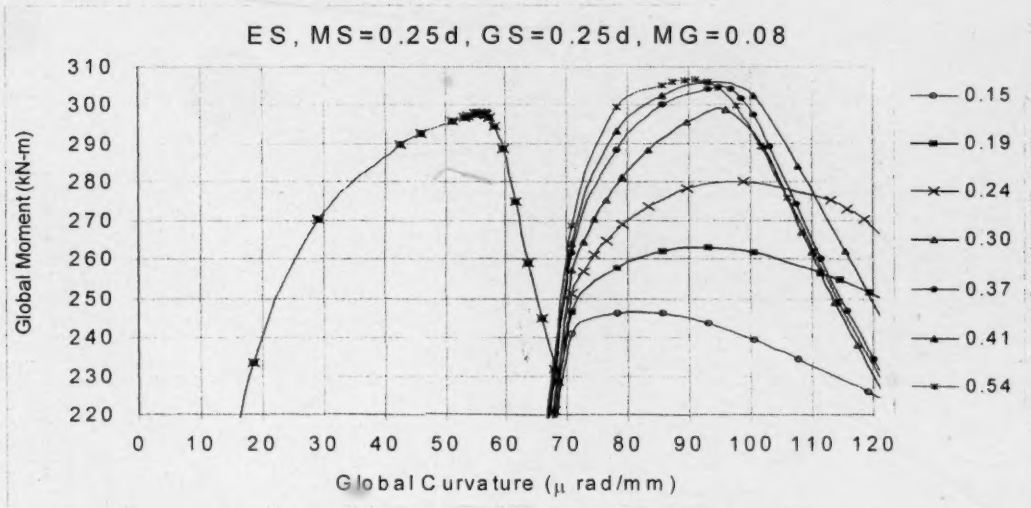

Figure 5.32 The effect of varying stiffness ratios for even sleeve configuration

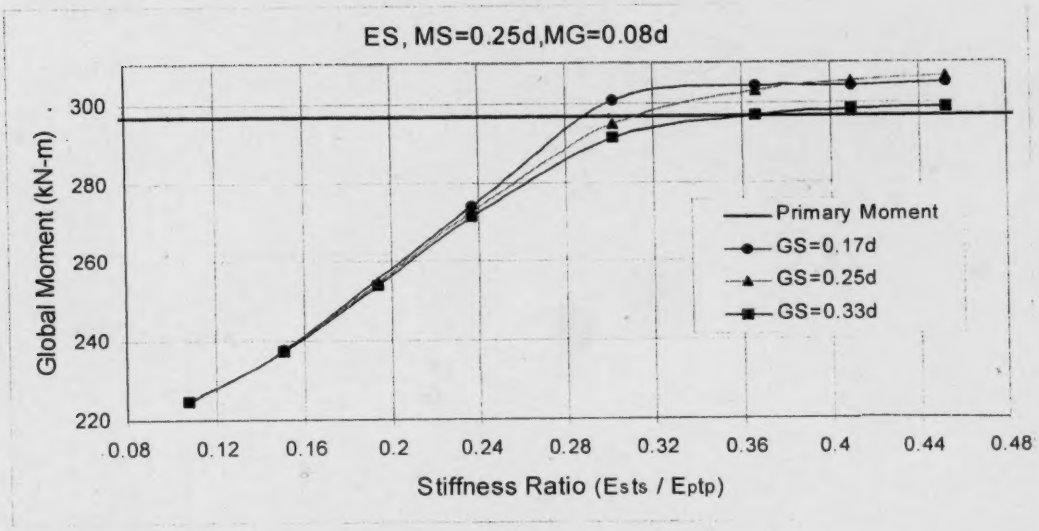

Figure 5.33 Combined effect of varying stiffness ratios and side gap sizes on the secondary moment for even sleeve configuration

ES, MS=0.25d, ρ=0.15, GS=0.17d, MG=0.08d

Figure 5.34 The growth of the primary wrinkle for lower stiffness ratio

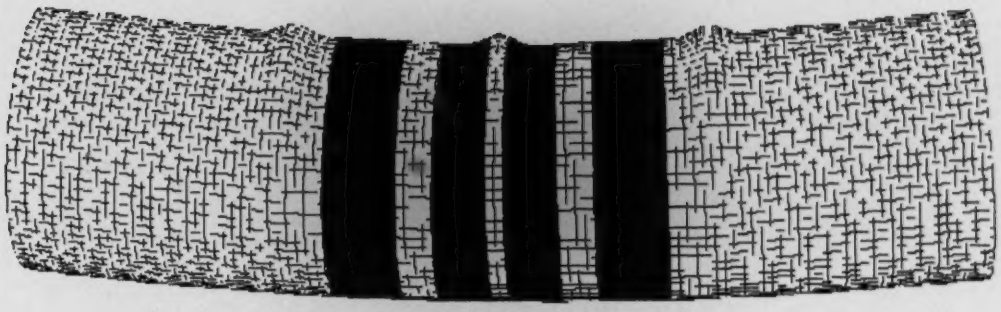

ES, MS=0.25d, ρ=0.37, GS=0.17d, MG=0.08d

Figure 5.35 Secondary wrinkle outside sleeved region

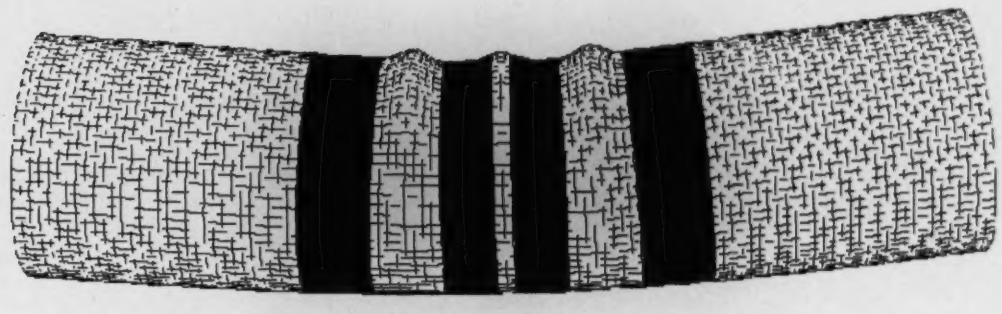

ES, MS=0.25d, ρ=0.37, GS=0.33d, MG=0.08d

Figure 5.36 Secondary wrinkle inside sleeved region

Effect of varying side gap sizes on the location of secondary wrinkle

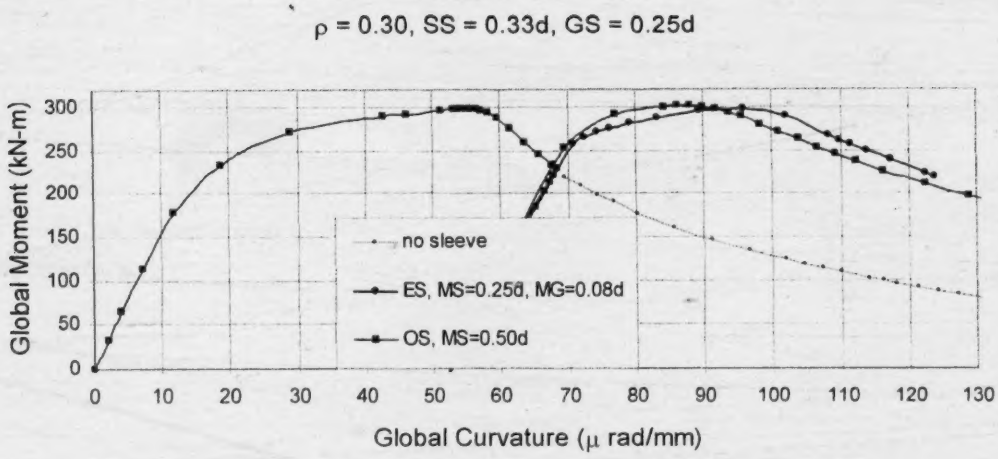

Figure 5.37 Comparison between even and odd sleeve configuration

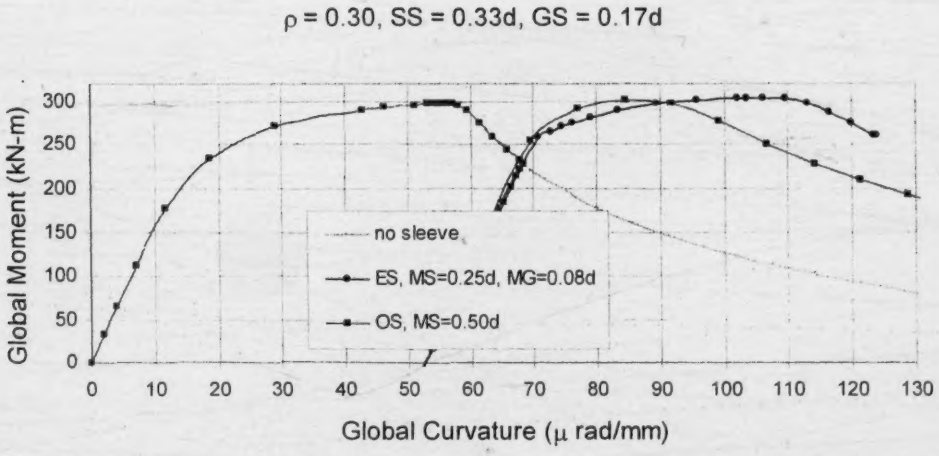

Figure 5.38 Comparison between even and odd sleeve configuration

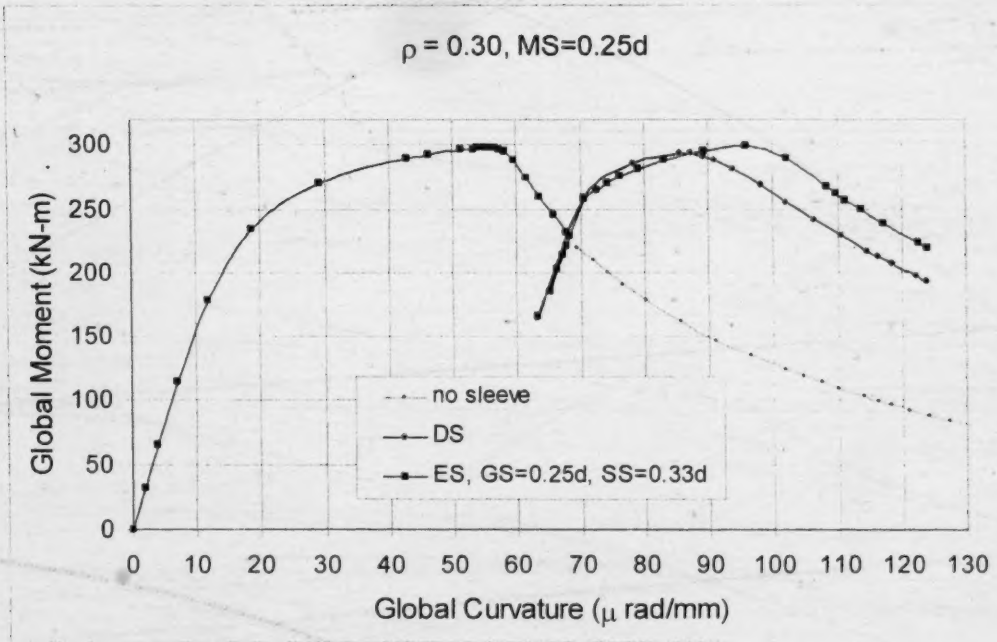

Figure 5.39 Comparison between double and even sleeve configuration

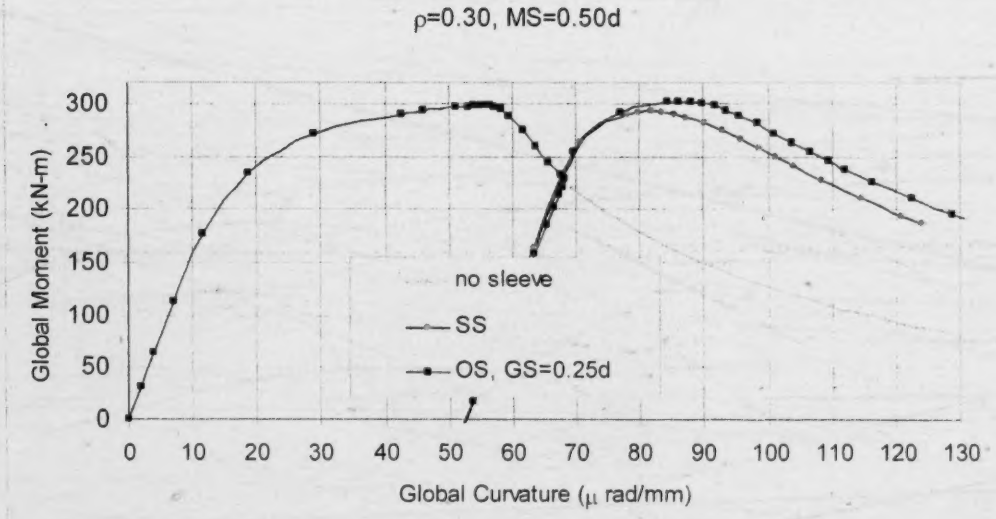

Figure 5.40 Comparison between single and odd sleeve configuration

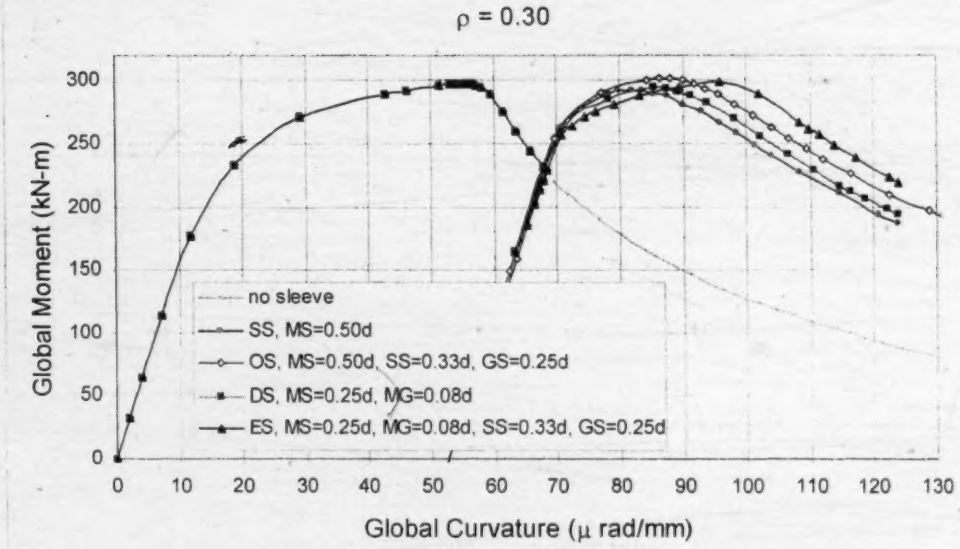

Figure 5.41 Comparison among all sleeve configurations

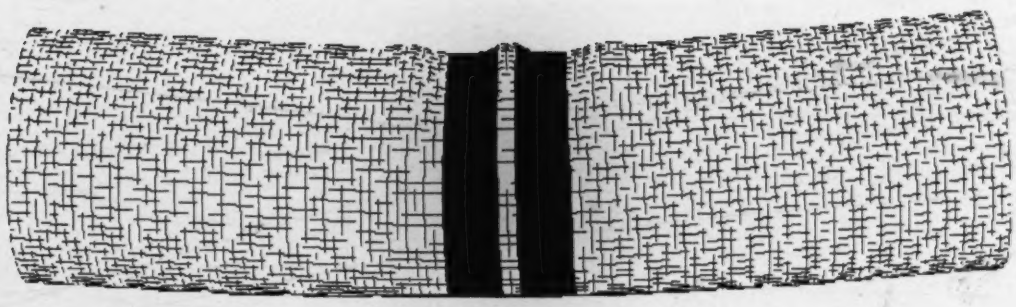

DS, MS=0.25d, ρ=0.37, GS=0.17d, MG=0.08d

Figure 5.42 Initially double sleeves were applied for a sequential repair

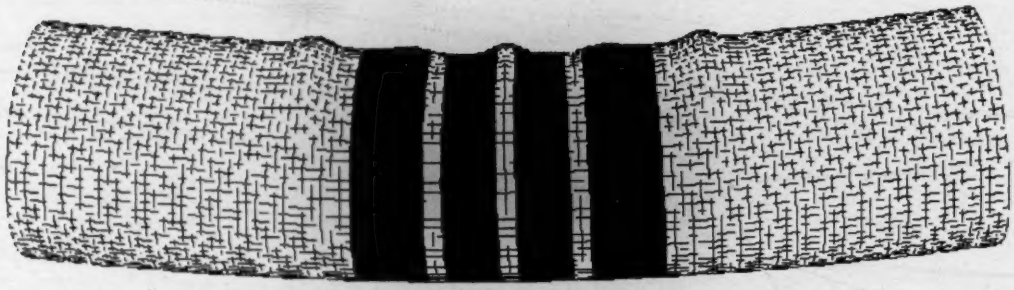

Figure 5.43 0.33d side sleeves were applied on secondary wrinkle

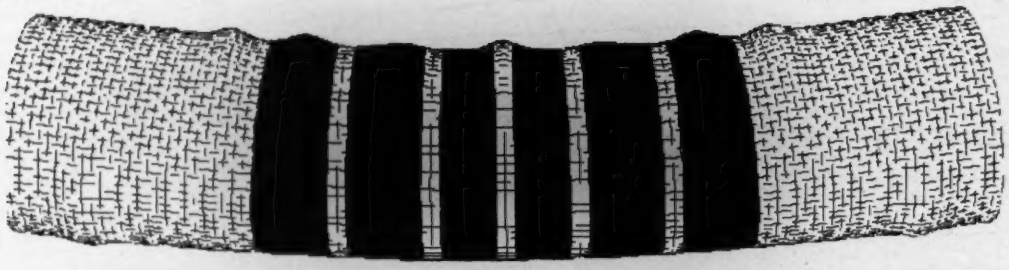

Figure 5.44 0.33d sleeves were applied on the tertiary wrinkle

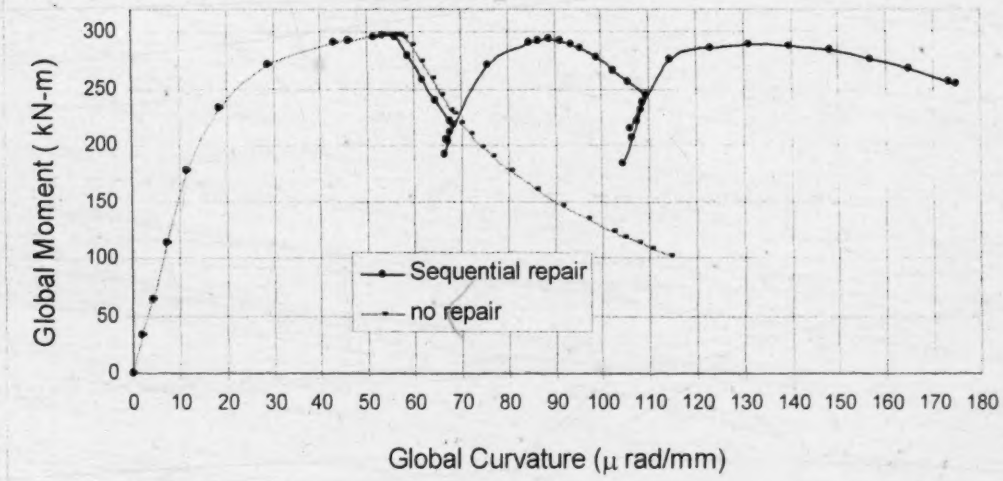

Figure 5.45 Moment-curvature behaviour of a sequential repair

6. CONCLUSIONS AND RECOMMENDATIONS

6.1 GENERAL

The effect of various repair techniques using FRP sleeves on the post buckling behaviour of the pipe has been discussed in chapters 4 and 5 on the basis of experimental results and finite element analysis (FEA). The importance of geometrical and material properties of the FRP sleeve(s) on the post buckling capacity and the mode of failure of the pipe is evident from the results discussed in chapter 5 and an efficient sleeve design can be chosen based on the performance of each sleeve.

It is a general trend of the repaired pipe that post buckling capacity increases when sleeves are applied and eventually decreases followed by either the appearance of a secondary wrinkle or further growth of the primary wrinkle. In order to assure long service life of a buckled pipe, it is advised that a sleeve design be used that allow for sequential (further or subsequent) repair, while providing more ductility and flexural strength to the pipe. In the following sections, notable findings on the major parameters of sleeve(s) are discussed. It should be noted that the following proposed sleeve details are based on the pipe geometry and material, and the operational conditions of Norman Wells Pipeline.

6.2 SLEEVE LENGTH

The length of the middle sleeve performs an important role in the post-buckling behaviour of the pipe.

The post buckling capacity and the mode of failure of the pipe may vary if the length of middle sleeve(s) is varied. If the length of the middle sleeve is increased in the case of odd sleeves configuration, a post buckling capacity equal to the primary moment capacity can be achieved at a lower stiffness ratio. Shorter sleeves require a higher stiffness ratio

to resist a particular post buckling capacity. The length of the middle sleeve should be selected so that it may enable the wrinkled pipe to resist more flexural capacity and cause an outward secondary wrinkle so that the pipe can be rehabilitated sequentially.

For odd sleeve configuration, 0.33d or 0.50d middle sleeves have appeared to be an optimum sleeve length. A middle sleeve length of less than 0.33d may not provide enough moment capacity.

For even sleeve configuration, middle sleeves shorter than 0.25d provide very low post buckling capacity as shown in **Figures 5.12** and **5.13**. 0.25d middle sleeves appeared to be the optimum sleeve length for even sleeves.

The effect of sleeve length on the post buckling capacity of the pipe is not significant in the case of single sleeve configuration but a sleeve shorter than 0.50d may produce an inward buckle as shown in **Figure 5.18** which is not a desirable mode of failure. It is recommended that at least a 0.50d single sleeve be used.

The length of the side sleeves may not have major impact on the post buckling capacity of the pipe as discussed in section 5.4.3 and shown in **Figure 5.17**. However it is suggested that 0.33d side sleeves be used for all odd and even sleeves.

6.3 GAP SIZE

For odd sleeve configuration, the post buckling capacity of a rehabilitated pipe increases when the side gap size decreases or vice versa as shown in **Figure 5.8**. Longer gap sizes disregard the effectiveness of side sleeves and produce a single sleeve effect in the case of odd sleeve configuration. The gap size also affects the location of the secondary wrinkle, causing it to appear either within or outside the sleeved regions. The sleeved region is referred to as the portion of the pipe length strengthened by the sleeves. If 0.17d or smaller gaps are provided, the secondary wrinkle is observed to appear outside the

sleeved region. 0.17d or smaller gaps may not allow a secondary wrinkle to appear within the sleeved region since the wrinkle requires a minimum gap of around 0.25d to appear.

For an odd sleeve configuration, a 0.17d gap seems to be the optimum size, since it may force the secondary wrinkle to appear outside the sleeved region and therefore sequential repair might be possible. This gap size may also improve the ductility and the post buckling capacity of the pipe.

For an even sleeve configuration, the post buckling capacity and the ductility of the pipe increase when side gap size decreases, provided other parameters remain the same, as showed in **Figures 5.13** and **5.14**. A side gap of 0.08d or 0.17d may provide more ductility and strength to the pipe and is therefore considered to be an optimum side gap for even sleeves.

In addition to side gaps, the middle gap also has a major impact on the behaviour of the pipe. The post buckling capacity of the pipe increases if the middle gap decreases or vice versa. It seems that other parameters of the sleeves may not affect the behaviour of the pipe significantly when a middle gap longer than 0.08d is provided as shown in **Figure 5.16**. A longer middle gap may not be able to stop the growth of the primary wrinkle. It is recommended that a middle gap of 0.08d be used for all even sleeve configurations.

In Summary, the post buckling capacity of the pipe increases when side gap sizes decrease or vice versa. Shorter gaps may provide more strength to the pipe to resist external loads. Side gap sizes also affect the location of secondary wrinkle. Smaller gap sizes (0.17d or less) may cause the secondary wrinkle to appear outside the sleeved region as shown in **Figures 5.30** and **5.35** and longer (0.25d or more) gaps may cause the wrinkle to appear within the sleeved region as shown in **Figures 5.31 and 5.36**. If the secondary wrinkle appears outside the sleeved region, it might be easy to rehabilitate the pipe again.

6.4 SLEEVE STIFFNESS

FEA shows that the stiffness of the sleeve(s) may alter the post buckling capacity and the mode of failure of the pipe. In order to achieve a non-dimensional value for the stiffness, the ratio of sleeve to pipe stiffness ($E_s t_s / E_p t_p$) is used and denoted by "ρ" in this research. The stiffness of the pipe is constant since the thickness and the modulus of elasticity are constant. The stiffness of the FRP sleeve(s) is varied by altering only the thickness of the sleeve(s) since the modulus of elasticity of the material (FRP) is constant.

The stiffer the sleeve, the higher is the post buckling capacity of the pipe. A stiffer sleeve may decrease the growth rate of the primary wrinkle and provide more strength to the pipe to resist external loads. It is shown in **Figures 5.19**, **5.23** and **5.32** that the post buckling capacity of the pipe increases by increasing the stiffness ratio for all configurations.

The failure mode of the pipe largely depends on sleeve stiffness. The growth of the primary wrinkle may not be stopped if less stiff sleeves are used as shown in **Figures 5.21**, **5.27**, and **5.34**. It is necessary that the sleeve must be stiff enough to control the growth of the primary wrinkle and causes an outward secondary wrinkle.

For each configuration, a stiffness ratio of less than 0.30 may not produce a secondary wrinkle. For a single sleeve of 0.50d or longer, the stiffness ratio of 0.41 appears to be optimum. In the case of odd sleeves having a middle sleeve length of 0.50d, a stiffness ratio of 0.30 (or more) seems to be optimum. For even sleeves, a stiffness ratio of 0.37 or more seems to be an optimum design.

During the experimental program, the fibre fracture problem has appeared in the case of odd sleeves. This problem did not appear in even sleeve configuration. In the cases of single and odd sleeve configurations, the middle sleeve is placed directly on the wrinkle crest applying high strains on the sleeve and thereby causes a fracture in the sleeve. This problem might be overcome by increasing the stiffness of the sleeve or choosing even

sleeve configuration. The sleeve fracture problem makes even sleeves more attractive than single and odd sleeves.

6.5 CONCLUSIONS

- The post buckling capacity of a locally buckled pipe increases when FRP composite sleeves are applied but eventually decreases followed by the formation of a secondary wrinkle or further growth of the primary wrinkle.

- By adjusting certain parameters or properties of the sleeve design, the post buckling capacity and the ductility of the pipe can be improved. It is very easy and economical to adjust those parameters for FRP composites since many of their properties can be custom-designed.

- The post buckling capacity and the ductility of the pipe can be increased by increasing the sleeve to pipe stiffness ratio, provided the length and gap sizes of the sleeve(s) are kept within a certain limit.

- Multiple sleeve configurations (odd and even) provide a wider variety of behaviour patterns than a single sleeve.

- In the case of a single sleeve, geometrical and material properties of the sleeve have little effect on the behaviour of the pipe. However, shorter single sleeves (less than 0.42d) may produce inward buckling.

- The post buckling capacity for odd sleeves increases if the length of the middle sleeve is increased.

- The mode of failure of the pipe changes according to the stiffness ratio.

- There is a trade off between the length of the middle sleeve and the stiffness ratio for an odd sleeve. For a longer middle sleeve, the maximum post buckling capacity is achieved at a lower stiffness ratio and for a shorter sleeve the same capacity is achieved at higher stiffness ratios.

- For odd sleeves, if the gap sizes are small, the maximum post buckling capacity is achieved at a lower stiffness ratio, and for larger gap sizes the same level of post buckling capacity is achieved at higher stiffness ratios.

- In order to achieve sufficient post buckling capacity, the middle gap size for even sleeves may not be more than 0.08d. A middle gap size of more than 0.08d may disregard the effectiveness of all other parameters.

- The ductility of the pipe can be increased by decreasing the side gap sizes.

- For almost all even sleeve configurations, the growth of the primary wrinkle may not be stopped if the stiffness ratio is less than 0.30.

- The side gap size should not be more than 0.33d.

- For even sleeves the post buckling capacity and the ductility increase if the length of the middle sleeves is increased. The length of middle sleeves should not be less than 0.17d and the middle gap size should not be more than 0.08d.

6.6 OPTIMUM SLEEVE DESIGN

On the basis of FEA it is concluded that each of the following design configurations may produce optimum results for the Norman Wells Pipeline on the basis of post buckling capacity and the mode of failure of a rehabilitated pipe:

1. Double sleeves having a sleeve length of 0.25d, a middle gap of 0.08d and a stiffness ratio of 0.37.

2. Even sleeves having middle and side sleeve lengths of 0.25d and 0.33d respectively, middle and side gaps of 0.08d and 0.17d respectively, and a stiffness ratio of 0.37.

3. Even sleeves having middle and side sleeve lengths of 0.25d and 0.33d respectively, middle and side gaps of 0.08d and 0.25d respectively, and a stiffness ratio of 0.45.

4. Odd sleeves having middle and side lengths of 0.42d and 0.33d respectively, side gaps of 0.17d, and a stiffness ratio of 0.37.

5. Odd sleeves having middle and side lengths of 0.50d and 0.33d respectively, side gaps of 0.17d, and a stiffness ratio of 0.30.

6. Single sleeves having a sleeve length of 0.5d and stiffness ratio of 0.41.

6.7 RECOMMENDATIONS

- Pipe geometries (d/t ratios) and operational conditions (internal pressure and axial load) other than the Norman Wells Pipeline should be studied to develop a comprehensive repair technique using FRP sleeves.

- More experiments should be conducted to observe the behaviour of even sleeves and sequential sleeve repairs.

- Studies should be conducted to overcome the fibre fracture problem of odd sleeve configurations.

- Optimum sleeve design should be studied for other FRP materials or systems, such as carbon FRP sleeves or combination of steel and FRP sleeves.

REFERENCES

1. Das, S., Cheng, J.J.R., Murray, D.W., 2002. "*Fracture of Wrinkled Energy Pipelines*". Department of Civil and Environmental Engineering, University of Alberta, Edmonton, Alberta, Canada.

2. Das, S., Cheng, J.J.R., Murray, D.W., Wilkie, S.A., and Zhou, Z.J. 2000. "Laboratory Study of Local Buckling, Wrinkle Development, and Strains for NPS12 Line pipe". *International Pipeline Conference* – Volume 2, ASME, Calgary, Alberta, Canada, pp. 909-915.

3. Dorey, A.B., Cheng, J.J.R. and Murray, D.W. 2001. "*Critical Buckling Strains for Energy Pipelines*". Structural Engineering Report No. 237. Department of Civil and Environmental Engineering, University of Alberta, Edmonton, Alberta, Canada.

4. Dorey, A.B., Murray, D.W., Cheng, J.J.R., Grondin, G.Y. and Zhou, Z.J. 1999. "*Testing and Experimental Results for NPS30 Line Pipe under Combined Loads*". Proceedings of OMAE99, 18th International Conference on Offshore Mechanics and Arctic Engineering, St. Johns, Newfoundland, Canada.

5. DeGeer, D. and Cheng, J.J.R. 2000. "*Predicting Pipeline Collapse Resistance*" International Pipeline Conference – Volume 2, ASME, Calgary, Alberta, pp. 1083-1091.

6. Hibbitt, Karlsson and Sorenson, Inc. (HKS) 1999a. ABAQUS/Standard, Version 5.8-1 (computer software). Hibbitt, Karlsson, & Sorenson Inc., Pawtucket, Rhode Island.

7. Hibbitt, Karlsson, and Sorenson, Inc. (HKS) (1999b). ABAQUS/Standard User's Manual, Version 5.8. Hibbitt, Karlsson, & Sorenson Inc., Pawtucket, Rhode Island.

8. Jones, R.M. 1999. "Mechanics of Composite Material", (2nd Edition,). Taylor and Francis, Philadelphia, PA.

9. Kaw, A.K., 1997. "*Mechanics of Composite Materials*", CRC Press, Boca Raton, Florida.

10. Mohareb, M., Elwi, A.E., Kulak, G.L., and Murray, D.W. 1994. "*Deformational Behaviour of Line Pipe*" Structural Engineering Report No. 202, Department of Civil and Environmental Engineering, University of Alberta, Edmonton, Alberta.

11. Mohareb, M., Alexander, S.D.B. and Murray, D.W. 1993. "*Laboratory Testing of Line Pipe to Determine Deformational Behaviour*". Proceedings of the 12th International Conference on OMAE, Vol. V – Pipeline Technology, ASME, pp. 109-114.

12. Murray, D.W. 1997. "*Local Buckling, Strain Localization, Wrinkling, and Post-Buckling Response of Line Pipe*" Engineering Structures, Vol. 19, No. 5, pp. 360-371.

13. Souza, L.T. and Murray, D.W. 1996. "*Analysis for Wrinkling Behaviour of Girth-Welded Line Pipe*" International Pipeline Conference – Volume 2, ASME, Calgary, Alberta, pp. 835-844.

14. Souza, L.T. and Murray, D.W. 1994. "*Prediction of Wrinkling Behaviour of Girth-Welded Line Pipe*" Structural Engineering Report No. 197, Department of Civil and Environmental Engineering, University of Alberta, Edmonton, Alberta.

15. Wilkie, S.A., Doblanko, R.M. and Fladager, S.J. 2000. "*Case History of Local Wrinkling of a Pipeline*" International Pipeline Conference – Volume 2, ASME, Calgary, Alberta, Canada, pp. 917-922.

16. Yao and Murray, D.W. 2000. "*Steel Sleeve Repairs for Buckled Pipelines*". Draft Report Prepared for Enbridge Pipelines Inc., Department of Civil and Environmental Engineering, University of Alberta, Edmonton, Alberta.

17. Yoosef-Ghodsi, N., Cheng, J.J.R., Murray, D.W., Doblanko, R. and Wilkie, S. 2000. "*Analytical Simulation and Field Measurements for a Wrinkle on the Norman Wells Pipeline*". International Pipeline Conference of ASME, Calgary, Alberta.

18. Yoosef-Ghodsi, N. and Murray, D.W. 1999. "*Numerical Study of the Buckle at KP 311+745 of Norman Wells – Zama Pipeline*" Report Prepared for Enbridge Pipelines (NW) Inc., Department of Civil and Environmental Engineering, University of Alberta, Edmonton, Alberta.

19. Youzwishen, O. and Cheng, J.J.R. 2001. "*Flexural Rehabilitation of Energy Pipelines using Fibre-Reinforced Polymer Composites*", Department of Civil and Environmental Engineering, University of Alberta, Edmonton, Alberta, Canada.

20. Zhou, Z.J., Boivin, R.P., Glover, A.G. and Kormann, P.J. 1996. "*Pipeline Integrity Design for Differential Settlement in Discontinuous Permafrost Areas*" International Pipeline Conference, ASME, Calgary, Alberta, pp. 603-612.

21. Zhou Z. and Murray D.W. 1994. "*Analysis of Postbuckling Behaviour of Line Pipe Subjected to Combined Loads*" International Journal of Solids and Structures Vol.32, No. 20, pp.3015-3036, 1995.

22. Zhou, Z.J. and Murray, D.W. 1993. "*Behaviour of Buried Pipelines Subjected to Imposed Deformations*". Proceedings of the 12th International Conference on OMAE, Vol. V – Pipeline Technology, ASME, pp. 115-122.